

Mathematical model for optimising the performance of a ground source heat pump.

PALLEDA, Siva Prakash.

Available from Sheffield Hallam University Research Archive (SHURA) at:

<http://shura.shu.ac.uk/20159/>

This document is the author deposited version. You are advised to consult the publisher's version if you wish to cite from it.

Published version

PALLEDA, Siva Prakash. (2009). Mathematical model for optimising the performance of a ground source heat pump. Masters, Sheffield Hallam University (United Kingdom)..

Copyright and re-use policy

See <http://shura.shu.ac.uk/information.html>

REFERENCE

ProQuest Number: 10697466

All rights reserved

INFORMATION TO ALL USERS

The quality of this reproduction is dependent upon the quality of the copy submitted.

In the unlikely event that the author did not send a complete manuscript and there are missing pages, these will be noted. Also, if material had to be removed, a note will indicate the deletion.

uest

ProQuest 10697466

Published by ProQuest LLC(2017). Copyright of the Dissertation is held by the Author.

All rights reserved.

This work is protected against unauthorized copying under Title 17, United States Code
Microform Edition © ProQuest LLC.

ProQuest LLC.
789 East Eisenhower Parkway
P.O. Box 1346
Ann Arbor, MI 48106- 1346

MATHEMATICAL MODEL FOR OPTIMISING THE PERFORMANCE OF A
GROUND SOURCE HEAT PUMP

By

Siva Prakash Palleda

The thesis is submitted in partial fulfilment of the requirement of Sheffield Hallam
University for the degree of Master of Philosophy

October 2009

Abstract

Energy demand for the twenty first century is expected to increase many fold along with corresponding diversification of energy sources and generation methods. Of the many energy sources available, use of Ground Source Heat Pump (GSHP) system is the focus of the analysis in this research.

This work is carried out to identify the key parameters which affect the performance of the GSHP system. A mathematical model has been developed to understand the complex operation of the heat pump under typical working conditions. Individual sub-systems, such as Ground Heat Exchanger (GHE), evaporator, condenser, compressor and radiator are modelled in MathCAD and coupled together and solved simultaneously. The performance of the system is predicted while varying air temperature, power input to the compressor and the ground temperature beneath the earth's surface. In addition a special sub-model was developed for the single vertical U-tube GHE in FLUENT, a Computational Fluid Dynamics (CFD) software, to calculate the overall heat transfer coefficient for varying outer surface temperature of the borehole.

The overall system results are validated against the published results with the system operating range of 18°C to 33°C with around 10 percent deviations.

It is determined that the COP of the system increases with surface area and overall heat transfer coefficient (OHTC) of the heat exchanger. An increase in up to 500 m² surface area, steep raise of COP from 10.05 to 10.3 is observed. Similarly increase of 10 W/m²K of OHTC has steep COP rise from 10.05 to 10.28. The temperature gradient across the system also has influence on its operating performance, where a 15°C increase in the ground temperature for cooling mode reduces the COP by around 5%. Finally the degree of refrigerant sub-cooling has a positive effect, for every 5°C temperature drop the COP improves by 0.5 similarly for degree of super-heating, COP improves by 0.25.

Scope for performance enhancement for GSHP is investigated by tuning operating conditions. The effect of operating variables to the sensitivity of performance of heat pump is also determined.

Contents

Structure of the Thesis	1
Chapter 1	
Introduction	4
1.1 Ground temperature variations.....	6
1.2 Types of GSHP configurations	9
1.3 Cost comparison	11
1.4 Typical Heat pump cycle operation	13
1.5 Role of GSHP in reducing CO ₂ emissions	14
1.6 Methodology.....	17
1.7 Research objectives	21
1.8 Block diagram of the project.....	23
Conclusion	24
Chapter 2	
Introduction	25
2.1 Literature Review	25
2.1.1 Coefficient of Performance (COP)	28
2.1.2 Ground Heat Exchanger (U tubes)	30
2.1.3 Condenser and evaporator	34
2.1.4 Methodologies used to model the Heat Pump System	36
2.1.4.1 Ground temperature variation modelling.....	38
2.1.4.2 Thermal loading on the borehole	41
2.1.4.3 Heat transfer modelling of GHE	44
2.1.5 Development of GSHP.....	51
2.1.6 Refrigerant.....	53
2.1.7 Scope and limitations.....	59
2.1.8 Computational Fluid Dynamics (CFD)	60
2.1.9 MathCAD	65
Conclusion	66
Chapter 3	
Introduction	67
3.1 Steady state of analytical model.....	67
3.1.1 GSHP system	68
3.1.1.1 Ground Heat Exchanger	71

3.1.1.2 Heat Pump system	72
3.1.1.3 Compressor	72
3.1.1.4 Evaporator	73
3.1.1.5 Throttle valve	74
3.1.1.6 Radiators	76
3.1.1.7 Room wall	77
3.1.2 Calculation of Thermal resistance.....	79
3.1.3 Solving procedure.....	83
Conclusion	85

Chapter 4

Introduction	86
4.1 CFD modelling in FLUENT.....	86
4.1.1 Modelling the U-tube.....	86
4.1.1.2 Meshing	90
4.1.1.3 Boundary condition and Solving	91
Conclusion	92

Chapter 5

Introduction	93
5.1 Results and discussions.....	93
5.1.1 Results from the analytical model.....	94
5.1.2 Validation with experimental model (Bench mark model)	96
5.1.3 Comparison with Ideal Carnot COP.....	99
5.1.4 Parametric study.....	100
5.1.5 CFD model.....	106
Conclusion	109

Chapter 6

Introduction	110
6.1 Conclusion and future scope of work	110
6.2 Future scope of work.....	113
Conclusion	114
References.....	115
Appendix A - Numerical values for the variables	122
Appendix B: Calculation of Overall Heat transfer Coefficient for heat exchangers	124
Appendix C: MathCAD Calculations- Uses values given in Appendix A.....	126
Residue calculation for an initial guess.....	133

List of Figures

Figure 1 Renewable energy delivered by a heat pump system with COP of 4	5
Figure 2 Monthly variation of outdoor air temperature Erzurum, Turkey	7
Figure 3 Monthly variation of mean ground temperatures at several depths Erzurum, Turkey.....	7
Figure 4 Temperature variations with depth of ground	8
Figure 5 Horizontal closed loop heat pump system.....	10
Figure 6 Horizontal closed loop slinky coil system	10
Figure 7 Vertical U tube closed loop heat pump system	11
Figure 8 Capital costs for different configurations	12
Figure 9 Typical Heat Pump Unit.....	13
Figure 10 Comparison of several renewable energy techniques.....	15
Figure 11 Comparison of fuel costs and CO ₂ emissions for GSHPs and fossil fuel Boilers	16
Figure 12 Comparison of carbon dioxides emissions from GSHPs and other forms of heating	17
Figure 13 Flow chart for the project.....	23
Figure 14 Vertical U-tube in symmetry plane.....	30
Figure 15 Basic configurations of Vertical U tubes	31
Figure 16 Basic configurations of vertical U tubes.....	31
Figure 17 Evolution of daily average subterranean temperature and outdoor air temperature.....	33
Figure 18 Evolution of daily average temperatures of outdoor air, circulating water, surface of ground heat exchanger.....	34
Figure 19 Typical Plate Heat Exchanger	36
Figure 20 SGSHP System pumping efficiently required pumping water to cooling capacity.....	38
Figure 21 Earth temperature distribution surrounding buried coil at different depth after 4 hour operation of GSHP.....	39
Figure 22 Earth temperature variation with the operation time of GSHP at a depth of 5 m for different radius	40
Figure 23 The borehole temperature rise profiles at different times	41

Figure 24 Borehole loading profile against a dimensionless parameter ($z-d/H$) (with value one at bottom and zero at borehole top).....	42
Figure 25 GHE thermal load as a function of the load duration with the inlet and out let temperatures of water at 10°C initial ground temperature	43
Figure 26 The GHE thermal load as a function of the load duration with the inlet and outlet temperatures of water as parameter 15°C intial ground temperature	44
Figure 27 Shape factors for three different positions.....	47
Figure 28 Mean fluid temperature: numerical and theoretical line-source solution	48
Figure 29 Thermal balance on ground surface.....	50
Figure 30 Variation of COP with increase in the temperature of heat source.....	51
Figure 31 Refrigerants with ODP and GWP values.....	54
Figure 32 Temperature entropy diagram for refrigerant cycle	55
Figure 33 Pressure enthalpy diagram for refrigerant cycle.....	56
Figure 34 The three dimensions of computational fluid dynamics.....	60
Figure 35 Basic structure of the CFD modelling tree.....	62
Figure 36 Line diagram of GSHP system	69
Figure 37 Line diagram of GHE.....	71
Figure 38 Line diagram of condenser.....	72
Figure 39 Line diagram of heat pump system	73
Figure 40 Line diagram of evaporator	74
Figure 41 Line diagram of Throttle value.....	75
Figure 42 Line diagram of Radiator.....	76
Figure 43 Line diagram of heat transfer through wall	79
Figure 44 Various components within the system with their UA values.....	82
Figure 45 Pipe and water geometry in GAMBIT	88
Figure 46 Pipe geometry with grout in GAMBIT	89
Figure 47 Meshed geometry water in the pipe	91
Figure 48 COP varying with temperature gradient with T_g at 18°C.....	94
Figure 49 COP varying with temperature gradient with T_{air} at 33°C	95
Figure 50 Experimental and actual COP for varying compressor power	96
Figure 51 Air temperature V/S circulating water temperature in GHE both actual and experimental.....	98
Figure 52 Comparison of actual and Carnot COP	99

Figure 53 Variation of COP with area of grout.....	100
Figure 54 Varying outlet temperature of water from the GHE with area of grout	101
Figure 55 Effect of degree of super heat on COP	102
Figure 56 Effect of degree of sub cooling on COP	103
Figure 57 P-h diagram with sub cooling and super heating for a typical cycle ...	104
Figure 58 Variation of COP with U value of grout.....	105
Figure 59 Contours of temperature distribution in the pipe.....	106
Figure 60 Contours of velocity profile in the pipe.....	107
Figure 61 Contours of velocity in U tube	108
Figure 62 Surface heat transfer coefficient on the inner surface of the pipe	109

Nomenclature

A = Surface area of heat transfer (m^2)

C_p = Specific heat ($J/kg\ K$)

d = Diameter of pipe(m)

h = Enthalpy ($J/Kg\ K$)

h_f = Convective heat transfer coefficient (W/m^2K)

k = Thermal conductivity($W/m\ K$)

K_{pipe} =Thermal conductivity of pipe ($W/m\ K$)

K_{grout} =Thermal conductivity of grout ($W/m\ K$)

K_{ground} =Thermal conductivity of ground ($W/m\ K$)

l = length of pipe (m)

M = Mass flow rate(Kg/s)

m_1 = Mass flow rate of radiator water (Kg/s)

n = Number of bore holes

Q_{sr} = Cooling load (Watts)

Q_s = Condenser load (Watts)

Re = Reynolds number

r_1 =Internal radius of pipe(m)

r_2 =External radius of pipe(m)

r_3 =External radius of grout(m)

r_4 =External radius of ground (m)

T_{air} = Outside air temperature ($^{\circ}C$)

T = Temperature ($^{\circ}C$)

U =Overall heat transfer coefficient ($W/m\ K$)

v = Velocity of water (m/s)

W_{in} = Power input (Watts)

$W1$ = Radiator loop circulating water (Kg/s)

List of symbols

ΔT_{Lm} = Log Mean Temperature Difference ($^{\circ}K$)

ρ = Density of water (Kg/m^3)

μ = Dynamic viscosity ($Kg/m\ s$)

Subscripts

ai = Air inside

ao = Air outside

fi = Water inlet to heat pump ($^{\circ}C$)

fo = Water outlet from heat pump ($^{\circ}C$)

g = Grout

in = Water inlet temperature to the radiator ($^{\circ}C$)

out = Water exit temperature from the radiator ($^{\circ}C$)

r = Room

ref = Refrigerant

w = Wall

W = Water

1 = Condenser side

2 = Evaporator side

4 = Condenser exit

DECLARATION

This thesis is submitted in partial fulfilment of the requirements of Sheffield Hallam University for the degree of Master of Philosophy. It contains an account of research carried out between October 2007 to October 2009 in Materials Engineering and Research Institute, Sheffield Hallam University under the supervision of Dr Andy Young and Dr Saud Ghani. Except where acknowledgement and reference is appropriately made, this work is, to the best of my knowledge, original and has been carried out independently. No part of this thesis has been, or is currently being submitted for any degree or diploma at this or any other University.

ACKNOWLEDGMENTS

I would like to acknowledge the support and encouragement of my director of studies Dr Andy Young and Dr Saud Ghani during the course of this research project. I also acknowledge the Materials Engineering and Research Institute and the Faculty of Arts Computing Engineering and Sciences at Sheffield Hallam University for the provision of computing facilities.

My special thanks extend to Kasara farahani for his unfailing help in using MathCAD and I would like to thank Dr. Osman Baig and Dr. Ben Hughes for their constructive ideas and discussions.

I thank all the technical staff in the Materials Engineering and Research Institute for their help and assistance during the course of research work. Special thanks are extended to Professor Doug Cleaver and Mrs. Rachael Ogden.

Thanks are also extended to my family and my dear friends Shivaraj Alavandimath and Narasimha Raju for their unfailing support and encouragement. I also want to thank Mr. Anura Uthumange for his ideas and inspiration to complete this thesis.

Dedicated to

My beloved Parents

Palleda Thipperudra Swamy

Palleda Nagarathamma

Structure of the Thesis

Chapter 1 Introduction

This chapter gives the initiation of the project, answering why this topic has been chosen and sufficient information about the scope and the developments in the recent past. It also introduces to the availability of the non-conventional energy resources and its applications and research objectives. The block diagram of the research carried out has been explained.

Chapter 2 Literature Review

In this chapter the detailed work undertaken by many authors and the methodologies used to represent the system is discussed in detail. The progress in the area of GSHP has been highlighted at appropriate instances. There have been many attempts to develop analytical model of the system and the true representation of the model in the numerical form as well. Numerous numerical procedures available to solve the system especially the ground surrounding the vertical U tube heat exchangers have been discussed. Calculation methods of the thermodynamic properties of the refrigerant adopted by different authors have been discussed.

Chapter 3 Steady state modelling of Ground Source Heat Pump

Each sub system of the GSHP is modelled representing heat balance and heat transfer equations. Overall there are five heat exchangers in the complete system. The system is represented by a set of simultaneous equations. Since heat transfer

is modelled in Log Mean Temperature Difference (LMTD) method, they are nonlinear in nature. These equations are solved simultaneously with some good initial guess work. Once the model is established, the variables are fine tuned to match with the published data. The validated model is used to calculate the new values of COP. With increase in the surface area of ground heat exchanger and better thermal properties for the pipe and grout material, the expected COP is much improved.

Chapter 4 Ground Heat Exchanger (GHE) modelling in FLUENT

FLUENT is versatile CFD software, used to model and analyse the complex physical problems. Methodology is developed to model, analyse the GHX and use results from Chapter 3, and the boundary conditions were used from the published data for the analysis. The value of the thermal resistance of the grout and pipe material is used in the analytical model to verify the results. This chapter explains conditions used to model the system, mesh quality and solution techniques. Different configurations are modelled to increase the surface area of heat transfer to observe the effect on COP of the system. Thermal properties of the grout and pipe material are improved to observe the improvement in the COP of the overall system.

Chapter 5 Results and discussions

Results from the analysis are discussed and the comparison is made with the published data to represent the reference model. Normal operating parameters are used to validate against the standard mode, the deviation for the analysis and the assumptions made are discussed.

Chapter 6 Conclusions

Conclusions are made with reference to the influence of operating parameters and the assumptions made. Power input to the compressor, Air temperature and Ground temperature are the three main variables which drives the system. Water inlet temperature, degree of superheating and sub cooling effect is also considered as variables and appropriate conclusions were made for the hybrid model

Chapter 7 Future scope of work

It is out of the scope of the work to implement all the practical operating and time varying parameters in the current study. Ground modelling for the grout and time variations might be a good approach for better understanding of the system. Different configuration of the ground pipe is worth the try. Future suggestions are made to improve the research to achieve the higher performance.

Chapter 1

Introduction

Generating power to meet the growing demand of the developing world with limited resources calls for more efficient, safe, economical and environmental friendly means and has been a growing challenge for many years. Various non-conventional methods to generate power and heat from natural resources have been developed. They are wide spread from wind turbines, solar energy systems to tidal power systems. Air Source Heat Pumps (ASHP) and geothermal heat pump systems are environment friendly and greener energy systems. Generally the geothermal heat pumps are also called as geo-exchange systems. Ground-Source Heat Pump (GSHP) system uses ground as source or sink and this very basic energy exchange distinguishes the technology from air-source heat pumps. Since ASHP uses air as source or sink for the thermal energy exchange for heating or cooling, auxiliary heating sources are used as its efficiency and capacity decrease with outside air temperature [1].

GSHP can be used in almost any region, irrespective of any weather conditions. GSHP uses energy well below the earth surface, which is unaffected by the outside air temperature, hence it is more reliable technology compared to ASHP. Mechanical pumps were used directly to circulate the high underground temperatures water available like hot springs and steam vents for heating indoor spaces without the use of a heat pump system. Systems such as mechanical ventilation heat recovery system MVHR show the scope available to develop newer technologies in sustainable energy [2].

In developed countries, approximately 40% of the total energy consumed is account for space heating and cooling [3]. With the increasing demand for the power, use of fossil fuel has a greater concern over global warming due to harmful emissions. Every effort is being made to develop and use energy efficient, environmentally friendly and less maintenance systems. This need gives rise to the development of the GSHP system for its less maintenance costs compared to the conventional alternatives available.

Today GSHP systems are considered to be one of the widely accepted systems in the renewable energy sector. Around one million GSHP system units have been installed worldwide in about 30 countries with annual increases of 10% over the period of last 10 years [4]. Energy consumption is reduced up to 50% in cooling to 70% in heating mode can be observed [5]. This potential for significant energy savings has led to the use of GSHPs in a variety of applications.

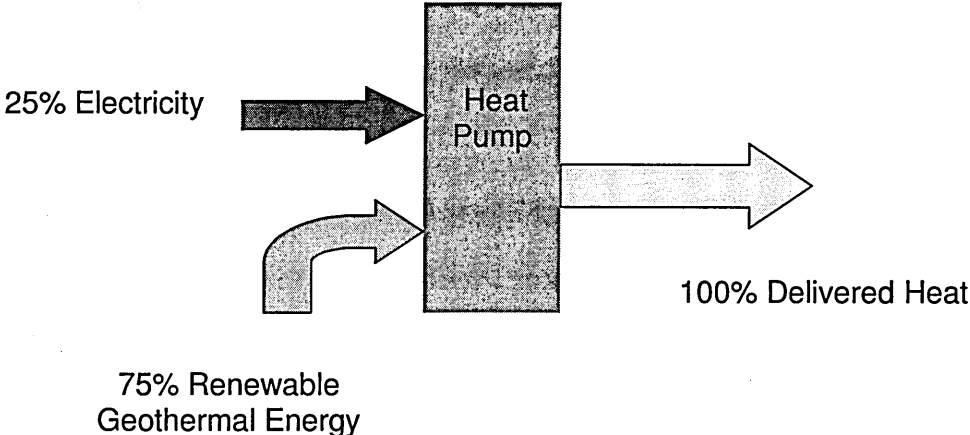


Figure 1 Renewable energy delivered by a heat pump system with COP of 4

The performance of the heat pump system is measured in Coefficient Of Performance (COP) as that is the ratio of work done to the energy supplied. In refrigeration cycle, either in heating or cooling mode, the COP is always greater

than one, but ASHP with defrost cycle COP can be less than one. The drop in performance can be accounted for the energy consumed to defrost the heat exchanger exposed to the outside air. The ranges of COP for practical application are around 3 to 5; the output is 3 to 5 times the power input to the compressor [6]. As shown in Figure1, these heat pumps with external energy input, cause the heat to flow from a lower temperature region to higher temperature region, which is the refrigeration unit that is being used other way round as heat pump system. The use of heat pump technology is not new, in 1852 Lord Kelvin developed the concept and Robert Webber was then modified as a GSHP in the 1940s. During 1960s and 1970s these heat pumps gained commercial popularity.

1.1 Ground temperature variations

Earth's temperature is relatively constant after certain depth throughout the year and increases as it goes further in depth. GSHPs utilise the relatively constant temperature of the Earth to provide heating and cooling. Figure 2 shows typical monthly outdoor temperature variations in Erzurum, Turkey between October 2005 and May 2006. This shows that mean temperature is around -10°C and max around 10°C for winter and summer respectively.

It is observed in the following Figure 3 that ground temperature is very much dependent on the air temperature [7]. At -10°C to 10°C outside temperature, the ground temperature is varying from -5°C to 8°C from months 1 to 5 for a depth of 5 cm. The variation at much greater depth of around 100 cm, the variation is ranging from 5°C to 10°C .

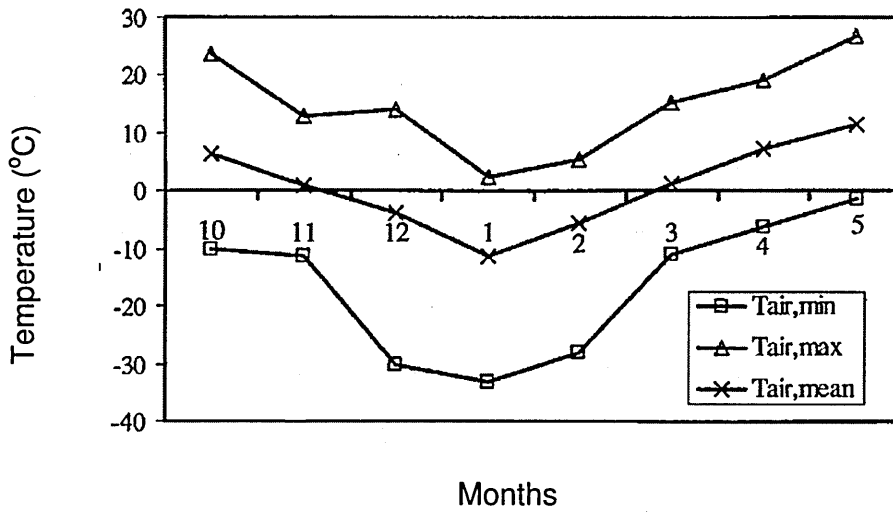


Figure 2 Monthly variation of outdoor air temperature from October 2005 to May 2006 for Erzurum, Turkey

It is evident that the ground temperature very much depends on the outside air temperature for certain depth [7]. . It is almost linear to the temperature outside and is resilient for small changes.

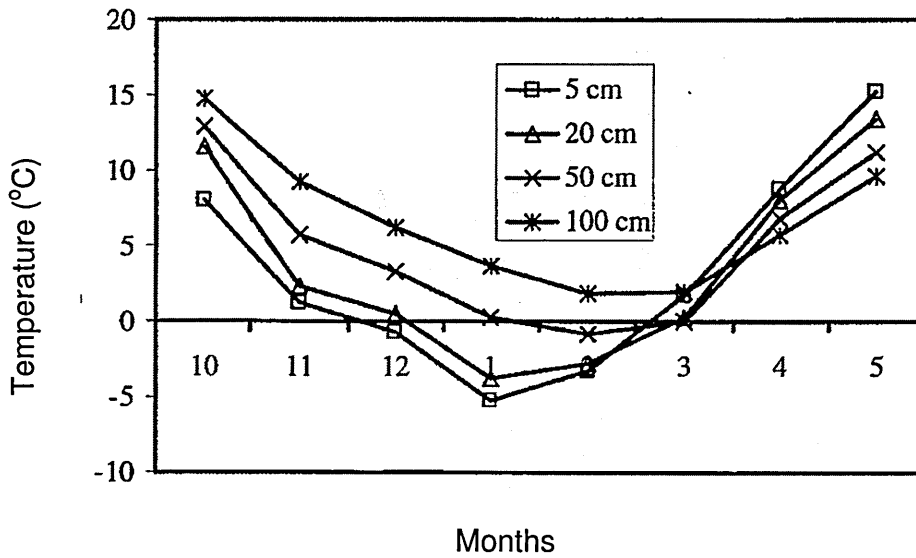


Figure 3 Monthly variation of mean ground temperatures at several depths from October 2005 to May 2006 in Erzurum, Turkey

As the depth increases, temperature increases and eventually stabilises around constant value for greater depths and is no more affected by the outside air temperature.

As the heat is absorbed from the ground, high thermal inertia of the ground makes the temperature of the surrounding ground decrease very slowly. Before the temperature further drops, energy from the surrounding ground is extracted. This very nature of the ground makes it possible to use it as the infinite reservoir for heat exchange.

Below Figure 4 shows the temperature of the ground is nearly constant after certain depth the variations are shown from summer (August) and winter (January) in Nicosia, Cyprus [8]. It is evident that earth temperature is nearly stabilised to a constant value after certain depth irrespective of the geographical locations.

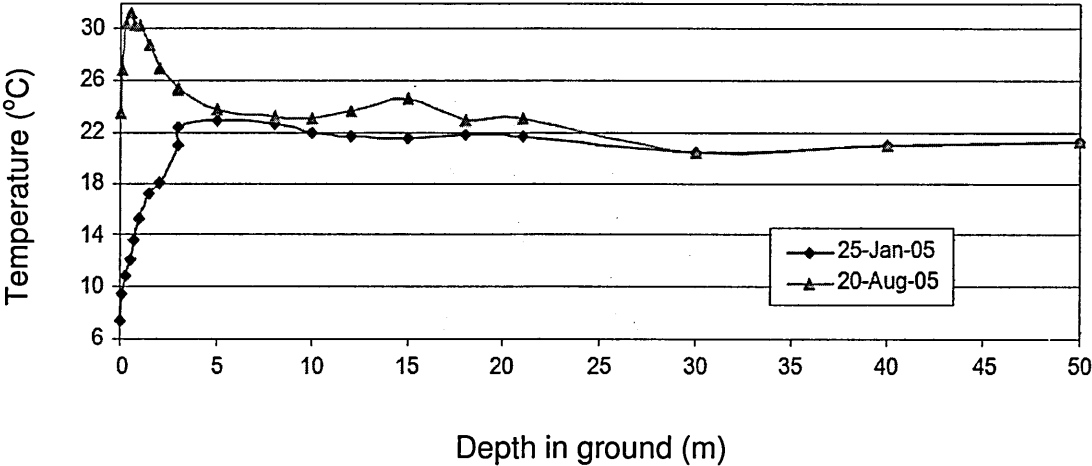


Figure 4 Temperature variations with depth of ground

1.2 Types of GSHP configurations

1.2.1 Open loop systems

In this system the water from the wells or ponds is used directly to add or reject the heat to the primary loop heat exchanger in the system. The water from the secondary loop is pumped back to the well or pond again. The cycle uses fresh water each and every time it exchanges heat from the primary loop.

1.2.2 Closed loop system

In this system the secondary loop which carries the water or glycol exchanges the heat with the source (water or ground) on one side and with primary loop on the other side. The primary loop is the main system loop of the heat pump system which involves compressor, condenser and evaporator and throttle valve. The water in the secondary loop is re circulated.

1.2.2.1 Horizontal trenches (Closed loop)

Horizontal trenches are made for the pipes to be laid usually at 1-3m deep underground. The area of the ground required depends on the heating capacity of the building, but usually it is also dependent on the space availability and it requires large area when compared to vertical borehole types. Below Figure 5 shows the arrangement of the system [5]

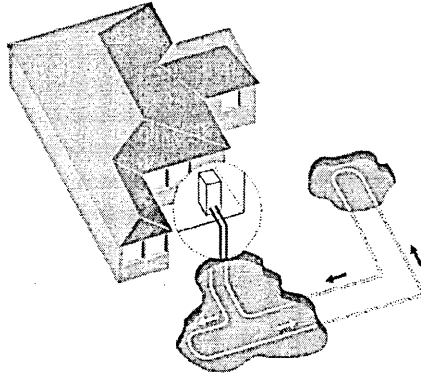


Figure 5 Horizontal closed loop heat pump system

1.2.2.2 Slinky coil horizontal system (Close loop)

Slinky coil system is another type of arrangement of horizontal loop systems, pipes are laid in coil shape on the horizontal trench rather than the straight pipe. This increases the surface area of the pipe for the given length of the trench laid hence it increase the heat transfer process. The overlapped looped pipes can be 30 to 60% shorter than the traditional horizontal types and cheaper to install [9].

Following Figure 6 shows the general arrangement of the slinky coil system [9]

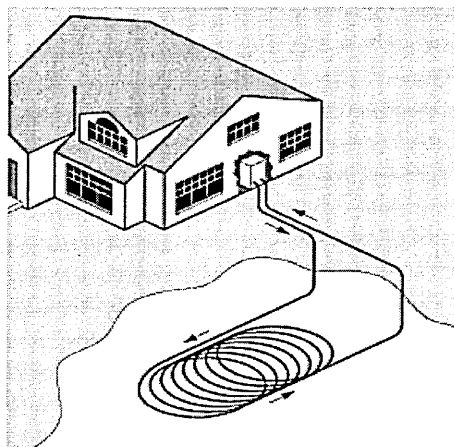


Figure 6 Horizontal closed loop slinky coil system

1.2.2.3 U- tube vertical boreholes (Closed loop)

On the other hand, vertical borehole type configurations are widely used because of the space restrictions [4]. Vertical borehole types or the U-tube as they generally called as require 30- 50% less tube length compared with horizontal types for the same thermal loading, due to effect of high temperature at different depths [10]. The borehole depths of up to 200m are being used for these types of arrangements. Below Figure 7 shows the arrangement of vertical borehole system [5]

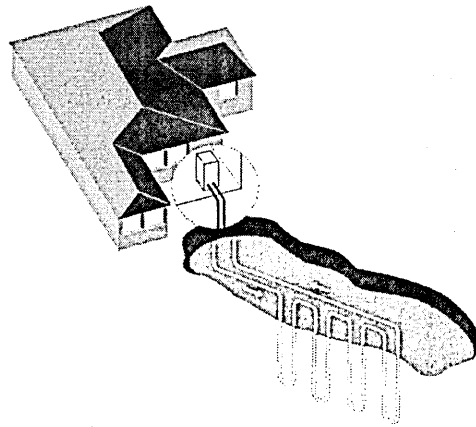


Figure 7 Vertical U tube closed loop heat pump system

1.3 Cost comparison

The choice of different configuration is influenced by the cost associated with each type. Following Figure 8 gives the capital costs for different configurations for ground to water heat pump systems [11]. The investment on the coil for the vertical system is more when compared to the horizontal system. On the other hand it saves on the length of ground coil required for the same capacity as explained earlier. Vertical drilling costs more compared to the horizontal trenches.

System Type	Ground coil Costs (£/KW)	Heat pump Costs (£/KW)	Total system Costs (£/KW)
Horizontal	250-350	350-650	600-1000
Vertical Indirect	450-600	350-650	800-1250

(Costs include installation and commissioning but exclude distribution system)

Figure 8 Capital costs for different configurations

Direct exchange systems

It is the simple cycle in which the refrigerant from the heat pump is directly circulated in the copper tubes buried in the ground. The heat is directly exchanged between the refrigerant and the ground which in contrast to the secondary loop containing water or antifreeze solution to exchange the heat with the indirect heat pump system. This avoids the secondary loop; copper being good conductor of heat, heat transfer rate is higher compared to the conventional pipes. It requires copper tubes for greater length and more quantity of refrigerant for circulation makes it expensive.

1.4 Typical Heat pump cycle operation

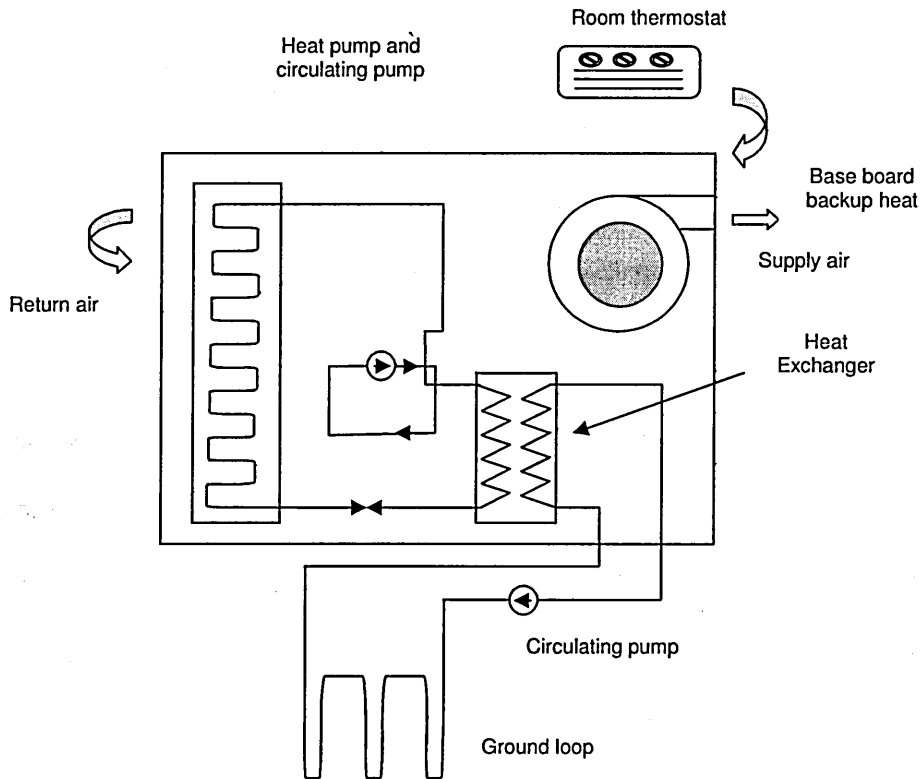


Figure 9 Typical Heat Pump Unit

GSHP system consists of three systems loops as shown in Figure 9 a ground loop, a refrigerant loop, distribution loop and optional domestic hot water loop [5] ground loop circulates the water in to the ground and extracts the heat, then enters the refrigeration loop where it exchanges the heat with the refrigerant. The cooled water will then enter the ground loop; hence the water keeps circulating in the same loop. The refrigerant loop once getting heat from the ground water will evaporate; the compressor then compresses the refrigerant vapour. The compressed high temperature refrigerant enters the condenser and loses the heat by heating the water in the distribution loop. The condensed refrigerant is

then expanded in the throttle valve before entering the evaporator. The heated water in the distributed loop will be circulated in the building for heating purposes.

In cooling the building for summer conditions, the heat is absorbed by the cold water in the distribution loop and transferred to the relatively cold refrigerant in the evaporator. The evaporated refrigerants are then compressed in the compressor and make its way to condenser to loose heat to the ground loop circulation water. Warm water in the ground loop rejects the heat to the relatively cold surrounding ground and it re-circulates again for the next cycle. The refrigerant after loosing heat in the condenser, pass through expansion valve and enters the evaporator to absorb heat from the distribution loop and this cycle repeats.

1.5 Role of GSHP in reducing CO₂ emissions

Properly sized and installed GSHPs have shown significant CO₂ reductions compared to conventional fossil fuel boilers, in the UK context with the current power station mix, 1kWh of electricity emits 0.43kg of CO₂[12]. At a Seasonal Performance Factor (SPF) of 3.8, this can lead to overall CO₂ reductions in excess of 40% compared to a 'natural' gas boiler. For gas grid, the CO₂ savings against oil, LPG, coal or direct electric heating, the CO₂ emission savings are even higher [6]. In the context of the Stern review, it is now interesting to 'cost' carbon savings. Figure 10, extracted from a UK government report tabulates the relative costs and outputs of different renewable energy technologies. The final row of the table makes interesting reading for GSHPs. The existing capacity of the GSHPs is much less in comparison with the solar thermal energy generation. Capital cost of the

solar photovoltaic system is much higher than the ground source heat pump; it is a clear choice for the other systems to be replaced with GSHP.

Over the last few years, GSHPs have gained significant popularity, especially in the domestic market. Ease of maintenance and reasonable pay back period with impressive savings of the energy bills makes it a more viable alternative than the conventional systems.

	Existing Capacity	Capital Cost £/kW	kWh/yr per kW	Pay back (years)	Saving Tonne CO ₂ /yr Per kW	Saving kgC/yr /£1000CAP EX
Solar PV	8MW	6300	750	120	0.32	14
Micro-Wind	-	2500 – 5000	1700	30	0.7	47
Solar Hot water	35MW 70,000 Installation	1250 – 2000	1000	80	0.2	54
GSHP	5MW 600 Units	1000 – 500	3000	15 - 20	0.4	91

(Source: UK DTI report-Renewable Heat and Heat from Combined Heat and Power Plants-2005)

Figure 10 Comparison of several renewable energy techniques

From Figures 10 & 11 significant reduction in CO₂ emissions can be achieved by using GSHP systems. Figure 11 shows the relative fuel costs of the different technologies, as well as the CO₂ savings. All heating and hot water supplied by the heat pump, at an affordable cost, is a very satisfactory outcome. The table has to be evaluated for each country and region to be relevant.

Annual fuel cost to run the GSHP system is very low compared to all the other systems. The interesting fact remains that the emissions is the lowest among all the conventional methods.

System	Annual Fuel Costs	Annual CO ₂ Emissions (tonnes)
GSHP	£215	1.6
Natural Gas (Condensing Boiler)	£300	2.9
Natural Gas (Non-Condensing)	£345	3.3
Liquid Petroleum Gas (Bulk-Non-Condensing)	£500	4.3
Liquid Petroleum Gas (Bottle-Non-Condensing)	£670	4.3
Oil (35 sec) (Non-Condensing)	£300	4.4
Direct Electric-Storage and Panels With night time Low Cost Tariff	£510	6.5
House Coal	£380	6.6
Smokeless Coal	£515	7.5

(House =100m²-12500KWh/yr as per SAP 2001)

Figure 11 Comparison of fuel costs and CO₂ emissions for GSHPs and fossil fuel Boilers

The following Figure 12 shows the Kg of CO₂ emissions for KW of energy produced [13]. It is very clear from the table that GSHP is the lowest producer of emissions compared to the other conventional and non-conventional methods of heating .It is evident from the following figure that GSHP performs 50% better than the ASHP. One more advantage being, the ground temperature is relatively constant for all the seasons; hence the system can maintain its performance all year around.

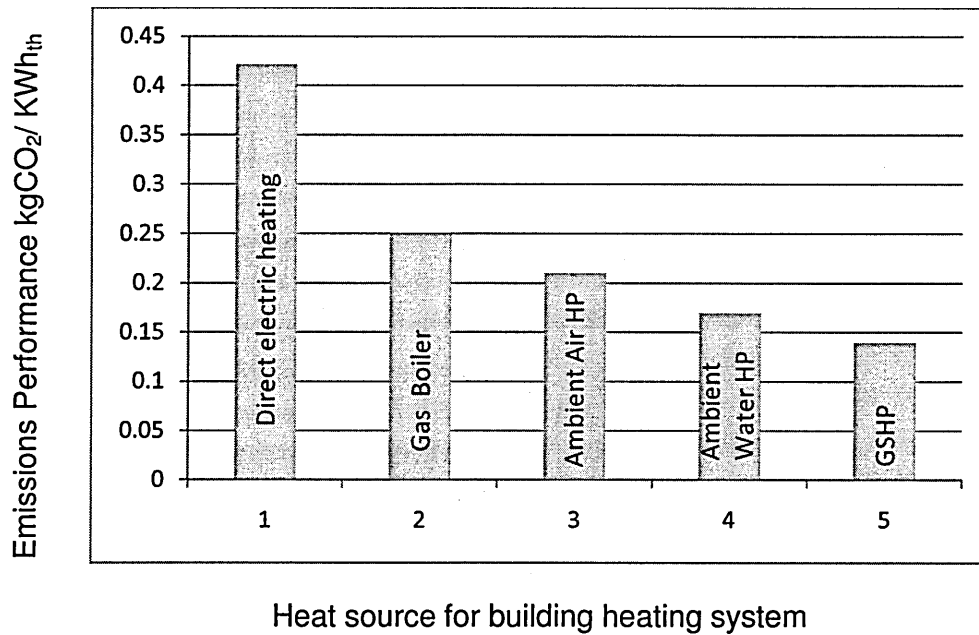


Figure 12 Comparison of carbon dioxides emissions from GSHPs and other forms of heating

1.6 Methodology

Calculating annual building loads as well as long-term ground thermal response for the demand, multi-year simulation is an invaluable tool in the design and development of GSHP systems [14]. Predicting the performance of GSHP for varying underground thermal properties, temperature and heating requirements has been a difficult task. GHE operates with various dynamically operating parameters, this gives an opportunity to study and improves its effectiveness, so as to improve the performance of the whole system. It has to operate with varying parameters such as load, soil temperature, configurations, thermal properties of ground and soil condition. Since the pipe is buried in the ground, it is a difficult task to calculate the thermal resistance between the borehole surface and pipe external surface. The configuration of the pipe and deep ground characteristics adds to the complexity of the resistance measurement. A method to calculate

thermal resistance has been introduced by Kavanaugh et al [15, 16] in which a pipe represented as a hollow cylinder with effective radius by assuming that the external surface of the pipe is completely in contact with borehole surface.

The work of Eskilson [17] presents the methods based on non-dimensional thermal responses for thermal interference between boreholes for multiple borehole systems. These functions are computed numerically and the values are given for various configurations of the pipes in the borehole. There have been a number of models based on some analytical solutions suggested by Ingersoll [18] and Hellstrom [19], but these models used oversimplified approaches to treat the boreholes for short time behaviour. In many design programmes, the time of interest is in the order of months or years. Boundary element method to calculate thermal resistance in the grout has limited use for simple, straight-line flows, which are practically not common. There are many programmes available for evaluation of GSHP systems [20]; these tools only deal with a peak load and for simple or basic heat exchangers.

This work is undertaken to develop a hybrid model combining analytical and numerical solution techniques known as Computational Fluid Dynamics (CFD) to predict the performance of GSHP and to identify the critical parameters, which governs the COP of the heat pump by considering response of changes in the load and the temperature difference between the room and the ground. The use of CFD techniques in thermal analysis and turbulence modelling is widely gaining popularity in design and research of heat exchangers [21].

Having gained much popularity, CFD deals with some limitations; it is difficult to calculate the response for longer time of the ground and associated climatic conditions. In order to deal with the climatic conditions over the year, a powerful mathematical tool called MathCAD is used to develop the model of the borehole along with the pipe. Performance evaluation is carried out for steady state conditions by assuming the temperature on the outer surface of the grout as an initial start. The simulations are also carried out for changing temperature of room, ground, surface area of the grout and other varying parameters to observe the effect on COP of the system.

From Fourier's law, heat conduction without the temperature gradient indicates the material having no resistance to heat transfer or having infinite thermal conductivity. Practically existence of these condition is clearly not possible, however such condition is never be satisfied exactly. Such conditions can be approximated, considering the resistance to the conduction within the solid is small or negligible compared to the resistance to heat transfer between the solid and its surroundings [22].

The temperature from the outer surface of the tube is modelled for Logarithmic Mean Temperature Method (LMTD) for temperature distribution to the circulation fluid. LMTD is the logarithmic average of the temperature difference between the hot and cold sides of the fluid at each end of the exchanger. The larger the LMTD, the more heat is transferred

Incropera et al. [22] shows that the steady-state average fluid temperature is the average log mean difference defined by LMTD.

$$\Delta T_{lm} = \frac{|\Delta T_{out}| - |\Delta T_{in}|}{\ln\left(\frac{\Delta T_{out}}{\Delta T_{in}}\right)} \quad \text{----- (1)}$$

Where

ΔT_{in} and ΔT_{out} are the fluid temperature variations, at the inlet and outlet, with respect to the ground temperature (i.e. $\Delta T_{in} = T_{in} - T_g$) and T_g is the grout temperature. This method is more accurate compared to the generally used average temperature method which generally over predicts the temperature.

1.6.1 Use of CFD and MathCAD

The CFD model is used for calculating the overall thermal resistance of the borehole by fixing the temperature on the surface of the grout. Previously the attempts were made to calculate the thermal resistance of the borehole by using Boundary Element Method (BEM) [20]. Here Finite Volume Method (FVM) does the simulation. This method is more accurate since it integrates the residuals over the entire domain before reaching the next iteration. This method converges quickly and is more reliable compared to the boundary element method which consumes both time and memory.

In this analysis, a 50 meter pipe is modelled with single u tube surrounding the grout. The geometry and the properties of the complete system are obtained from the manufacturer's handbook. Convergence is obtained for the values given in the

published data; this model is used as a reference model for varying parameters. The temperature on the surface of the grout is varied along the length to observe the outlet temperature variations. To improve the model, different geometries and material properties were suggested.

Each subsystem is represented by a set of equations and assembling each subsystems represents the complete system. Simultaneous equations were solved in MathCAD for the convergence and compared with the published data to validate the model. The overall heat transfer coefficient from the CFD model is used to verify the temperature variations and compared with published data, this represent the complete system hybrid model.

1.7 Research objectives

To build the whole system model in MathCAD and use the operating conditions for the model from the published data as input, to create a reference model. Once the reference model is created the system is checked for the stability by changing predefined variable and to look for change in the solution. If the unique solution exists, the variables calculated will converge at the same value and with negligible or no residuals.

Then the initial guess for the variables to be calculated is changed and checked for the residue so that the convergence is achieved. This process gives the affect of variables on the system performance. The procedure is repeated for different

values of material properties, flow rate, inlet water temperature to the GHE and area of grout.

The results were analysed and the key parameter which affect the performance are identified. The CFD model of the GHE is modelled and solved for the same boundary conditions used for the MathCAD model to calculate the thermal resistance of the GHE. The CFD results are analysed for temperature and velocity distribution in water and temperature distribution in the grout material and pipe. It also gives the surface heat transfer coefficient which can intern used to calculate the thermal resistance. The results were analysed and discussed at the end and necessary conclusions were drawn. Finally future scope for the model analysis is discussed.

1.8 Block diagram of the project

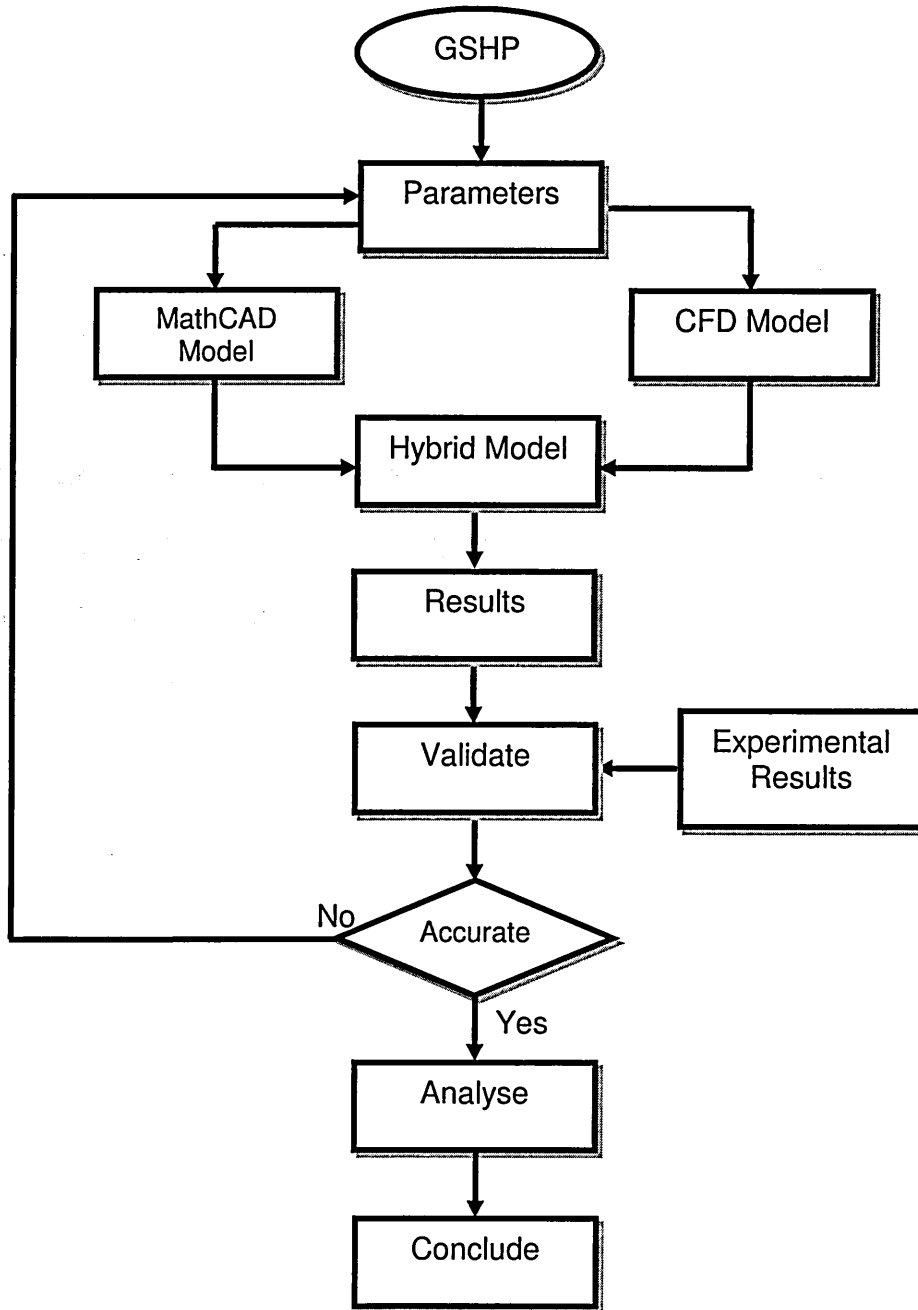


Figure 13 Flow chart for the project

Above Figure 13 shows the steps followed to complete the cycle of the project. The analytical model developed in MathCAD is compared with the experimental values published. The key parameters are identified and the bench model is

created. The CFD model of the GHE gives additional information of the overall heat transfer resistance of the heat exchanger. The final model is validated against the published data. The results are discussed and the necessary assumptions are made and discussed as appropriate.

Conclusion

The purpose of this first chapter has been to introduce the full scope of the project and define the main objectives for such a study. It gives brief introduction about the work to be carried out to build hybrid system. These remains centred upon how ground heat has become important to study and evaluate as an important alternative energy resource.

Chapter 2

Introduction

The purpose to this section is to establish a working definition and framework for the GSHP and its potential toward becoming a primary energy saving system. A literature review acts a framework from which the analysis can be conducted and continue towards further development of GSHP. Further exploration is needed in order to build a foundation toward understanding new energy heat sources, which may work better toward 'green' initiatives. Methodologies use do model ground, thermal loading and environmental variables which affects the ground thermal storage, developed by different authors has been discussed. Building hybrid model in MathCAD and CFD has been outlined. Assumptions made for the modelling and its limitation due to complex working nature have also been discussed.

2.1 Literature Review

Until 1980's not much significance was given to the ground thermal storage systems. Growing demand for the green energy initiative has given significant rise, since then much work is done in geothermal energy extraction techniques.

One of the projects such as Metropolitan housing trust head quarters in Nottingham, UK has invested in greener energy initiatives. Major research work and development of GSHP technology with innovative applications such as hybrid GSHP systems and development of environmentally-friendly refrigerants are being carried out across many universities in the UK [23, 24]. The major deriving force in this research is to identify technologies that may be utilised by industries in the

commercial market to strengthen GSHP's competitiveness at the global level [25]. Countries such as US, Canada, China, South Korea installed and successfully operating the GSHP systems for industrials and domestic applications.

A geothermal heat pump can transfer heat stored in the earth into a building during the winter, and vice versa during the summer. GSHPs are increasingly becoming popular due to their reduced primary energy consumption and there by reducing emissions of greenhouse gases. The technology is well established and adopted in USA and Europe.

A typical heat pump require 100kWh of power input to turn 200kWh of freely available environmental or waste heat into 300kWh of useful energy [26]. This saving of 200kWh correspondingly reduces the emissions of harmful gases such as carbon dioxide (CO_2), Nitrogen oxides (NO_x) and Sulphur dioxide (SO_2).

Approximately the total number of globally installed GSHP-systems sums up to about 12,000 MW_{th} [27]. This as almost equalling to the total number of global systems estimated around 1,100,000 units, of all the GHE types available, it was found that vertical closed loop type contribute to 46% of the systems and horizontal closed loop type contribute to 38% in USA alone, while the remaining are open loop systems [28]. In the last two to three decades, significant research has gone in to relating the effect of properties of ground, pipe and grout material on the performance of the GHE system. The goal being optimisation of the heat transfer mechanism and installation method used for the given ground type. Kavanaugh [29] suggested, during steady state operation the maximum expected

thermal power is 50–80 W/m. For vertical GHE's one or two U tubes per bore hole is the most commonly used configurations. The sizing of the GHE depends on the load, thermal and physical properties of the soil such as thermal diffusivity, density, specific heat capacity, thermal conductivity, etc. Thermal conductivity of the tubing, grout material and the ground temperature plays important role in designing of the GHE system. For typical ground conditions, Pahud and Matthey [30] suggest 50 W/m thermal power to be considered in designing a GHE, with ASHRAE [31] as also confirming around the same value. Taking into account, however; the parameters such as:

- The thermal loading on the building is not a steady state condition
- The time required by the GHE to reach steady state condition is comparatively longer due to its high thermal inertia. It is estimated around 30 tonnes of soil per m² of building area is required for heating and cooling operations.
- System is used alternatively for both heating and cooling purposes, it is important to consider the energy sustainability in the ground in response to the change in working nature of the heat pump system.

The critical parameter in designing the vertical system is the thermal power per meter of borehole that the GHE can handle [32]. With this mind, it is important to test the performance of the system with following equations.

2.1.1 Coefficient of Performance (COP)

According to the first law of thermodynamics, in a reversible system we can show that

$$Q_{\text{hot}} = Q_{\text{cold}} + W \quad \text{-----(2)}$$

and

$$W = Q_{\text{hot}} - Q_{\text{cold}} \quad \text{-----(3)}$$

Where

Q_{hot} = heat given off by the heat reservoir (Watts)

Q_{cold} = heat taken in by the cold heat reservoir (Watts)

W = Work input (Watts)

Therefore, substituting for W from the definition of COP,

$$\text{COP}_{\text{heating}} = \frac{Q_{\text{hot}}}{Q_{\text{hot}} - Q_{\text{cold}}} \quad \text{-----(4)}$$

For a heat pump operating at maximum theoretical efficiency (i.e. Carnot efficiency) it can be shown that

$$\frac{Q_{\text{hot}}}{T_{\text{hot}}} = \frac{Q_{\text{cold}}}{T_{\text{cold}}} \quad \text{-----(5)}$$

and

$$Q_{\text{cold}} = \frac{Q_{\text{hot}} T_{\text{cold}}}{T_{\text{hot}}} \quad \text{-----(6)}$$

Where

T_{hot} = Temperature of the hot reservoir ($^{\circ}\text{K}$)

T_{cold} = Temperature of the cold reservoir ($^{\circ}\text{K}$)

Hence, at maximum theoretical efficiency,

$$\text{COP}_{\text{heating}} = \frac{T_{\text{hot}}}{T_{\text{hot}} - T_{\text{cold}}} \quad \text{----- (7)}$$

Similarly, for cooling

$$\text{COP}_{\text{cooling}} = \frac{Q_{\text{cold}}}{Q_{\text{hot}} - Q_{\text{cold}}} = \frac{T_{\text{cold}}}{T_{\text{hot}} - T_{\text{cold}}} \quad \text{----- (8)}$$

It can also be shown that $\text{COP}_{\text{cooling}} = \text{COP}_{\text{heating}} - 1$.

Note that these equations must use the absolute temperature, such as the Kelvin scale. $\text{COP}_{\text{heating}}$ applies to heat pumps and $\text{COP}_{\text{cooling}}$ applies to air conditioners or refrigerators.

Although COP can never be remotely approached in practice to the theoretical values, it is useful as a reference to indicate important influencing factors. It is evident that the COP increases as the temperature difference between the condenser and the evaporator decreases.

The $\text{COP}_{\text{system}}$ can be calculated from the following equation

$$\text{COP}_{\text{system}} = \frac{Q_{\text{sr}}}{W_{\text{in}} + W_{\text{pumps}} + W_{\text{fan}}} \quad \text{----- (9)}$$

Where,

$\text{COP}_{\text{system}}$ = COP of the whole system

Q_{sr} = Cooling Load (Watts)

W_{pumps} = Work input to the circulating pumps (Watts)

W_{fan} = Work input to the fans (Watts)

W_{in} = Work input to compressor (Watts)

For engines, efficiency is the general term in use for which values for actual systems will always be less than these theoretical maximums.

2.1.2 Ground Heat Exchanger (U tubes)

Vertical ground loop exchanger typically consists of High Density Polyethylene (HDPE) pipe U-tube as shown in Figure 14 inserted in to 50 meter deep vertical borehole drilled in the ground [33]. The borehole has a diameter of 150mm and a polyethylene pipe of 32mm internal diameter with 4mm thickness is used to circulate the water for the ground circuit. Circulating water in the pipe absorbs the heat from the refrigerant in the heat pump and rejects the heat to the ground on the other side or vice versa

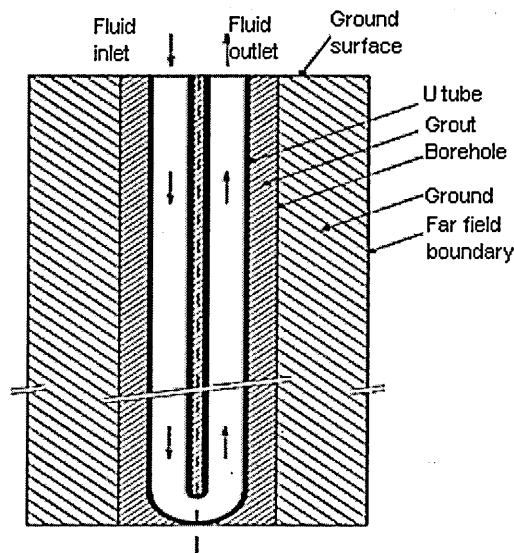


Figure 14 Vertical U-tube in symmetry plane

Once the U-tube is inserted in to the borehole, the rest of the gap between the U-tube and the borehole is filled with grout mixture. The very purpose of the grout being used is to improve the heat transfer between the soil and plastic pipes by providing a better contact surface and also to provide a seal around the U-tube to prevent against the contamination in the ground water system. For this very reason, the maintenance is nearly zero for such systems.

2.1.2.1 Configurations of ground tubes

There are basic configurations which are generally used are shown in 15 & 16 [8]

Single U pipe	Double U-Pipe
Pipe diameter = 25-32 mm	Pipe diameter = 25-32 mm
Width 50-70 mm	Max. Width= 70-80 mm

Figure 15 Basic configurations of Vertical U tubes

Simple Coaxial	~ ~ ,
External Diameter = 40-60 mm	Max. Width = 70-90mm

Figure 16 Basic configurations of vertical U tubes

The ground heat exchanger is the closed vertical type (U-shaped) and generally has 24-30 boreholes of depth ranging from 50- 175 m in depth depending on the load requirement. The distance between the boreholes generally maintained around 5 m. Thermocouples measures subterranean temperatures in the ground located at 1.5 m and 2.5 m away from the outer surface of the heat exchanger. Ground temperature might be varied with the temperature of the ground heat exchanger [34]. Ground temperature distribution may vary with different surface cover (such as bare ground, lawn, and snow), two different locations for example, bare land and grass lawn has been selected to measure the temperature distribution in the ground at different depths [35]. Cu-Konstantan thermocouple wires and thermocouple meters SR60 (Stanford Research System, USA) were used by POPIEL et al [36] to measure the temperature at different time intervals. Survey suggest that because of the complexity of acquiring the physical properties of ground and surface boundary conditions, simple empirical formulas such as for example formula proposed by Baggs [37,38] is commonly used.

For studying the heat transfer phenomena in transient condition most models uses step response for the heat transfer rate. Superimposing principle allows the final solution to be the form of convolution of these individual step contributions [39].

2.1.2.2 Effect of air temperature ground circulating water

Figure 17 shows evolution of daily averaged subterranean temperature at the depth range from 2.5–30 m and outdoor temperature measured during March 21–September 30, 2007 [34]. The ground is influenced by the outdoor air temperature till the depth up to 5 m,. However, it has no influence below 10 m depth and the

temperature of the ground was observed to keep constant around 16°C regardless of the abrupt change in the outdoor temperature

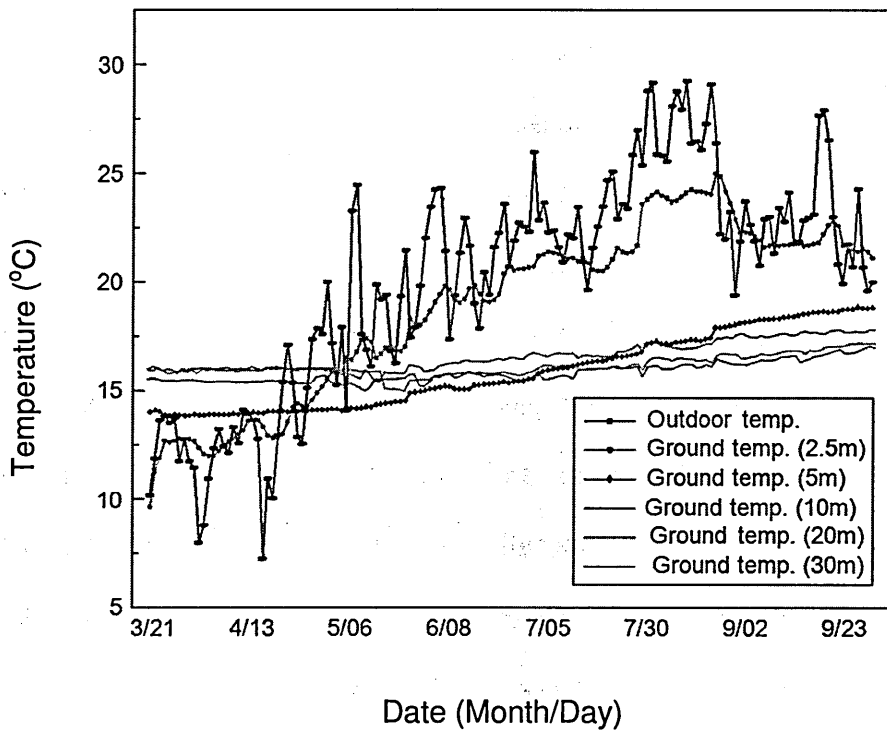


Figure 17 Evolution of daily average subterranean temperature and outdoor air temperature

Figure 18 shows the outside air temperature, average temperature of circulating water, the surface temperature of the ground heat exchanger at 1.5 m and 2.5 m away from the ground heat exchanger at the depth of 10 m [34].

As the outdoor temperature increased, the temperature of circulating water was increased up to 22 °C. This gives the indication that the cooling load increased as the outside air temperature.

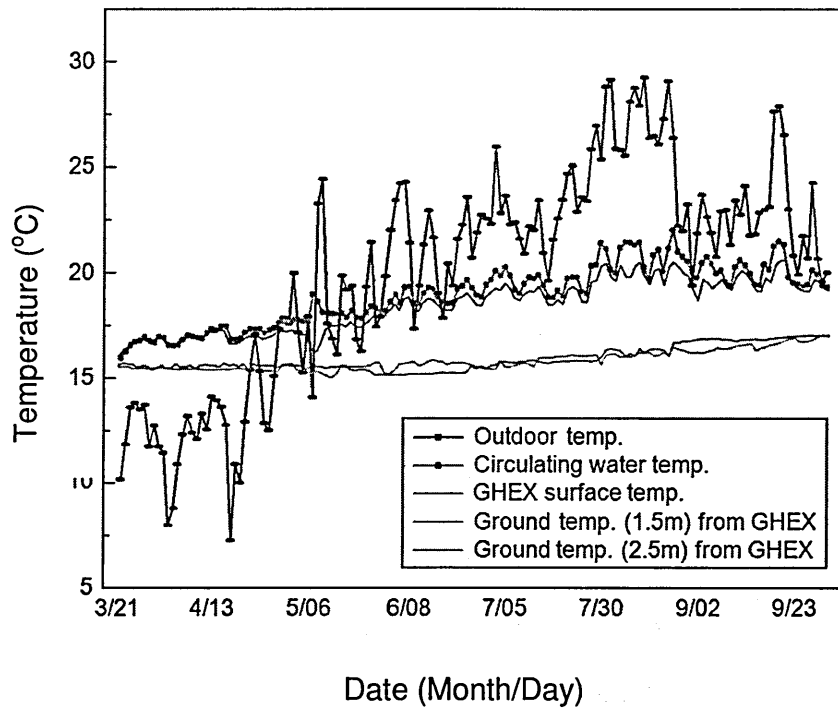


Figure 18 Evolution of daily average temperatures of outdoor air, circulating water, surface of ground heat exchanger

It can be seen that the temperature of circulating water strongly affected the surface temperature of the ground heat exchanger. The temperature of the ground appeared to be constant regardless of circulating water temperature at 1.5 m and 2.5 m away from the surface of the heat exchanger.

2.1.3 Condenser and evaporator

The heat balance and the heat exchange from the water circulating in the pipe is analysed in the water to refrigerant heat exchanger at the condenser side of the heat pump. Plated Heat Exchanger (PHE) is assumed to be used in the calculation. Plated heat exchangers are the natural choice for flexible chillers and climate control applications for its high effectiveness, versatility and ease of maintenance. Its advantage is its ability to offer full performance at both full and

half load. PHE is mainly made of thin, corrugated alloy plates held in a carbon steel frame, each plate is separated by a gasket to avoid leakage. Plates are arranged in a manner to make flow channels by the arrangement of the gasket pattern and the ports of each corner of the plate acts as a header for the main flow line.

It has a major advantage over a conventional heat exchanger in that the liquids spread out over the plate. This facilitates the transfer of Heat, and greatly increases the speed of the temperature change. In a PHE plates are generally arranged in such a way that it forms channels of hot and cold liquid alternately. Due to corrugations in the plate, high turbulent flow increases the heat transfer rate.

As compared to Shell & Tube heat exchanger, for the same amount of heat exchange the size of the PHE is small, because of the large heat transfer area afforded by the plates. Expansion of the heat transfer area is possible in PHE just by adding the number of corrugated plates. These types of heat exchangers are widely used in district heating and cooling especially where the heat transfers between two-phase liquids. Since the refrigerant in the condenser is partial mixture of gas and liquid the selection of such heat exchanger is valid.

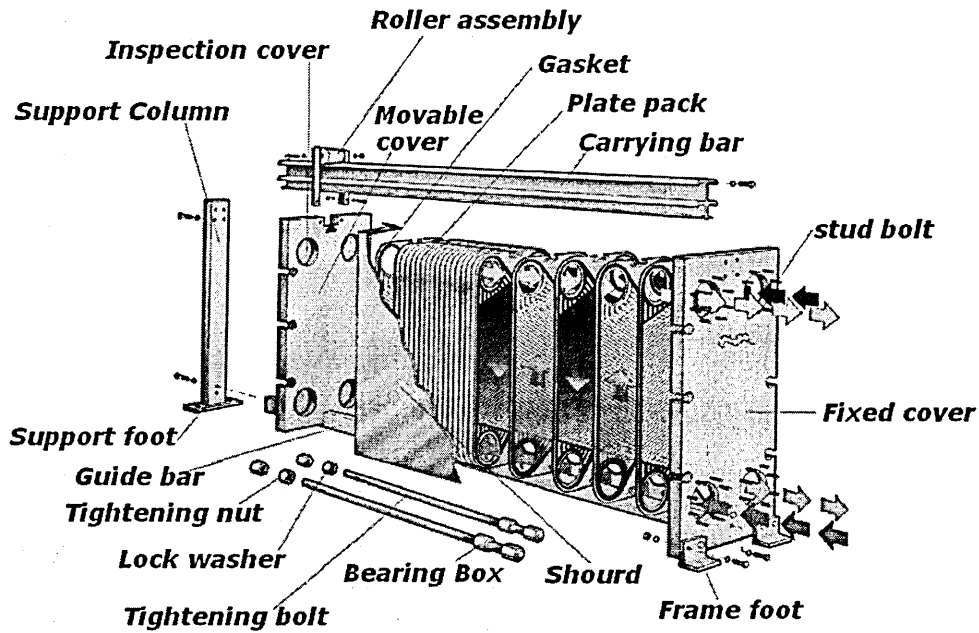


Figure 19 Typical Plate Heat Exchanger

Above Figure 19 gives the arrangement of the heat transfer between the warm water and relatively hot refrigerant or vice versa in case of evaporator [40]. Heat transfer in the condenser and evaporator occurs at phase change of the refrigerant; hence the temperature of the refrigerant is constant (latent heat transfer). The amount of heat transfer is calculated by taking the enthalpy change with the mass flow rate of the refrigerant.

2.1.4 Methodologies used to model the Heat Pump System

The equations developed earlier to represent the heat pump are based on the assumption of one-dimensional flow, which were replaced by two-dimensional models during the 1990s and three-dimensional systems during recent years. Models have been devised in three dimensions but it seems one-dimensional approach remains the best for heat transfer. Finite difference methods have been

extensively used to take account of thermal conductivity and heat flow in the ground surrounding the grout.

Borehole thermal resistance bears strong impact on the GHE performance. This is defined by the thermal properties of the construction material used and the arrangement of flow channel of the water pipes in the ground. The common methods for heat transfer in the semi-infinite medium from a perpendicular buried infinite cylinder were the cylindrical source and the line source solutions. While the cylindrical source solutions assume steady heat flux on the boundary of the borehole into the surrounding medium, the line source solution is based on the steady release of the heat of constant strength through an infinite line [40].

The thermodynamic analysis for the performance characteristics of the GSHP systems with U-tube ground heat exchanger for heating can be considered with mass, energy, entropy and exergy balance relations. It has been shown that the performance can be evaluated by energetic and exergetic aspects [41]. In thermodynamic analysis of energy systems, exergy analysis is proven to be a powerful tool. Exergy is calculated by setting a reference environment. It is used to detect and quantitatively evaluate the cause for the thermodynamic imperfection in the thermodynamic process. But only an economic analysis can decide the expediency of a possible improvement. The results of the exercise shows that the uncertainty analysis needed to prove the accuracy of the experiments [42]. According to Kavanaugh and Rafferty [43] energy performance of the system is also influenced by the pumping energy required to circulate the fluid through the heat pump and the ground loop. In the design of GSHP systems, Kavanaugh and

Rafferty [43] suggested the guidelines for pumping power for commercial GSHP systems. The values shown in Figure 20 is proposed as a benchmark for measuring the effectiveness of a pumping efficiency and piping system design for a minimum of 0.162m³ /h per KW of cooling, with optimum pumping flow rates ranging from 0.162 to 0.192m³ /h per KW of cooling [44].

Watts Input		Performance Efficiency	Grade
Per Tonne	Per KW		
≤ 50	≤ 14	Efficient Systems	A:excellent
50-75	14-21	Acceptable systems	B:good
75-100	21-28	Acceptable systems	C:medium
100-150	28-42	Inefficient Systems	D: poor
> 150	> 42	Inefficient Systems	E:bad

Figure 20 GSHP System pumping efficiently required pumping water to cooling capacity

2.1.4.1 Ground temperature variation modelling

Determining the temperature in the ground is a transient and complicated process. Over the past few years significant work has been done to develop algorithms to simulate the temperature inside the ground surrounding the pipe and heat carrier fluid in GHE. Developed algorithms should be tested against the experimental work to validate the calculation results. Reports are available relating to the comparisons made for various other simulation models [45]. Several field experiments and analysis of GSHP systems with multiple GHE designs are also developed [46, 47].

Below 21 shows the earth temperature is nearly constant far away from the outer surface of the pipe [48] Solar assisted GSHP is operated alternatively for a period 24 h with and without solar power for an interval of 4 hours of operation. The effect of the solar assist on the temperature distribution around the pipe is negligible. The ground seems to be more resilient in temperature for loading and unloading conditions.

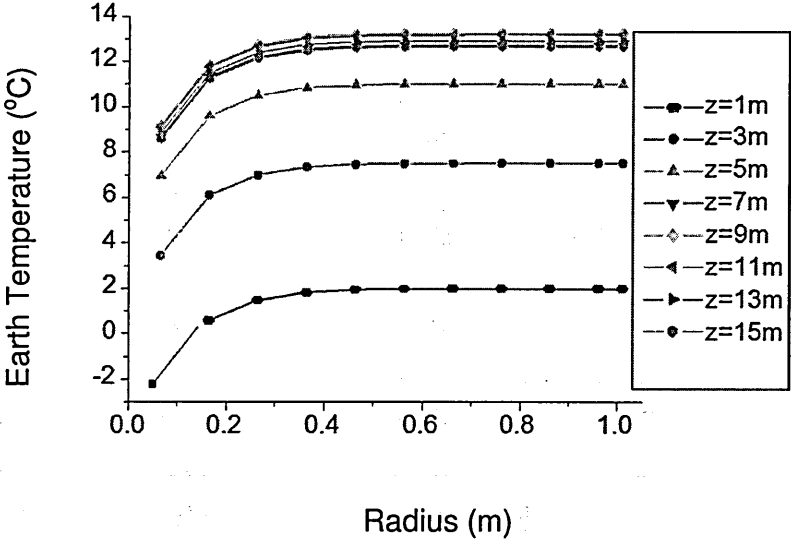


Figure 21 Earth temperature distribution surrounding buried coil at different depth after 4 hour operation of GSHP

Below figure 22 shows the temperature of the earth decreases near the outer surface of GHE as the operation time increases and seems not affected at far distance [48]. Its give the clear idea that because its thermal inertia, system should be operated intermittently in order to extract the temperature from the ground.

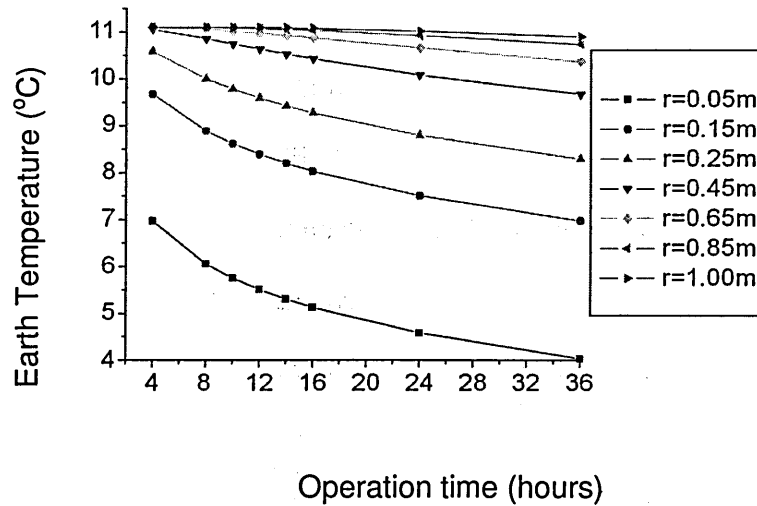


Figure 22 Earth temperature variation with the operation time of GSHP at a depth of 5 m for different radius

Investigation on narrow channel models is becoming more important lately. Research work on wide diameter ratios was carried out at significant levels. It is observed that heat transfer characteristics of narrow annuli are different from conventional channels. Measurements were carried out for heat transfer coefficients in a narrow channel for a mercury flow [49]. Experiments conducted to calculate heat transfer coefficient at the inner wall of concentric annuli with wide diameter ratios for turbulent flow was suggested [50]. It can also be seen that the choice of diameter ratio has an effect on the convective heat transfer coefficient. The Finite Element Model (FEM) developed to simulate natural convection and heat transfer around the annulus is interesting to observe how parameters such as flow rate and temperature can affect the heat transfer coefficient [51]. It is shown that the extended algebraic turbulence model is important for predicting flow pattern and wall heat transfer coefficient at transitional Rayleigh numbers [52].

On the basis of works conducted before, it can be observed that there is an affect on the heat transfer mechanism on the geometry of the pipe

2.1.4.2 Thermal loading on the borehole

Simulation conducted by C K LEE et al [53] shows the importance of loading on the performance of the system in which loading is done on the borehole with temperature profile for steady state condition. The temperature in the ground and temperature profile on the borehole is greatly influenced by the initial loading temperature profile. Figure 23 shows with constant load for single borehole, neither of the borehole temperature and borehole loading was constant along the length of the borehole. This shows that the single finite difference scheme is not sufficient to estimate the performance by superposition.

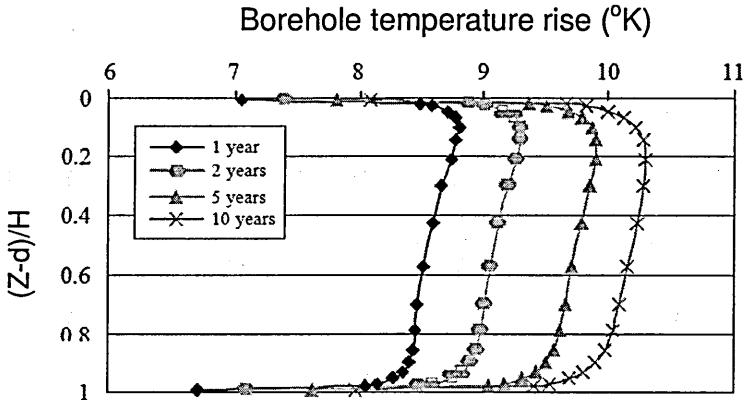


Figure 23 The borehole temperature rise profiles at different times

Where,

d= depth of borehole top from ground surface (m)

H= length of borehole (m)

z= Distance along the length of borehole (m)

It is evident that the temperature raise is very little over the years. At least for 10 years it shows that the system is very resilient.

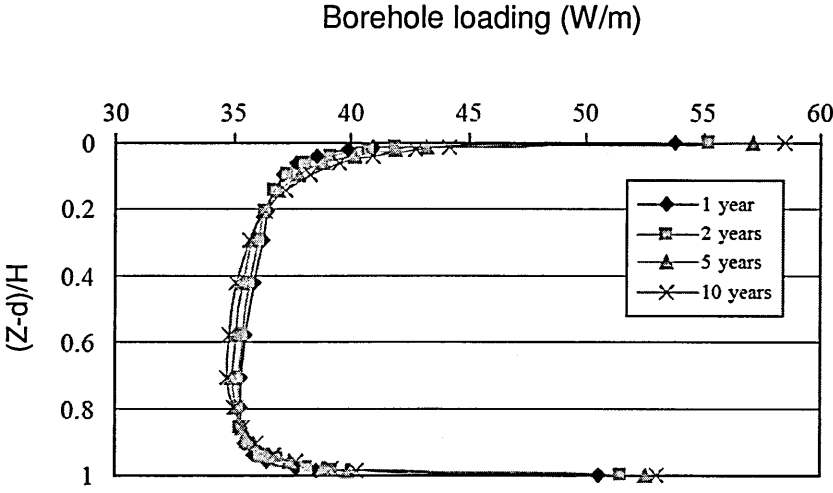


Figure 24 Borehole loading profile against a dimensionless parameter $(z-d)/H$ (with value one at bottom and zero at borehole top)

From Figure 24 it was found that neither the temperature nor the loading was constant along the borehole. Borehole temperature is maximum at the top if finite line source model is used. Then the loading is decreased till bottom end this could be assumed that the mean fluid temperature inside the borehole decreased with depth.

By assuming no thermal resistance between tube and surrounding soil, the heat flux can be calculated by temperature difference between inlet and outlet of GHE and mass flow rate of heat carrier fluid. Figure 25 shows considering convective resistance and conduction in pipe material, temperature at the outer surface of the

tube can be calculated which is the average temperature of inlet and outlet of GHE

[54].

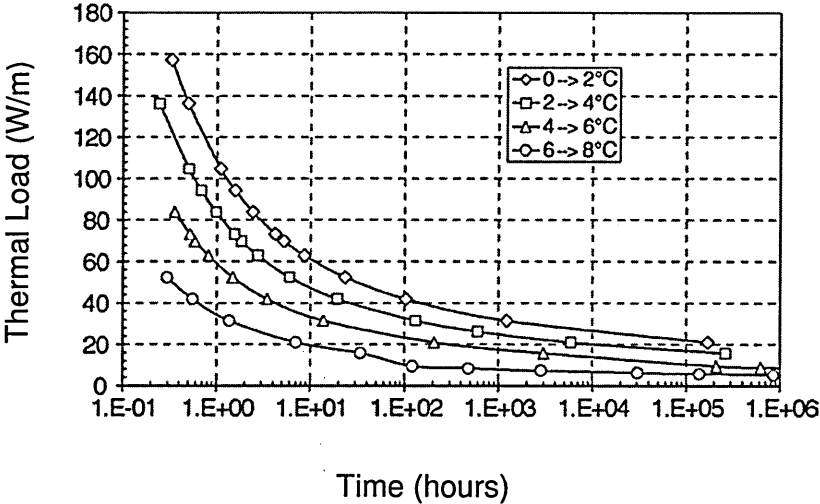


Figure 25 GHE thermal load as a function of the load duration with the inlet and outlet temperatures of water at 10°C initial ground temperature

The time for which GHE can provide a constant heat flux at maximum load which is used in the calculation can be determined.

The initial ground temperature was taken from 10 to 30 °C, the water temperature difference between GHE inlet and outlet was kept at 2 °C. Results shown in Figure 25 and Figure 26, for areas with milder climate the representative ground temperature is around 20 °C.

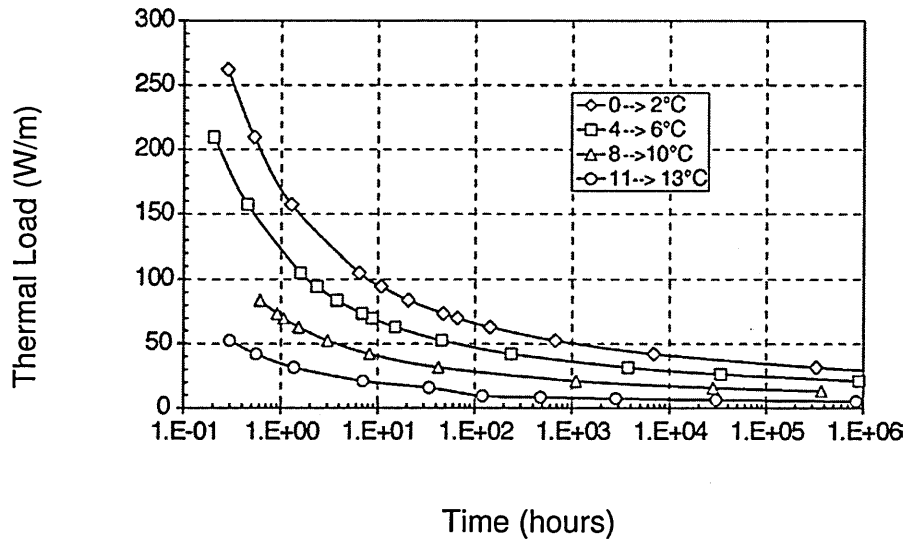


Figure 26 The GHE thermal load as a function of the load duration with the inlet and outlet temperatures of water as parameter 15°C initial ground temperature

it can be seen that for cold climates at 10 °C, GHE is capable of covering loads up to 140 W/m for 1 h, but as in initial literature it was suggested to use 50 W/m corresponds to steady-state operation.

The ground heat exchanger and heat pump systems are used both for heating and cooling. It can be understood that the initial ground temperature of 10°C is very low, this might be due to the additional heat absorbed from the ground during the heating period.

2.1.4.3 Heat transfer modelling of GHE

Sizing of GSHP depends on the ground thermal conductivity, capacity and the borehole thermal resistance. One popular method to estimate the thermal parameters is the interpretation of in situ thermal response tests.

The modelled response is average temperature which is calculated as

$$T_m = \frac{T_{in} + T_{out}}{2} \quad \text{----- (10)}$$

Where

T_m = average temperature of the fluid (°K)

T_{in} = fluid inlet temperature (°K)

T_{out} = fluid outlet temperature (°K)

Mean fluid temperature (T_m) calculated from above equation often deviates from the actual fluid temperature. By the use of three dimensional finite element model it shown that the mean temperature values are different from those used from the equation 10. This intern overestimates the thermal resistance and has economical impact on the system design. Another approach to approximate the temperature is suggested by Marotte et al [55] is a P-linear method. This method gives nearly accurate results with the numerical solution. The method followed is explained below the effective borehole resistance R_b .

$$R_b = R_{pipe} + R_{grout} \quad \text{----- (11)}$$

$$R_{grout} = \left(\frac{1}{S_b K_{grout}} \right) \quad \text{----- (12)}$$

$$R_{pipe} = R_{cond} + R_{conv} \quad \text{----- (13)}$$

$$R_{cond} = \left(\frac{\ln \left(\frac{D_o}{D_i} \right)}{4\pi K_{pipe}} \right) \quad \text{----- (14)}$$

$$R_{\text{conv}} = \left(\frac{1}{2\pi D_i h_i} \right) \text{-----(15)}$$

Where , D_i = inside pipe diameter (m)

D_o = are the and outside pipe diameter (m)

h_i = inside film coefficient

K_{grout} = grout thermal conductivity (W/m K)

K_{pipe} = pipe thermal conductivity (W/m K)

R_{cond} = resistance to conduction (K m/W)

R_{conv} = resistance to convection (K m²/W)

R_{grout} = grout thermal resistances (K m/W)

R_{pipe} = pipe thermal resistances (K m/W)

S_b = shape factor defined as



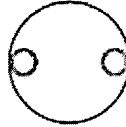
$$S_b = \beta_o \left(\frac{d}{D_o} \right)^{\beta_1} \text{-----(16)}$$

Where,

d = borehole diameter (m)

β_o & β_1 are geometrical parameters function of the U-tube's position in the borehole.

Following figure gives the shape factors for three different positions of a single U-tube in the borehole [55].

Coefficient	Pattern		
			
β_0	14.4509	17.4427	21.9059
β_1	-0.8176	-0.6052	-0.3796

S1: U-tube legs are close to the borehole centre, S2: intermediate case, S3: U-tube legs are close to borehole wall.

Figure 27 Shape factors for three different positions

When the heat flux is constant for the length of borehole the mean fluid temperature is equal to fluid temperature. However, this assumption is not entirely accurate.

Heat transfer in a borehole especially in the turbulent region where the propagation is quick, Marcotte et al [55] derived a numerical relation. The measured inlet and outlet temperatures and volume integration within the pipe give average temperature of the fluid (T_{num}). For simplicity resistance for convection is assumed to be zero and for the other boundary conditions assumed, the results for numerical and line-source solution were matched perfectly. Figure 28 shows the numerical model predicts exactly as the line source model [55].

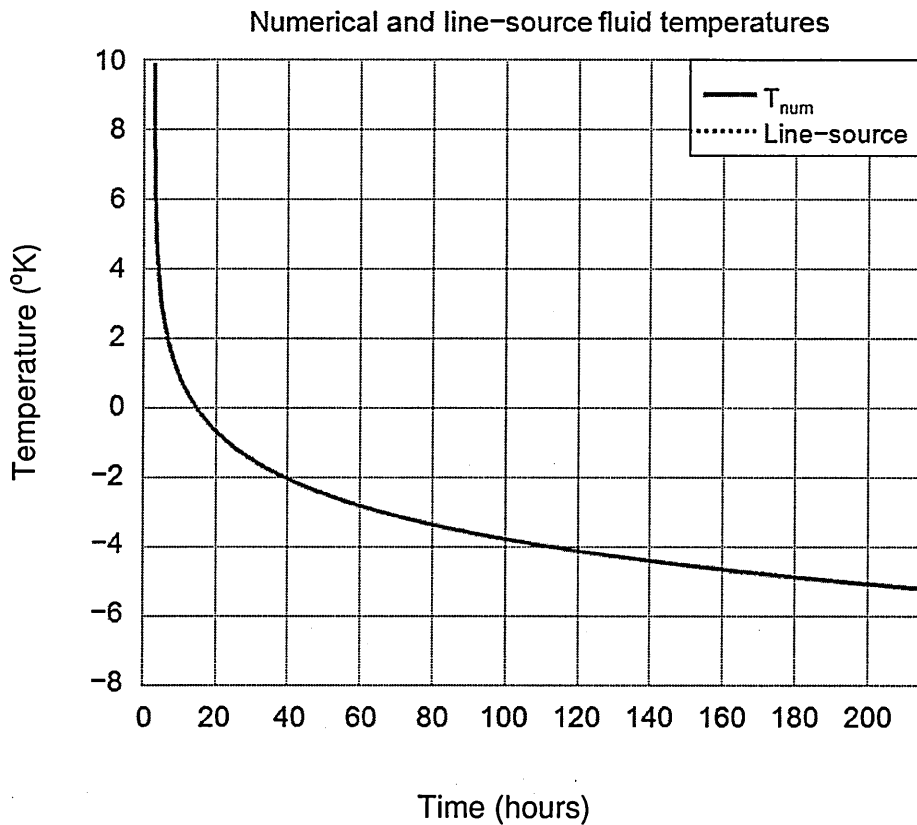


Figure 28 Mean fluid temperature: numerical and theoretical line-source solution

The scope of such models remains in the numerous use as many combine ground heat conduction and heat exchangers. It is important that predictions in heat extraction and injection rates should be accurate in promoting heat pump systems. The research field of heating, building ventilation and air coolant systems remain on the cusp due to these models. The only problem is that many analytical models extract data that remains inconclusive in their forecast especially for long term because they remain framed by the thermal conduction model. This model utilises the cylindrical coordinate system and sometimes the equivalent diameter model. For the purpose of further understanding these correlations, a numerical model is proposed because this model consider the heat transfer with ground flow. FEFLOW [56] proposed a calculation method to estimate the distribution of temperature and to calculate heat transfer rate between GHE and its surrounding

ground. In this method finite element model of the system for heat flow and fluid transport in the ground is simulated, which has attracted wide interest in analysis of ground water flow. The above model is based on the conservation of mass, momentum and energy to represent soil particles, liquid water and gas trapped in the ground. Fiji et al [57] used above model to study the FSHP's for dynamic working conditions for under eater and heat transport modelling.

Yujin et al [58] has developed the model of the ground heat exchanger considering the water pipe with 1-dimentional advection diffusion equation and convective heat transfer between the circulating water and the inner surface of the heat exchanger pipe. Figure 29 shows heat flux Q from the ground surface to ground is given by the following heat balance equation [58]

$$Q = R_{sol} + R_{sky} - R_{surf} - H_{surf} - L_{surf} \quad \text{--- (17)}$$

Where,

R_{sol} = total solar radiation

R_{sky} = Downward atmospheric radiation

R_{surf} =Upward long wave radiation from the ground surface

H_{surf} = Sensible heat flux

L_{surf} = Latent heat flux

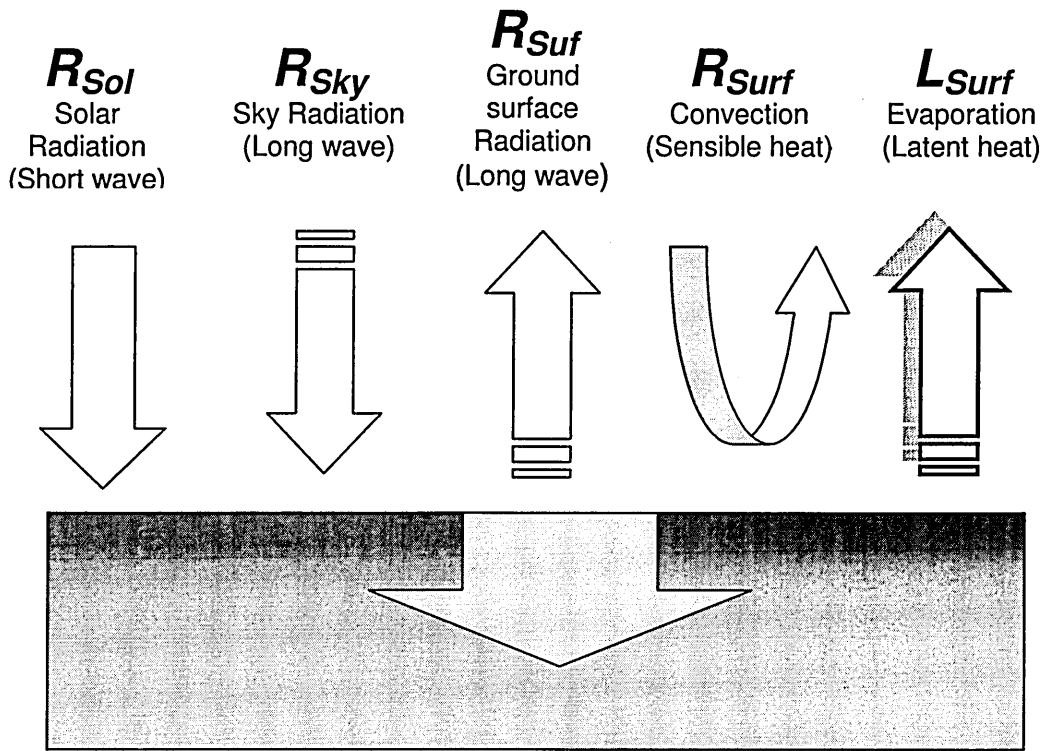


Figure 29 Thermal balance on ground surface

It is important to understand in the thermal analysis of soil the concept and effect of hydraulic conductivity or permeability on the performance [58]. It is also necessary to determine the thermal properties of soil for heat transfer analysis, such as soil conductivity and specific heat (volumetric). Most numerical model on GSHP is based on the principle of conduction. The temperature response of circulating fluid in single U- tube GHE for constant heat flux on the outer surface of the pipe is suggested by Austin et all [59]. Literature reveals that experimental formulations are available to estimate permeability of saturated soil. The overall heat transfer mechanism gives the temperature effect which couples all sub components the system. The temperature of the ground has significant effect on the performance. It is observed that during heating cycle, the increase in the source temperature has positive effect on the COP of the system while it has

negative effect on COP in cooling cycle [52]. The curve, which best fits the data at both the conditions is shown below.

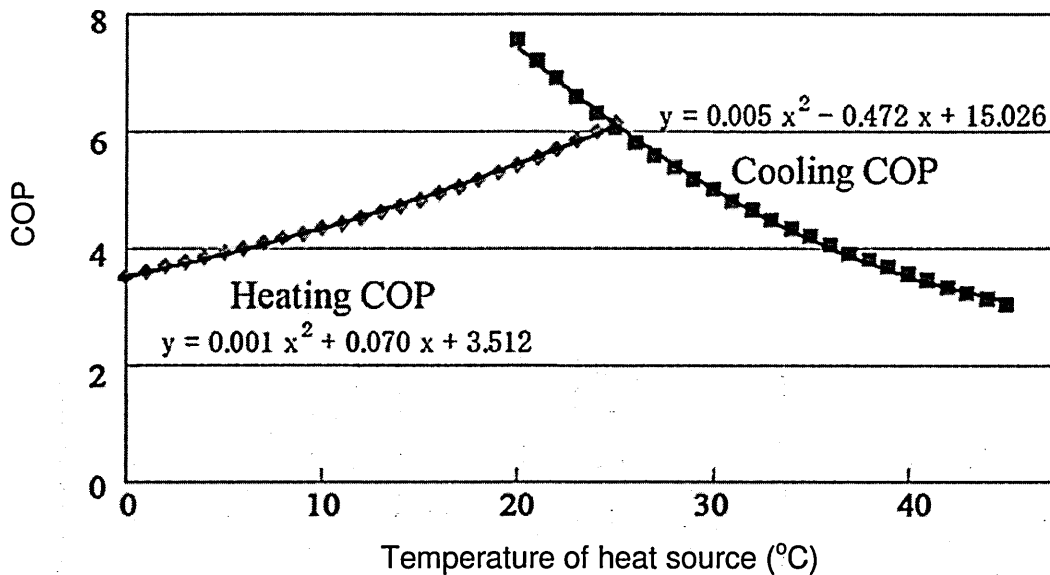


Figure 30 Variation of COP with increase in the temperature of heat source

2.1.5 Development of GSHP

over the past few years more work has gone in to the development of GSHP especially in understanding the influence of soil properties in the heat transfer process[60-63]. Saturated soil can be treated as a porous medium with aquifer without significant flow at under ground water level. It is high in permeability because of porous nature makes it to model as porous medium. In Europe and in America extensive studies were made since 80's. Studies shows that the GSHP performance is largely affected by thermal performance of the ground an efficiency of GHE [64, 65]. Down hole heat exchanger is developed in order to greatly improve heat transfer between GHE and the soil [66]. to better understand heat transfer characteristics of GHE earth probe model is developed [67]. As discussed earlier, the effect of ground water flow for a colsed loop system under the aquifer

with wide range of flow were analysed [68]. Moisture content in the soil can effect the performance, this work is modelled in three dimension for the ground surrounding GHE and heat exchanger and results were analysed [69]. Numerical algorithm called AUTOTOUGH was developed to simulate the performance between single U-tube and double U-tube shape pipes [70].

Thermal short circuiting between the legs of the U-tubes and axial convective heat transfer can have any effect on the heat transfer process [71]. However it is assumed that there is no conduction outside the borehole or the thermal resistance of the ground (porous medium) is neglected. This show from academic stand point there is lot of work needs to be done to understand the complex heat transfer mechanism for different soil types. Understanding of long-term time factor and the considerations of short time steps [71] is also important factor to model long term analysis. Similarly other methods for different time steps were also analysed [72,73]. Finite volume method model for U-tube heat exchanger with borehole is modelled to understand heat transfer mechanisms have been proposed [74]. However these numerical methods i.e FVM and FEM developed with considerable assumptions and does not reflect the complex nature of the system. These models works for short time durations, to simulate for all year models these models consume computing time and resource. On the other hand analytical model are easy to comprehend and difficult to solve without assumptions.

Kavanaugh [75] proposed the method developed in cylindrical solution for the heat transfer around the GHE as exact solution. Line source model assumptions are

the analytical solutions described by Ingersoll [76] and Jaeger [77] for cylindrical source solution. Both models are based on the assumptions of infinite borehole length for steady state condition. Above models proposed are in the form of line source solutions, but the integrals appeared in the solutions were modelled and analysed in exponential form by Igshpa and Cleland [78, 79].

However, above all surveys depend on the simplified models which still make some realistic assumptions to solve complex problems. With this information about the background work it gives opportunity to build the whole system and solve for the temperatures which couples all individual subsystems in GSHP system. Solving all equations simultaneously gives the understanding of the parameter which affects the COP of the whole system and also to analyse the critical parameters.

2.1.6 Refrigerant

Selection of the right type of the refrigerant is important for the range of the operating parameters. Much of the research has gone into developing new, nature friendly refrigerants and refrigerant mixtures without losing the significance of the performance of the system. R134a is a single Hydro-Fluorocarbon Compound (HFC) and is generally used for many applications from automotive to industrial refrigeration. R410a is a binary blend of HFC compounds 50% of R32 and 50% of R125. All the refrigerants are scale based on the Global Warming Potential (GWP) or the potential for ozone depletion better known as Ozone Depletion Potential (ODP). The GWP is a measurement that is usually measured over a 100-year period. This measurement can reflect how much a refrigerant can contribute to global warming when compared to carbon dioxide. CO₂ has a GWP = 1.0 potential

rate. The lower the value of GWP, the better the refrigerant is for the environment. ODP also reflects the potential of the single molecule of the refrigerant that has the destroying capacity of the ozone layer. All refrigerants use R11 as a datum reference, where R11 has an ODP = 1.0. The smaller the value of the ODP, the better the refrigerant is for the ozone layer and the environment.

Common refrigerants with corresponding values of ODP and GWP are given below:

Refrigerants	ODP	GWP
R11 (obsolete)	1	4000
R22 (obsolete)	0.05	1700
R134a	0	1300
R410a	0	1725

Figure 31 Refrigerants with ODP and GWP values

Creating a model for the refrigerant cycle has been a challenging task, development of algorithms and computational techniques has helped to an extent for understanding. This represents nearly accurate behaviour of the cycle. From the survey, it is found that the many authors have derived the means to fit the curve with standard coefficients at the saturation liquid and at saturated vapour regions.

2.1.6.1 Refrigerant cycle

A typical refrigeration cycle can be explained by the following figure. Following figure 32 shows the temperature and entropy relation of the cycle [22] and Figure 33 shows pressure enthalpy relationship for the complete cycle. Saturated vapour is compressed (W_{in}) isentropically in the compressor (process 1-2) and it leaves at the superheated state. It rejects the heat (Q_H) the condenser at constant pressure (process 2-3).

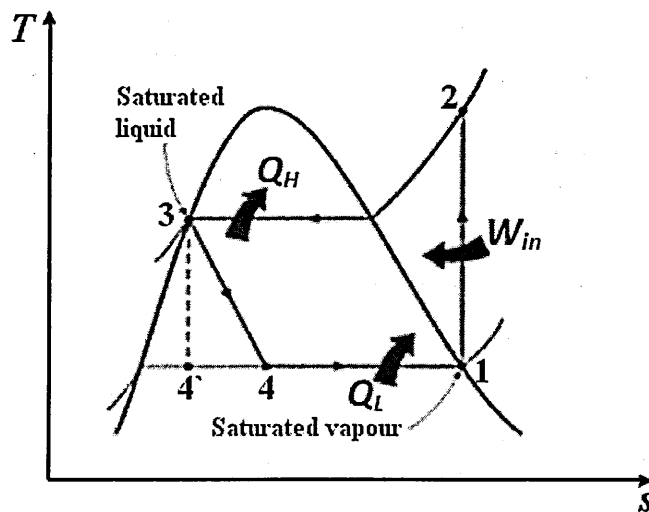


Figure 32 Temperature entropy diagram for refrigerant cycle

The refrigerant leaves the condenser at saturated liquid state and it is made to pass through the throttle valve where it expands at constant enthalpy (process 3-4). At reduced temperature and pressure, it enters the evaporator it absorbs heat (Q_L) and evaporates and enters the compressor at saturated point (Process 4-1) and the cycle repeats.

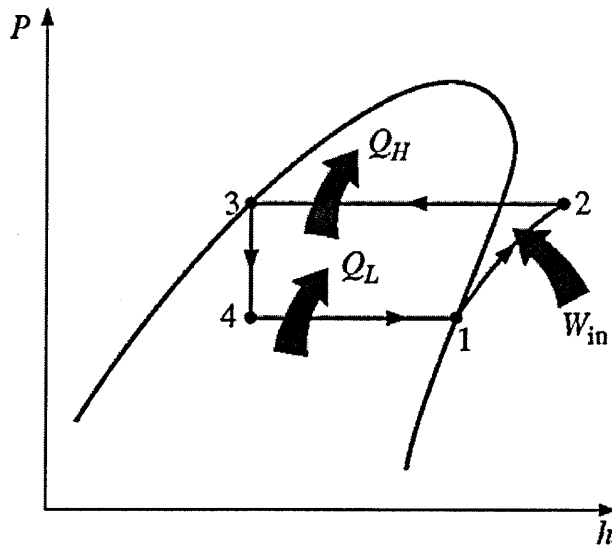


Figure 33 Pressure enthalpy diagram for refrigerant cycle

2.1.6.2 Temperature and pressure relation for refrigerant R 143a

Temperature and the pressure relations for R143a are given by A C CLELAND [79]

$$P_{\text{sat}} = \exp\left(21.51297 - \frac{2200.9809}{246.61 + T_{\text{sat}}}\right) \text{ ----- (18)}$$

$$T_{\text{sat}} = \left(\frac{-2200.9809}{\ln(P_{\text{sat}}) - 21.51297}\right) - 246.61 \text{ ----- (19)}$$

Across the full range of applicability ($-40^{\circ}\text{C} \leq T_{\text{sat}} \leq 70^{\circ}\text{C}$) at largest difference of P_{sat} from the source data is 0.46%, with the refrigerant application operating in the range of ($-30^{\circ}\text{C} \leq T_{\text{sat}} \leq 50^{\circ}\text{C}$) the largest difference is 0.22%.

The polynomial curve fit for saturated specific volume for R143a is given by

$$v = \exp\left(-12.4539 + \frac{2669.0}{273.15 + T_{\text{sat}}}\right) * (1.01357 + 1.067368 * 10^{-3} * T_{\text{sat}} - 9.2532 * 10^{-6} * T_{\text{sat}}^2 - 3.2192 * 10^{-7} * T_{\text{sat}}^3) \quad \text{----- (20)}$$

The method of CLELAND et al [79] uses the equation for ideal gas reversible compression process but replaces the ratio of specific heats with a curve fitted factor.

$$\Delta h = \frac{c}{c-1} \left[P_1 v_1 \left(\frac{P_2}{P_1} \right)^{\frac{c-1}{c}} - 1 \right] \quad \text{----- (21)}$$

Where

c = polynomial with constant coefficients

The saturated temperature or pressure is calculated by the given pressure or temperature during the experiment. Assuming the isentropic compression process in the compressor, the superheated vapour refrigerant enthalpy can be obtained if the exit pressure is known. Similarly the superheated temperature is known because of the isentropic compression and the superheated enthalpy can be calculated.

For most practical purposes, the condenser exit state of the refrigerant is assumed to be saturated liquid and hence the state of the refrigerant can be calculated on

the saturated region. Since the throttling process is the constant enthalpy process, the exit state of the condensed liquid is obtained on the P-h diagram of the refrigerant.

For many applications reasonably accurate evaluations are made for the thermodynamic properties of the refrigerant. Increasing number of algorithms rely on accurate information of refrigerants properties for each step for better approximation of the complex thermodynamic process. ease of programming adds another challenge to evaluate thermodynamic properties and algorithm calculation itself. Monte [80] has developed theoretical concept to evaluate thermodynamic properties of tow refrigerant mixtures of hydro fluorocarbon (HFC) R407C and R410a in the super heated region .Martin-Hou equation for state has been modelled for a long time response for pure HFC e g R134a with reasonable good accuracy. R407a and R410a have been fully investigated and well understood refrigerant. The analytical results were not considered for other factors, such as compressibility factor, isentropic and isothermal compressibility, volumetric expansively, etc are fully understood. This gives accurate refrigerant end temperature for isentropic compression. This also reflects the work exchanged or volumetric efficiency. Gas compressibility effect works in favourable role in isentropic compression. This allows work done to be reduced 10% for refrigerant 134a and refrigerant mixtures 407a and 410a. On the other hand it plays unfavourable role to reduce the compressor volumetric efficiency i. e refrigerant mass flow rate and consequently cooling and heating capacity of the vapour compression system.

This work is carried out to develop the steady state condition model to simulate the system with constant air and ground temperatures with fixed power input to the compressor. The configuration of the ground heat exchanger is the standard U-tube with grout surrounding the pipe. Assuming the ground is the infinite source or sink, constant surface temperature is used in the model simulation. Ground temperature, Air temperature and the work input to the heat pump varies each time to get the system response.

2.1.7 Scope and limitations

The literature survey above shows that the scope is endless for the complexity of the model to be analysed. It is limited by the capability of the algorithm, feasibility and the variations of the parameters for the range of operating conditions. However, it gives the scope for engineers to develop the near accurate model of the physical system for all weather, loading and geothermal conditions which will be a real challenge for the engineers for the years to come.

Performance parameters of heat exchanger design calculations are generally considered for steady state condition. It is general custom to prescribe temperature or heat flux at fluid wall interface on the other hand only energy equation has to be solved for the analysis. The results thus obtained only good to find out heat transfer flows bounded by wall having very small thermal resistance. However, in practical applications thermal boundary conditions are different from the once used for the analysis. The constant temperature or flux conditions will only work with some degree of accuracy. Line source model can not incorporate GHE modelling within few hours when compared to numerical solution because of line source model assumptions. Experiments for cooling and heating mode can be

conducted for short time period with proper assumptions comparisons show reasonable accuracy is maintained between numerical and experimental results. It can be observed that numerical model with proper assumptions can simulate GHE for short time scale.

2.1.8 Computational Fluid Dynamics (CFD)

In early 1980's anyone stepped in the history of aeronautics, where the major thrust was always been to fly faster and higher, never realised that one day that will be a reality. CFD made many such events possible with its computing techniques capable of solving complex and time varying problems. CFD is a numerical method of solving partial differential equations by finite volume (FV) approach, it acts as a communicator between the theory and the experiments [81].

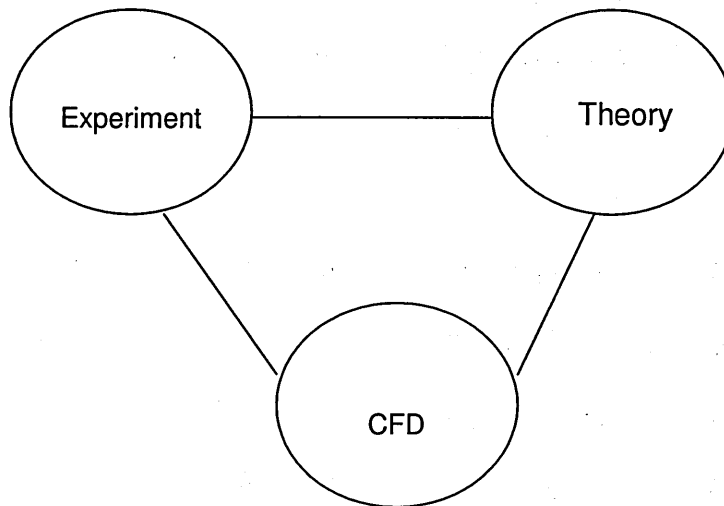


Figure 34 The three dimensions of computational fluid dynamics

As shown in Figure 34 it nicely complements the other two approaches of theory and experiment, but it can never replace either of these approaches. However, CFD is helping to interpret and understand the results of theory and experiment.

Over all since its development it has gained popularity and been tested as a versatile tool in the diversified research community.

2.1.8.1 CFD as research tool

CFD results are the simulation of the actual physical problem with some approximations, ranging from scaled wind tunnel model to actual pipe flow models.

The results from the simulation are more realistic as the methods use to represent the boundary condition and the solution techniques approaches the realistic in nature. However, exact physical system can be represented with complex equations, but to solve the complex equations without proper assumptions is still a challenging job for researches and engineers. The cost, time involved in solving the equations, the amount of computing power required, stability and reliability of the results obtained limits the extent to which the solutions techniques can be approximated.

Procedure for creating CFD model can be demonstrated as a pipeline of steps as shown in Figure 35 below [82].

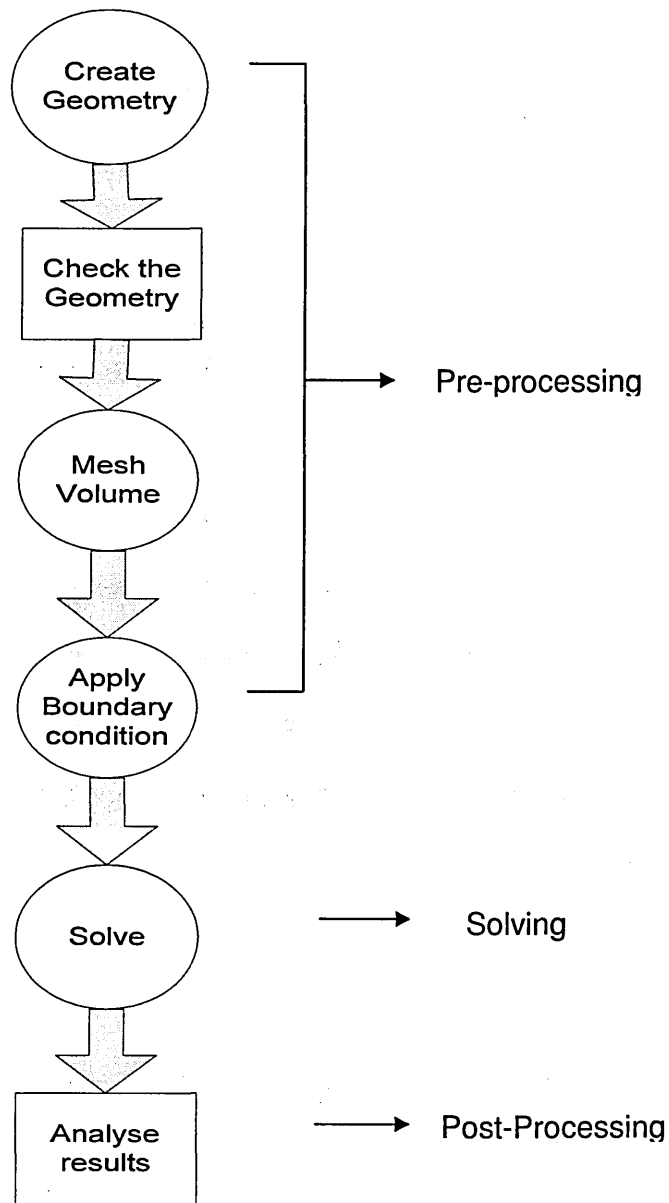


Figure 35 Basic structure of the CFD modelling tree

At first the part is created for which the analysis is to be carried out. this process generally known as geometry creation. Analysis generally deals with heat transfer and fluid flow. Once the geometry is built he geometry is referred to as the domain. This domain is discretised and boundary conditions are applied for the geometry and solved for the given boundary condition. Once the results were obtained, they are reviewed and analysed.

2.1.8.2 Pre Processing

Geometry creation, meshing and applying boundary conditions for the geometry is done in pre processing. Meshing is a process of discretising the geometry in to small elements also known as cells. All regions of the domain need to be connected before solving for the continuity of the region. Geometry also needs to be defined by a continuum either as a fluid or solid region. These steps are to be followed to completely define the system before solving. GHE is modelled in FLUENT 6.3, CFD software to analyse the heat transfer from fluid circulating in the pipe to the ground. GAMBIT pre processor is used to model the GHE.

2.1.8.3 Solving

The system is solved for a given boundary condition, or i.e. continuity, energy and momentum equations to get the temperature and flow distribution within the domain. These equations are solved iteratively since the exact value of the variable is unknown. This starts with the initial guess and solved for the entire domain for the conservation of mass energy and momentum equations. The difference starts as a residue is added for the next iteration and this is until the convergence is reached. The difference can be in the order of one millionth of the initial value. The end user has the control over the order of the difference for in order for the solution to reach the desired accuracy. The process is called convergence, which is the solution for the governing differential equation for a given boundary condition. Refining the mesh size and selecting the type of model for the type of flow, e.g. one equation, two equation models etc., allows desired convergence could be achieved.

2.1.8.4 Post Processing

The results obtained from the solution are analysed as data get generated by the solving process is finished. Plots were drawn, change of dependent variables along or across the domain is being analysed. Software gives various options to view the results in the form of a fringe plot, flow lines in the form of a legend are provided to interpret the results and analysis. Any changes to be incorporated with the appropriate measures in mind can be taken, such as changing the mesh or boundary conditions or modifying the geometry itself. The whole cycle repeats until the satisfactory results are obtained.

2.1.8.5 Turbulence modelling

In theory, if we know the diameter of the pipe, density of the fluid flowing in the pipe, velocity of the flow and the dynamic viscosity of the fluid, then we can calculate the local Reynolds number. But in practical situations it is not that simple, depending on the geometry of the pipe, e.g. flow across the bends. The flow inside the pipe of the GHE may be laminar or turbulent based on the Reynolds number. This is difficult to predict whether the flow is laminar or turbulent because of temperature variation on the pipe surface and from the ground. Still the problem becomes complicated. Thus overall, the heat transfer from the ground to the water is a complicated and transient phenomenon. This can be modelled in FLUENT with proper boundary conditions. In order for FLUENT to solve the equation correctly, the user has to define appropriate turbulence equation available in the software. No single turbulent model can be accepted universally for any problems. The type of model selected depends on the physics of the problem and degree of

accuracy expected from it. The computational time and resource availability also limits the type of the model to be used.

Spalart-Allmaras turbulence model solves turbulence viscosity for transport equation. This type of model is used in which it is not required to calculate length scale for local shear layer thickness. This model is widely used for turbomachinery applications. Since being low Reynolds number model, viscous region of the boundary layer should be resolved properly. It can be used for the cases where coarse mesh is generated and accurate turbulent flow calculations are not significant. On the other hand the standard $k - \varepsilon$ model is a two equation model for turbulent kinetic energy (k) and dissipation rate (ε). This equation can be used in the region where the flow is assumed to be fully turbulent and effect of viscosity is negligible, hence it is only valid for fully turbulent flows. The other turbulent model $k - \omega$ is a two equation model based on turbulent kinetic energy (k) and specific dissipation rate (ω), which is used to model shear flows with improved accuracy [83].

2.1.9 MathCAD

MathCAD is widely used software in many engineering applications for solving simple mathematical calculations to complex, nonlinear equations with built in functions to get exact or approximate solutions. For this project, MathCAD 13 is used for modelling a set of equations for the GSHP system. A standard in built function "*Minerr*" is used to solve all equations simultaneously for a given initial guess. The function seeks solutions to a solve block that minimize errors with the solution. It uses least square method to minimise the error. Since the equations are nonlinear, a good initial guess is very important to get the converged solution.

Conclusion

The purpose of this chapter was to provide extensive source material into the design, modelling and implementation of GSHP. This will allow the literature to be more than just good research but also reflect the design of such systems to build not only frameworks toward use, but also a step toward common acceptance within the consumer market. Though different approaches are available to model variable the nature has to offer, one step is to model the entire system with approximate assumptions. This makes such a choice more accepted and popular but also leads to cleaner ways of producing energy.

Chapter 3

Introduction

In the previous chapter author identified and discussed various literatures regarding GSHP systems, methods used to represent such physical systems. It is clear that there are numerous focuses of previous studies. The focus on this chapter is to represent the complete GSHP system. Subsystems are represented as heat transfer and heat balance equations and solved simultaneously for the whole system. Thermal resistance for all heat exchanges have been identified and scope available for the GHE to improve the system performance is considered. Commercially available plated heat exchanger is specified for the analysis.

3.1 Steady state of analytical model

A method has been developed to analytically solve the system of equations representing each sub system of the overall GSHP. Each sub system is represented by a set of two equations, representing heat balance and heat exchange between the two components. Temperature of the circulating water in the ground pipe, enthalpy of refrigerant in the heat pump and temperature of the air in the building couples these equations. These equations are then solved simultaneously with an initial guess until the convergence is achieved. The initial guess is from the working parameters of the test conducted and the results published. The geometric details of the heat exchanger and the heat pump are used from the manufacturer's data and pipe and grout properties are from the published data.

The main aim of the model is to:

- Calibrate the model for the results published
- Increase the surface area of heat transfer of the circulating water pipe by varying the configuration i.e. multiple passes, coils etc.
- Improve the thermal properties of the pipe and the grout material for improving the performance of the system.

3.1.1 GSHP system

Line diagram of the complete system shown in the Figure 36, the arrangement of the sub systems and the flow variables. Analysis of the system is carried out in cooling mode. T_{air} is the temperature of the outside air for summer and the heat transfer from outside to the wall is Q_{sr}

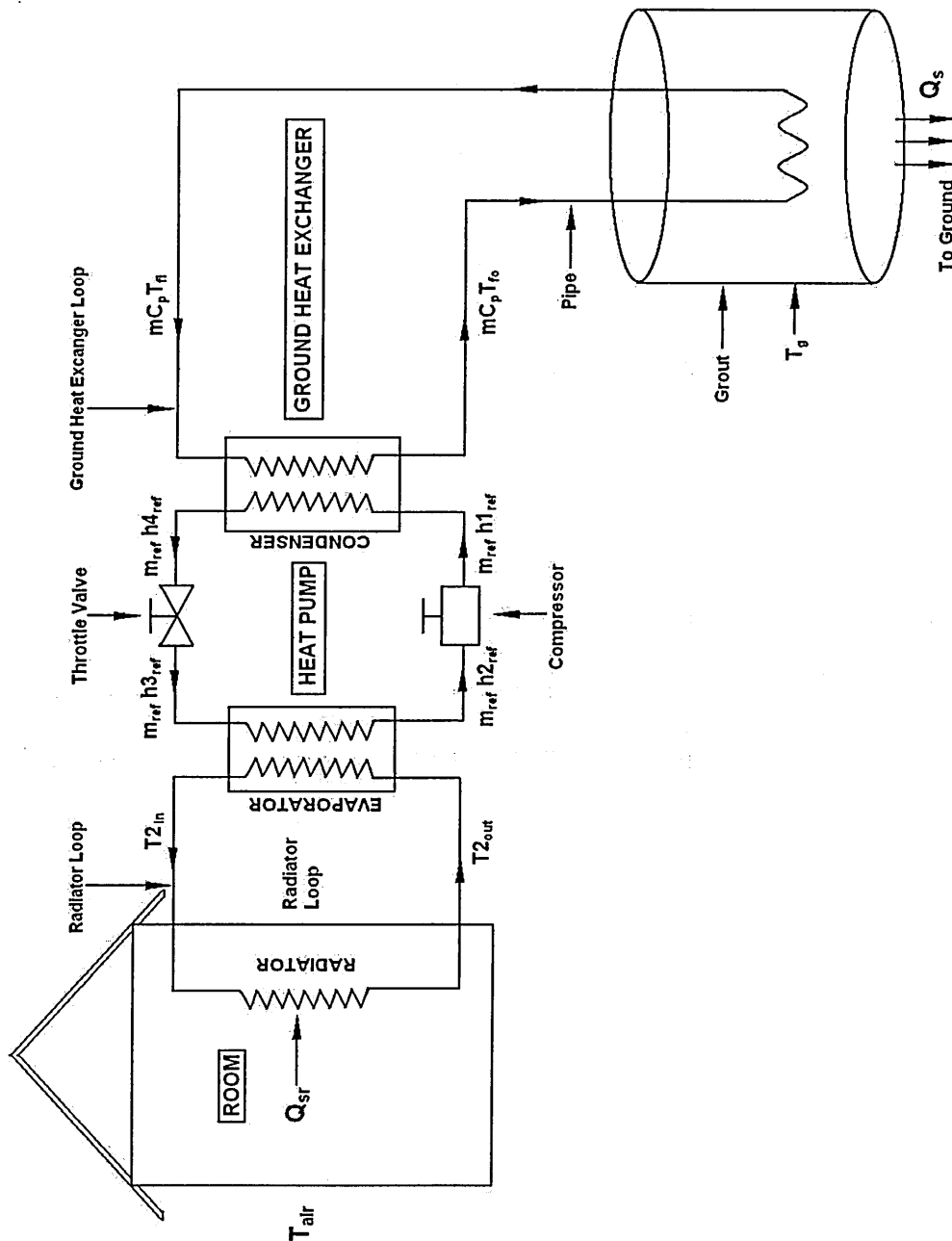


Figure 36 Line diagram of GSHP system

Overall heat transfer coefficient of the wall is used to calculate the heat transfer across the wall to the room using the equation 35. Heat gained in the room is balanced with the relatively cool water circulating in the radiator, which absorbs the heat and rejects in the evaporator. Circulating pump for the radiator loop maintains the constant flow of water.

Refrigerant enters the evaporator as a mixture of gas and fluid state and absorbs the low energy (Q_{sr}) from the warm water and evaporates. It leaves the evaporator in saturated vapour stage to the compressor.

The compressor compresses the saturated vapour to super heated vapour stage by increasing the temperature at constant entropy, which is also called as isentropic process. At high value of energy (Q_s), refrigerant leaves the compressor and condense in the condenser at constant pressure to saturated liquid state. At this stage the energy released (Q_s) equals compressor work (W_{in}) plus the heat added (Q_{sr}) by the circulating water the radiator loop.

$$Q_s = Q_{sr} + W_{in} \quad \text{----- (22)}$$

Condensed refrigerant enters the throttle valve at saturated liquid temperature and pressure is reduced to get vapour mixture. Thus the cycle repeats.

Heat gained by the ground circulating water rejects the heat to the grout buried in the deep ground, and circulates back to complete the cycle. The grout intern rejects the heat to the ground, which is relatively at lower temperature compared to the grout.

The sizing of the grout and the number of columns required depends on the amount of heat to be rejected or absorbed from the ground. For the analysis, the number of grout columns is 24 since the area of the room to be cooled is relatively

large. The diameter of the grout ranges from 120 to 150 mm and the depth varies from 50 to 200 meters.

3.1.1.1 Ground Heat Exchanger

The sub systems of GSHP are interesting to picture within a diagram that explain heat exchange and this is what Figure 37 serves to accomplish. The diagram explains how such position in the ground may contribute to better energy conduction.

The inlet (T_{fi}) and the outlet temperature (T_{fo}) of the water for the ground heat exchanger are obtained by solving heat balance and heat exchange equations 23 and 24 in the ground

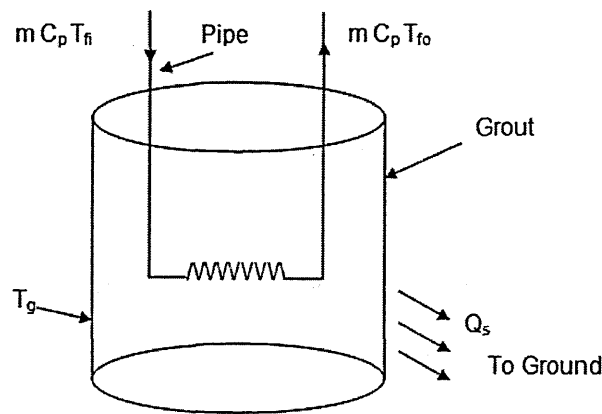


Figure 37 Line diagram of GHE

$$Q_s = U_g A_g \Delta T_{Lm} \quad \text{----- (23)}$$

$$Q_s = m_w C_p \Delta T \quad \text{----- (24)}$$

3.1.1.2 Heat Pump system

Super heated refrigerant gas is condensed by exchanging the heat to the ground circulating water in the pipe in the PHE as seen in the Figure 38 below.

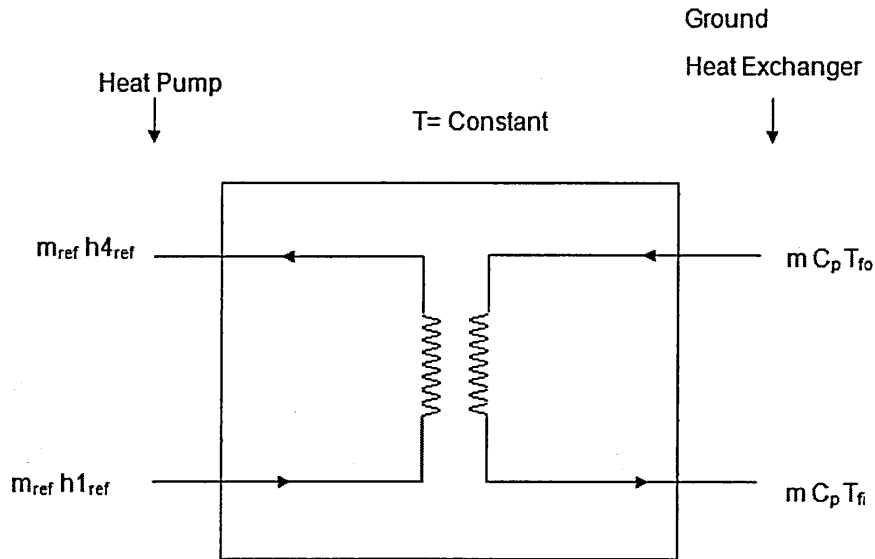


Figure 38 Line diagram of condenser

$$Q_s = U_1 A_1 \Delta T_{Lm} \quad \text{----- (25)}$$

$$Q_s = m_{ref} (h_{4ref} - h_{1ref}) \quad \text{----- (26)}$$

3.1.1.3 Compressor

Compressor can be modelled as a standard thermo sealed isentropic compressor. Since the entropy remains constant during the compression process. The rate of energy addition to the refrigerant can be modelled as

$$W_{in} = m C_{pref} (T_{1ref} - T_{2ref}) \quad \text{----- (27)}$$

In this analysis the compressor work is given. The line diagram of the compressor is shown in Figure 39 within the heat pump system. Saturated vapour from the

evaporator is entered to the compressor. The vapour is compressed to the superheated vapour in the compressor thus increasing the temperature and the enthalpy of the refrigerant. Thus the name is derived as the vapour compression refrigerant cycle.

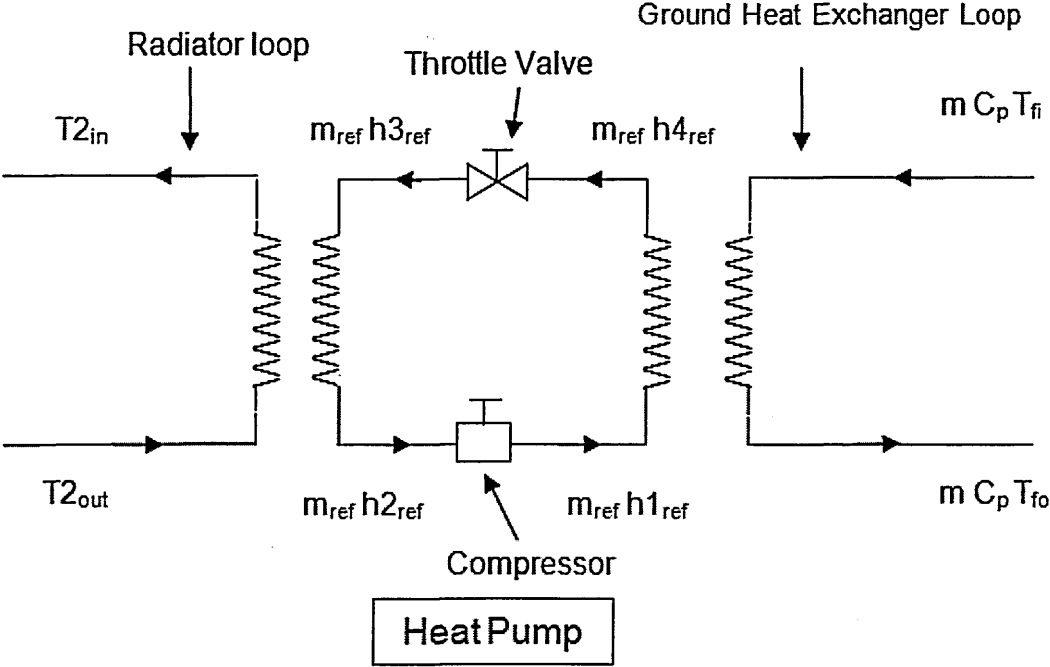


Figure 39 Line diagram of heat pump system

3.1.1.4 Evaporator

Evaporator is modelled similar to the condenser, only difference being that the evaporator is working at lower temperature. Refrigerant after throttling process enters the evaporator at low temperature saturated liquid. Liquid refrigerant absorbs the heat from the water-circulated from the room and evaporates. During the evaporation process temperature remains constant with gain in the enthalpy. The vapour refrigerant enters the compressor at saturated vapour condition.

The line diagram of the evaporator is shown in figure 40 with the flow of the refrigerant inside the loop. Equations 28 and 29 are modelled to represent the evaporator with enthalpy gain and heat exchange with log mean temperature difference. The overall heat transfer coefficient U_2 can be calculated by knowing the convective heat transfer coefficient of the hot and cold fluid and the conductivity of the plate material.

$$Q_{sr} = m_{ref} (h_{2ref} - h_{3ref}) - W_{in} \quad \text{----- (28)}$$

$$Q_{sr} = U_2 A_2 \Delta T_{Lm} \quad \text{----- (29)}$$

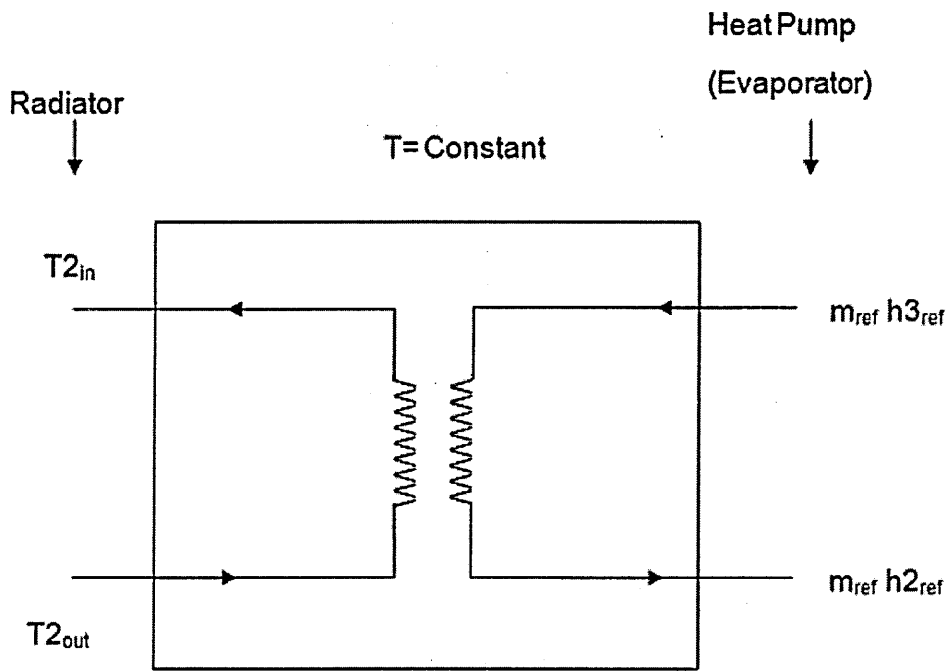


Figure 40 Line diagram of evaporator

3.1.1.5 Throttle valve

Primary function of throttle valve is to reduce the pressure significantly with constant enthalpy. There is a pressure drop often accompanied by temperature drop across the device. Thus drop in the temperature will condense the liquid

refrigerant, which enters the evaporator to absorb the heat from the hot water from the radiator loop. During the throttling process, there is no work done ($w=0$), change in potential energy if any is very small ($\Delta Pe \approx 0$). Though the exit velocity is often considerably higher, the change in kinetic energy is insignificant ($\Delta Ke \approx 0$). The conservation of energy equation is reduced to:

$$h_1 \approx h_2 \quad \text{----- (30)}$$

Where

h_1 and h_2 are the inlet and exit enthalpy of the fluid. Thus from the relation is formed.

$$u_1 + P_1 V_1 = u_2 + P_2 V_2 \quad \text{----- (31)}$$

Internal energy + Flow energy = Constant

The final outcome of a throttling process depends on which of the two quantities increase during the process. If the flow energy increases during the process ($P_2 V_2 > P_1 V_1$), it is done at the expense of the internal energy. As a result internal energy decreases, which is usually accompanied by a drop in temperature. If the product PV decreases, internal energy and the fluid temperature will increase during the throttling process.

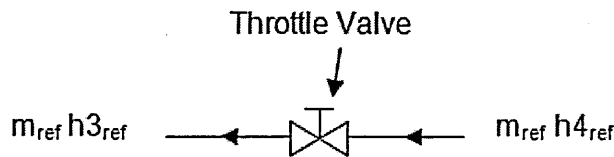


Figure 41 Line diagram of Throttle value

3.1.1.6 Radiators

Radiators are available with different sizes and capacities. The amount of heat to be removed or added to the room is given as Q_{rs} , from the manufacturer's catalogue. For the purpose of this study, only one of the standard radiator types has been selected. The area of the radiator surface is selected from the standard by assuming the type of the radiator to account for the amount of load Q_{rs} .

The radiator in the building is modelled as another heat exchanger absorbing the heat from the room by circulating relatively cold water from the evaporator side of the heat pump. Following figure 42 shows the radiator loop for circulating the water from the evaporator.

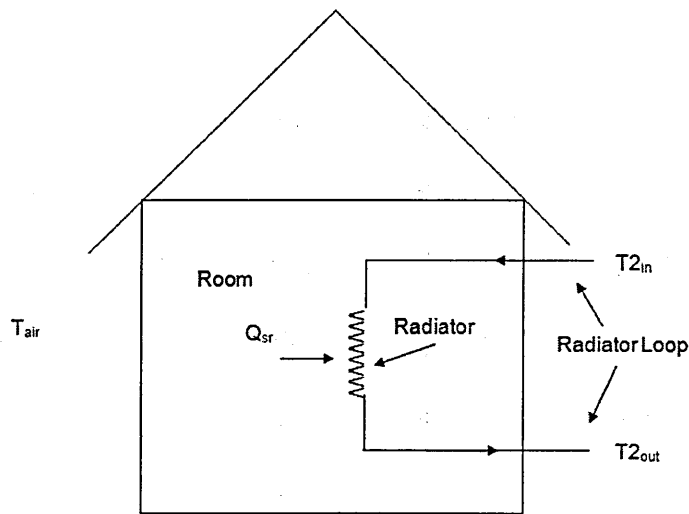


Figure 42 Line diagram of Radiator

Radiator is modelled using the following equations: U_r is the overall heat transfer coefficient of the radiator, which is calculated from convective heat transfer

coefficient of air in the room, conduction in the radiator material, and this is usually cast iron, with the circulating water in the radiator loop.

$$Q_{sr} = U_r A_r \Delta T_{Lm} \quad \text{----- (32)}$$

$$Q_{sr} = m_1 C_p \Delta T \quad \text{----- (33)}$$

3.1.1.7 Room wall

The heat transfer across the room's wall to the surrounding area is modelled as free convection in the room as well as outside air and the conduction through the wall. Assuming the outside air is still and the air inside the room is still, as well for the steady state condition, the convective heat transfer coefficient of the air is calculated. Free convection is obtained from thermal instability of the free convection boundary layer. The heat from the wall is transferred to the surrounding air, the warmer and lighter air moves vertically upward relative to the cooler and heavier air. Transition in a free convection boundary layer depends on the buoyancy and viscous forces in the fluid. It is correlated in terms of Rayleigh number, which is the product of the Grashof (G_r) and Prandtl (P_r) numbers. For vertical plates, the critical Rayleigh number is:

$$Ra = Gr Pr = \left(\frac{g\beta(T_s - T_\infty)}{\alpha \nu} \right) \approx 10^9 \quad \text{----- (34)}$$

Where,

Ra = Raleigh number

Pr = Prandtl number

Gr = Grashof number

g = Acceleration due to gravity (Kg/Sec)

β = Thermal expansion coefficient

ν = Kinematic Viscosity (m^2/Sec)

α = Thermal diffusivity (m^2/Sec)

T_s = Surface temperature of wall ($^{\circ}K$)

T_{∞} = Fluid temperature far from the surface ($^{\circ}K$)

In the following figure 43 the heat from outside air is transferred to the room which is maintained at T_r temperature. The temperature of the air outside is T_{air} and the temperature at the wall outside is T_{ao} . The inclined line in the wall shows the resistance offered by the wall for the heat transfer with in the wall, and the inside wall temperature is T_{ai} and the outside wall temperature is T_{ao} .

$$Q_{sr} = UA \Delta T \quad \text{----- (35)}$$

$$U = \left(U_{ao} + \frac{K_w}{L_w} + U_{ai} \right) \quad \text{----- (36)}$$

Where

L_w = thickness of wall (m)

K_w = thermal conductivity of wall (W/mK)

U_{ao} = free convective heat transfer coefficient of outside air (W/m^2K)

U_{ai} = free convective heat transfer coefficient of room air (W/m^2K)

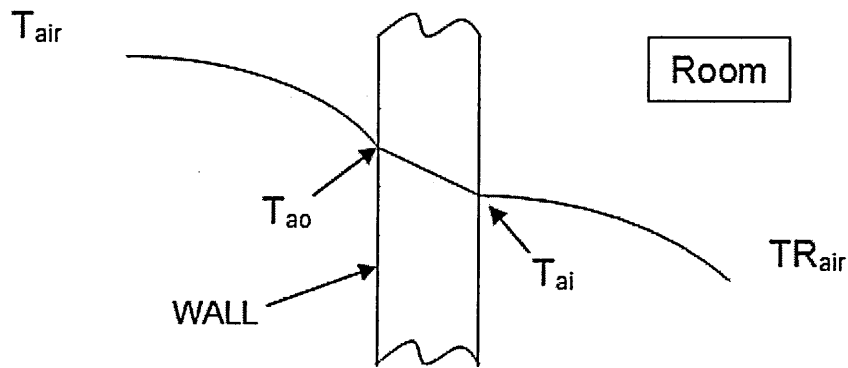


Figure 43 Line diagram of heat transfer through wall

3.1.2 Calculation of Thermal resistance

Heat transfer across a system, for a degree difference in temperature is measured by its UA values. It is calculated from the fundamental equations and the areas of heat exchangers are obtained by the standard manufacturer's catalogue. Inverse of UA gives the thermal resistance of each heat exchanger, which identifies the area and this is where the analysis to be carried out reduces the resistance to the heat transfer.

Convective heat transfer coefficient of the air inside the room and the outside air is calculated assuming free convection. Nusselt number is calculated from the standard relation for free convection with Reynolds number and the Prandtl number. Standard plated evaporator and condenser is selected based on the operating parameters and the range of workload. PHE P400T model is selected for evaporator and condenser. It is designed to operate efficiently during phase change of heat transfer fluid especially for air-conditioning and refrigeration industries [39]. Hence it makes a good choice to use for this model.

Dimensions and the operation conditions of the plates are as follows:

- 280 plates
- 0.601mX0.25 m
- Thickness of the plate 2.29mm
- Maximum working pressure at 155°C is 31 bar
- Plate material AISI 316.

The condenser DBD400 is selected with following dimensions:

- 282 plates
- 0.604mX0.216m
- Thickness of the plate 2.39mm
- Maximum working pressure at 155°C is 31 bar
- Plate material AISI 316.

The surface area of heat transfer is very high in plated heat exchangers and the number of plates being used can vary the area. For the selected model and the number of plates, the surface area will range from 36-42 m². Radiator is assumed to be cast iron with standard dimensions.

From Appendix B, it is clear that the values for PHEs are high and the opportunity is available to improve at the radiator. From research, it is found that the improvements are being made by:

- High thermal conductive material
- Various shapes for increasing the surface area
- Improved design
- Low maintenance

- Light weight
- High durability.

Although many factors will affect the performance with proper assumptions, still there is a scope for the improvement. From the following figure 43, , the UA values for the condenser and the evaporator are significantly high and the region of interest lies in making improvement in ground heat exchanger. The improvements in wall insulation and radiator design are limited owing to the space constraints. The clear choice is to improve the ground heat exchanger considering the flexibility and the methodologies available to optimise the performance the choice is justifiable.

Use of CFD to simulate the temperature and flow distribution in the pipe is very useful. CFD allows temperature, material properties, soil properties and the configuration of the pipe geometry to vary. This allows for calculations and its effect on the heat transfer rate from or to the fluid. By changing the configuration of the pipe inside the ground, the surface area of heat transfer can be varied. The length of the pipe can be varied to assess the variation of the temperature for each °C raise or drop. This information is very useful to calculate the cost associated for each meter depth of pipe to be buried.

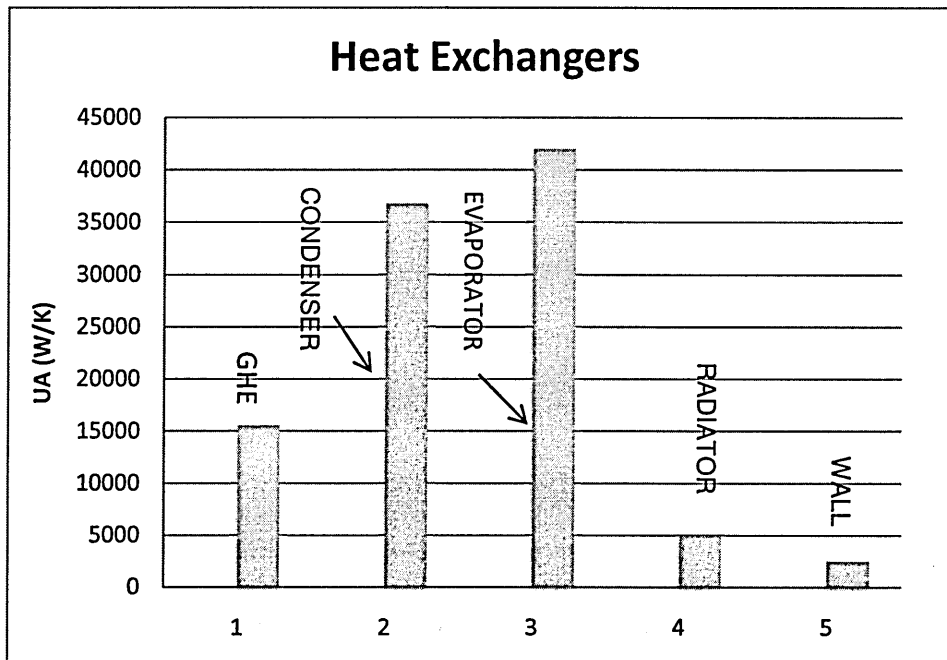


Figure 44 Various components within the system with their UA values

As an overview, the temperature and the enthalpy in the refrigerant connect the systems. Heat transfer from the outside air is coupled to the air inside the room. The circulating water in the radiator carries excess heat away. The radiator water is coupled to the heat pump with refrigerant exchanging heat in latent heat transfer. Power input to the compressor increases the pressure and temperature of the refrigerant, thus high-energy refrigerant exchanges the heat with cold water in the condenser with latent heat to the ground circulating water. The heated water rejects the heat in the ground heat exchanger to the ground at lower temperature.

All equations are solved for respective temperature; enthalpy and heat transfer between the systems. Initial guess is vital for the stable system. Once the system of equations is solved, the residues from each subsystem are tested for the maximum level of accuracy. In this model, the degree of convergence achieved is at acceptable level. The system uniqueness is tested with different room,

refrigerant temperatures the solution values converge to the original values. The stability is also checked by monitoring the residual values and it is observed that the residues are in acceptable level and the system is stable.

3.1.3 Solving procedure

The system of equations are solved for different air temperatures with all other variables to vary, the procedure is carried out for the range of air temperatures. In this analysis, power input, ground and air temperatures are the variables. MathCAD model is solved by varying one variable at a time. Work input (W_{in}) to the compressor is varied to observe the system response. Convergence is achieved if the residues are minimum or negligible, for this analysis, values are nearly zero as shown in the appendix C. Similarly the equations are solved for air temperature (T_{air}) and ground temperature (T_g) and the residues are checked for convergence.

Sample values used for the calculations are

Room temperature (T_r) = 21°C

Refrigerant temperature at the evaporator side (T_{2ref}) = 7°C

Refrigerant temperature at the condenser side (T_{1ref}) = 25°C

Ground loop water inlet to condenser (T_{fi}) = 21°C

Ground loop water outlet to condense (T_{fo}) = 25°C

Radiator water temperature inlet to evaporator (T_{2out}) = 21°C

Radiator water temperature outlet to evaporator (T_{2in}) = 15°C

Enthalpy of refrigerant before compression (h_{2ref}) = 424299 J/Kg K

Enthalpy of refrigerant after compression (h_{1ref}) = 442112 J/Kg K

Enthalpy after the condenser (h_{4ref}) = 240716 J/Kg K

Heat transferred by the outside air (Q_{sr}) = 64391 Watts

Heat transferred to the ground (Q_s) = 70591 Watts

Compressor power input (W_{in}) = 6200 Watts

The residuals of the some equations are

Heat balance between grout and ground loop water = -3.2×10^{-10} Watts

Energy balance between grout and ground loop water = -1.164×10^{-10} Watts

Heat balance between condenser and ground loop water = 8.73×10^{-10} Watts

Energy balance between condenser and ground loop water = -1.45×10^{-10} Watts

Overall balance of the heat pump = 0 Watts

Heat balance between evaporator and distribution loop = 0 Watts

Energy balance between evaporator and distribution loop = 1.4×10^{-10} Watts

Heat balance between radiator and distribution loop = 2.9×10^{-10} Watts

Energy balance between radiator and distribution loop = -1.14×10^{-10} Watts

Heat balance between evaporator and distribution loop = 1.3×10^{-10} Watts

Energy balance between evaporator and distribution loop = 0 Watts

Heat balance between room and the outside air = 1.3×10^{-10} Watts

COP for the above values is 10.38 which is nearly the values at the published data as discussed in the results section. For all the equations, the residues are around the order of -9 to -10 magnitude which is well received for the convergence criteria.

The effect of thermodynamic properties of the refrigerant in the system performance is out of the scope of this work. Methods have been modelled to simulate the properties have been discussed in the literature review.

Conclusion

Each sub system was modelled as a pair of heat transfer and heat balance equations. Coupling each sub system by temperatures and enthalpies to represent the complete GSHP system is the method proposed. Solving for range of temperatures and enthalpy shows the system response for the operating conditions. Values of residue and COP calculation for sample data are shown. The scope available to develop and improve the GHE has been discussed and selected for CFD modelling in the next chapter. The purpose here is to show how innovative and important to develop such hybrid model for future energy solutions.

Chapter 4

Introduction

This chapter focuses upon modelling GHE with varying temperatures on the outer surface of the grout to represent the varying temperature of the ground. The inlet and outlet temp of circulating water is taken from the published data for reference. The results are analysed and overall thermal resistance is calculated. Analysis is carried out with symmetry boundary conditions to reduce computing time and memory. Geometry is modelled in GAMBIT and solved in FLUENT 6.3

4.1 CFD modelling in FLUENT

A method has been developed to model the pipe carrying the water, which is buried in the ground. The model is built in gambit and the temperature gradient is used as boundary condition for different depth of the ground. The temperature for different depth of the pipe is used from the published data to, which the results to be compared. The geometric material properties for the pipe and the flowing water are obtained from the standard material data handbook. Necessary assumptions are made to implement all the aspects of the process to model the complete cycle.

4.1.1 Modelling the U-tube

The pipe outside diameter is 40mm with 4mm thickness; the length of the pipe used is 100 meter. The depth of the borehole is 50 meters with 150mm diameter. The internal diameter of the u-bends of the pipe is 42 mm. The borehole is filled with grout material to have maximum surface contact with the surface of the pipe

for better heat transfer and it also prevents the pipe from contamination from the foreign materials in the soil.

The circulation of the water in the pipe is analysed by periodic boundaries. The methodology commonly used in the analysis in which a section of the pipe is modelled and the output of the pipe is again used as input several times, remains until the exact length of the pipe is accounted. This avoids the modelling of several hundred meter of pipe and physics of the flow is not compromised. Assuming the length of pipe 400 meter for 200 meter borehole, considering the U tube configuration, the 50 meter model is made for simplicity and the water is recalculated for four times to capture the same effect of the 200 meter length pipe.

Periodic boundary conditions model the repetitive nature of flow considering space as variable for the length of pipe. It records the previous values of the variable at the outlet and feeds in to the inlet. The variables are calculated again for that given length as long as there are no geometric variations. This avoids modelling entire length of pipe.

Symmetric boundary conditions are used in cases where the flow parameters such as temperature, velocity etc do not change for fully developed flow across the particular plane. For temperature variations, the heat flux across the symmetric plane is assumed to be zero this reflects the exact properties of the fluid at the plane of symmetry of the geometry and flow.

Since the model is symmetric above the vertical plane, only half of the model is modelled and the results were reflected on the other side of the symmetric plane. Assuming the ground as infinite source or sink, the ground surrounding the pipe is modelled considering enough distance from the pipe to have steady distribution of the temperature. The diameter of the ground considered is about 5 meters to reflect the temperature measurements made from the sensors in the publication against which the results will be compared. Following figure 45 shows the basic geometry.

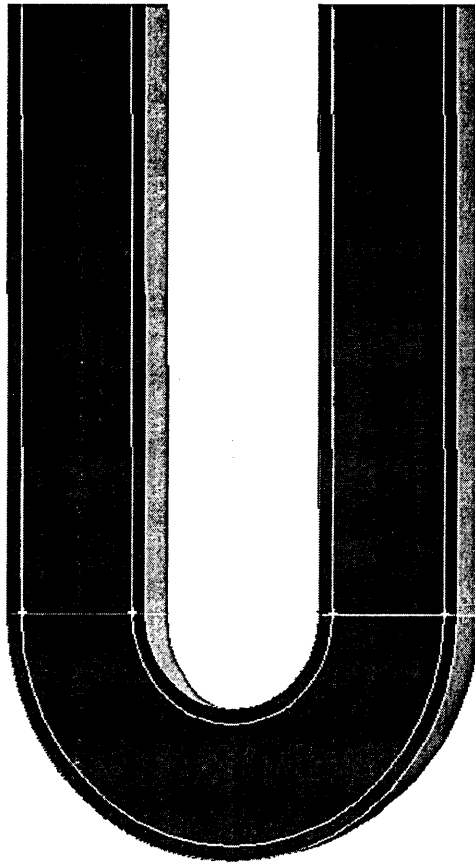


Figure 45 Pipe and water geometry in GAMBIT

The following figure 46 shows the sectional view of the water and the pipe along the vertical plane. Properties of high-density polyethylene pipe and water or some times water with glycol mixture can be used for calculating heat transfer coefficient. The overall heat transfer coefficient is calculated by convection heat transfer coefficient of the water flowing in the pipe and the conduction of heat through the pipe to the surrounding ground.

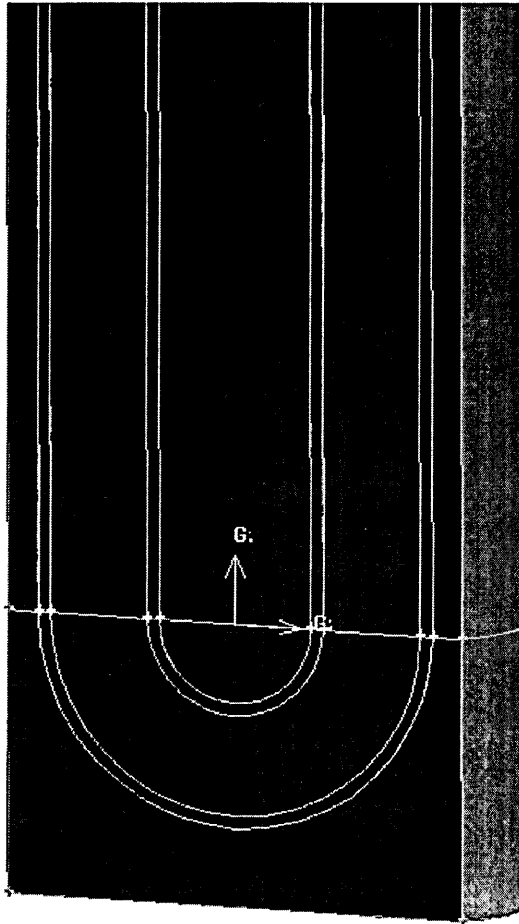


Figure 46 Pipe geometry with grout in GAMBIT

In summer, the surface temperature of the ground is high and as the depth in the ground increases, the temperature in the ground decreases. The varying temperature is used on the surface of the grout as the temperature boundary

condition. The typical summer temperature of 33°C is used and from the data published. It is observed that the temperature gradient is higher for the first few meters from the surface of the ground, and is maintained nearly constant for after certain depth. The temperature at 20m depths is around 18°C from the literature hence the same temperature is used for the analysis. Soil property can be found on the FLUENT material properties data base which is used for this analysis, for different soil types user can use other properties. Impact of these properties can be analysed based on the type of boundary conditions used.

4.1.1.2 Meshing

Meshing is a process of discretising the domain into small cells as the governing differential equation is conserved on each small cell and integrated over all the cells to complete the geometry. Hexahedral cells have greater accuracy and fast convergence when compared to tetrahedral cells [84]. Hexahedral cells with their degree of polynomials it converges accurately but relies on geometric simplicity. Tetrahedral mesh with high node numbers and degree of approximation used, takes more memory and time but on the geometry it has the advantage it can be used for any complicated geometries.

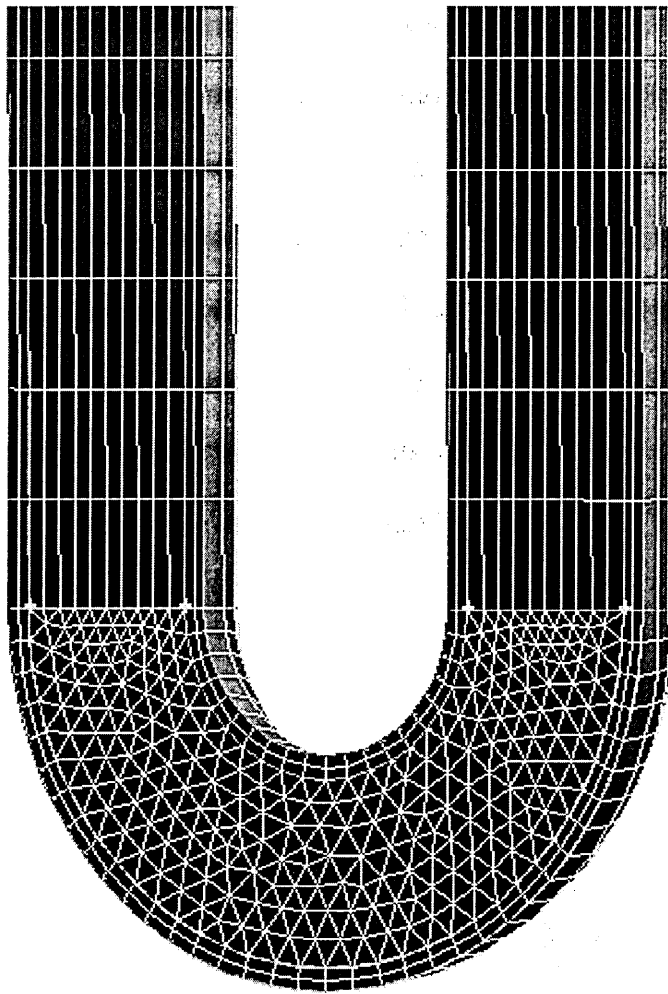


Figure 47 Meshed geometry water in the pipe

4.1.1.3 Boundary condition and Solving

Velocity inlet with temperature of the water entering the GHE is assumed for this model. The velocity and the temperatures are obtained from the experimental data published. For the given geometry and the velocity the Reynolds number is well above 2100, the flow is turbulent. Stand $k - \varepsilon$ model is used to solve turbulent quantities. Continuity, energy equations and turbulent equations are solved for the flow field. With standard material properties and operating conditions, symmetric model of the GHE is solved for the given boundary conditions.

Conclusion

Modelling of GHE with simple U-tube is demonstrated in this chapter. The geometry being simple, hexahedral mesh used for the straight length of the pipe and tetrahedral mesh for the U bend is appropriate. For the value of Reynolds number, type of flow use of two equation turbulent model is justifiable. Use of symmetric and periodic boundary conditions is valid for the type of the geometry and the analysis carried out. The results of this section is discussed in the following chapter

Chapter 5

Introduction

This chapter discuss the results obtained from the above analysis and analyse the results. The variables are selected based on the real parameters which have an effect on the system performance for steady state conditions. Variables are also taken in to account the physical feasibility to implement them if performance shoots up, for example surface area of grout, grout thermal properties and ground and air temperature difference and degree of sub cooling and super heating etc.

5.1 Results and discussions

An analytical model is developed to observe the parameters affect the performance of the ground source heat pump system. This study reproduces the results of the experimental work carried out by Yujin Hwang et all [33] for a school building in South Korea. The dimensions of the geometry in the analytical model, material properties and working parameters are used from the same publication to validate the model. The CFD model of the ground heat exchanger is used to calculate the thermal resistance of the borehole.

The geometric details and the thermal properties of the materials used for the calculation are listed in Appendix A. The variables are the air temperature (T_{air}), power in put to compressor (W_{in}) and the ground temperature (T_g). Temperatures of circulating water and refrigerant, enthalpies of the refrigerant at evaporator and the condenser exit are calculated directly. The enthalpy after the isentropic

compression is derived from the temperature at the evaporator exit, which is assumed to be at the saturated vapour condition.

5.1.1 Results from the analytical model

This model is analysed in cooling mode. It is observed that for the typical outside air temperature ranging from 18°C to 50°C at constant ground temperature at 18°C and at constant power input, the figure 48 shows the COP increases almost linearly

It is reasonable to understand that in cooling mode as the load increases for the constant power input, the COP will increase. The increase in temperature gradient above the practical working range limits the performance due to surface area of the ground heat exchanger.

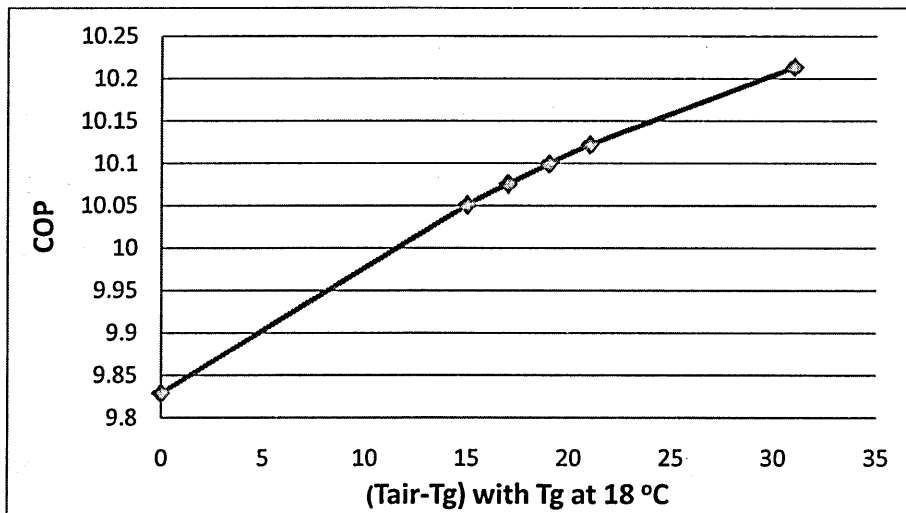
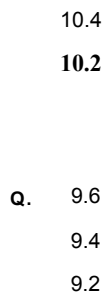


Figure 48 COP varying with temperature gradient with T_g at 18°C

High values of COP are observed for not taking in to account the power consumed by the circulating pumps. The 7500 watts power input suggested by Yujin Hwang

et al [33] to the pumps will bring the values down to more than half the above shown values, which are quite near to the practical range of operations.

The ground is a vast reservoir for heat transfer, above conditions are assumed with negligible or no temperature variation of the ground surrounding the grout over the long period of time. The dynamic working nature of the system and the local condition of the ground the temperature might vary. Considering the long term working nature of the system if the ground temperature varies the effect on the system is adverse. In the following figure 49 it is observed that the system has to work against the temperature gradient.



20

(T_{air}-T_g) with T_{air} at 33°C

Figure 49 COP varying with temperature gradient with T_{air} at 33°C

The increase in ground temperature reduces the amount of energy transfer to the ground. This affects the overall performance since the additional heat cannot be transfer to the ground and the cooling load is reduced for the given power input.

The effect of working temperature on the performance can be observed in figure 48 when the (T_{air}-T_g) is zero at T_g = 18°C the COP is around 9.85 and it is 8.7 when (T_{air}-T_g) is zero at T_{air} = 33°C in figure 49. For the same temperature

gradient of about 17°C it is observed that fixing the ground at lower temperature at 18°C average COP increases around 5.14% when compared to fixing the air temperature at 33°C. The model is tested against the standard Carnot COP to check whether the actual COP should not be exceeded.

5.1.2 Validation with experimental model (Bench mark model)

The model is tested against the experimental values under the similar working parameters. Power in put and the temperature difference of the circulating water from the ground heat exchanger are considered as the parameters to compare. The performance is dependent on the power input to the compressor below figure shows the decrease of performance with power input for fixed air and the ground temperature. The experimental results were collected from Yujin Hwang et al [33].

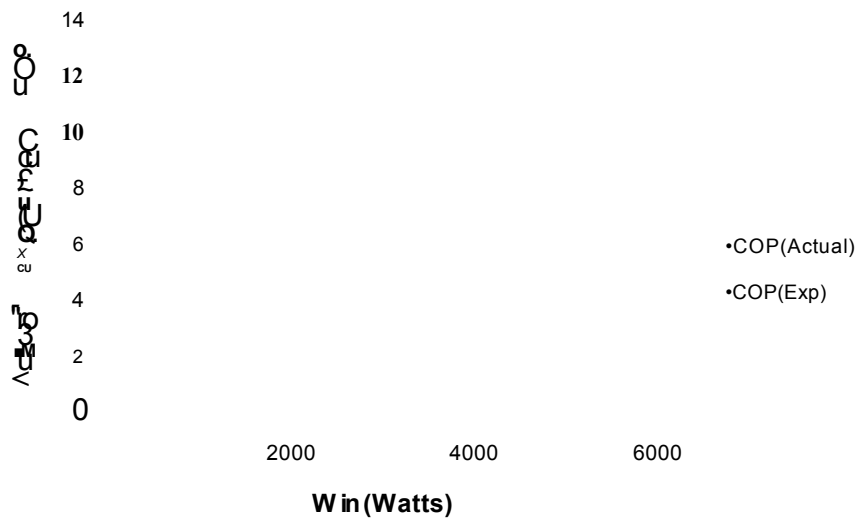


Figure 50 Experimental and actual COP for varying compressor power

The corresponding power input to the compressor is used to compare the results with the experimental results. It is seen that the actual model over predicts the

experimental model. The average actual COP is 9.14 and the experimental is 8.28 the prediction is around 10.38% higher to the experimental.

This model would work for operating temperature below the one considered for this analysis for example for the case of the UK scenario. The effect on the COP is also depend on the other factors such as ground temperature at certain depth as it can be seen the temperature difference which drives the system have an effect on the performance. As it can be seen from the figure 47 & 48 by extrapolating, COP might be at the lower values.

Possible causes for the deviation:

- Methodology used to calculate the load on the compressor
- Thermal properties used in the calculation of the heat load
- Type of sensor used and the assumptions made in the measurement of room temperature

The temperature of the circulating water in the ground heat exchanger largely depends on the temperature at the inlet and the surface area for the heat transfer.

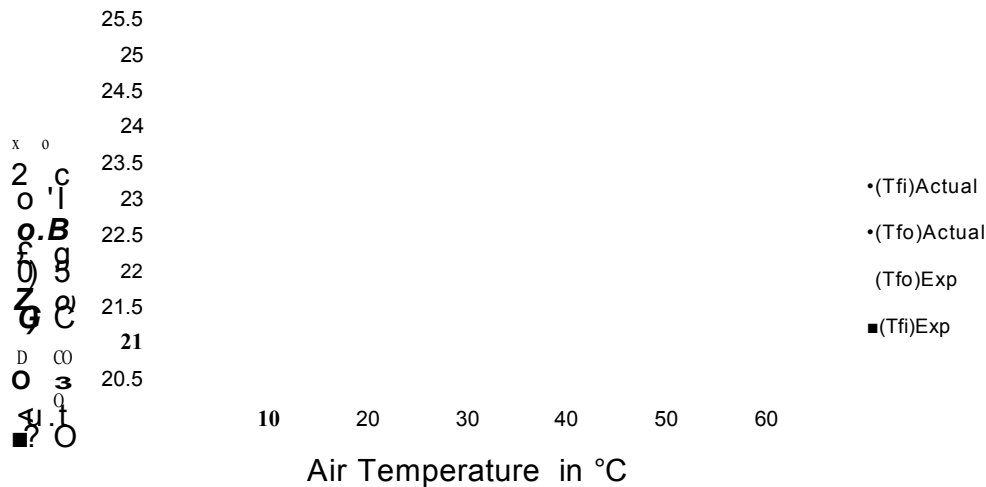


Figure 51 Air temperature V/S circulating water temperature in GHE both actual and experimental

Since the surface area is constant, the inlet temperature varies with the independent our side air temperature. As the air temperature increases the cooling load increases and so the temperature in the condenser. The inlet temperature of water to the ground increases and leaves the ground loop at higher temperature. The values of the temperature in the chart above nearly agree with the experimental results. The model under predicts the temperature at the entry to the heat pump about 0.5°C and over predicts by 0.5°C at the exit. The net raise in the temperature is nearly same as the experimental results. The average difference between the temperatures is around 2%, which are very nearly matches to the experimental results

The deviation for the results in comparison to experimental may be due to

- Thermal resistance of the ground, since the temperatures are measured at 2.5 meters from the surface of the grout

- Input temperature profile on the surface of the grout.
- Method used to relate the temperatures of the working fluid

5.1.3 Comparison with Ideal Carnot COP

Ideal Carnot COP depends on the hot and cold temperatures and is used to measure the scale of the actual cycle COP. This comparison gives the limit to the actual cycle COP to operate; it is impossible to have any cycle to operate above this value. Results show that the actual COP is far less than the Carnot COP. Initial temperature difference between the source and the sink is very low hence a very high value of COP is expected. As the temperature gradient increases the Carnot COP decreases as shown in Figure 52 Comparison of actual and Carnot COP

As the temperature difference increases rapidly, the ground temperature will increase marginally. This causes the gradient of the curve for Carnot COP to reduce and eventually get steady well above the actual COP value.

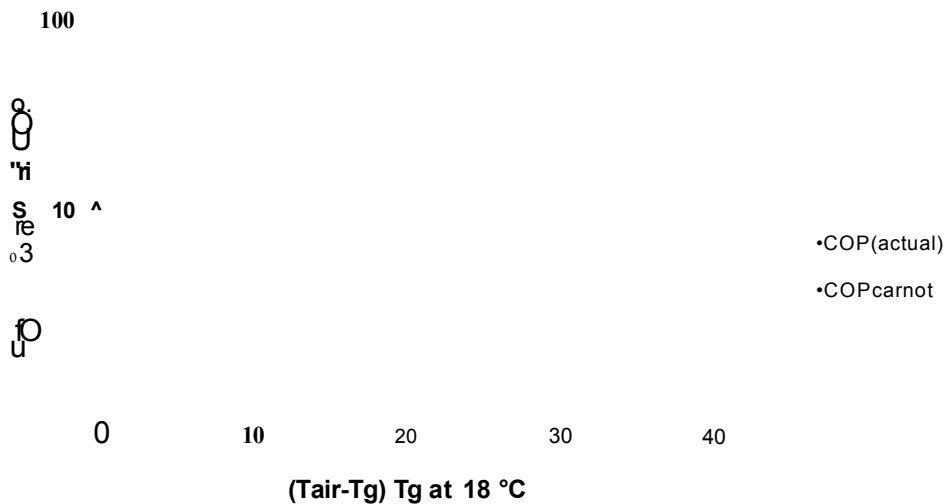


Figure 52 Comparison of actual and Carnot COP

5.1.4 Parametric study

5.1.4.1 Effect of area of the grout on the performance

Apart from the operating parameters, the geometric parameters and the material properties might also affect the performance of the system. Consider the affect of surface area of the grout to improve the heat transfer rate to the ground. Theoretically, by increasing the area of the grout the heat transfer will increase the effect is analysed in the model. Below figure shows the improvement of the COP with increase in the surface area of the grout.

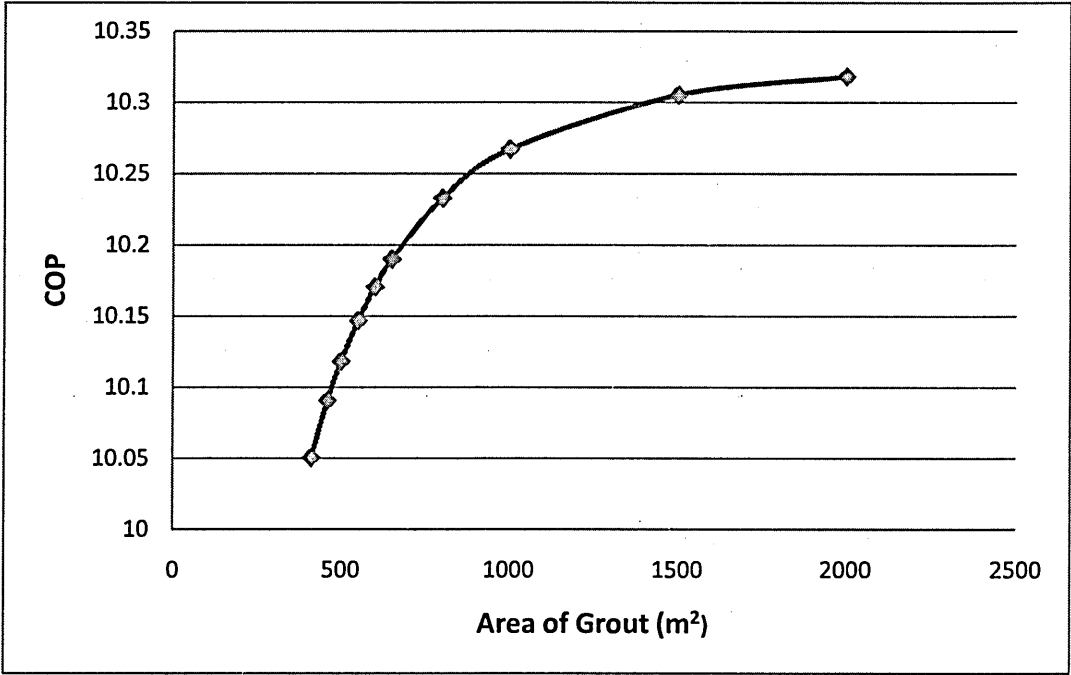


Figure 53 Variation of COP with area of grout

The curve shows that the increase in COP will be significant to the area around 900-1000m² after that value the curve reduces the slope. After around 2000m² the value of COP will almost remain same. The overall improvement of the performance is around 0.5-0.6 % for 1000m² of increased area and it is around

0.2-0.25% above 1000m² area. Changing the configuration of the pipe in the ground can increase the surface area. Two different types U-tube and the coil type are suggested in previous chapter.

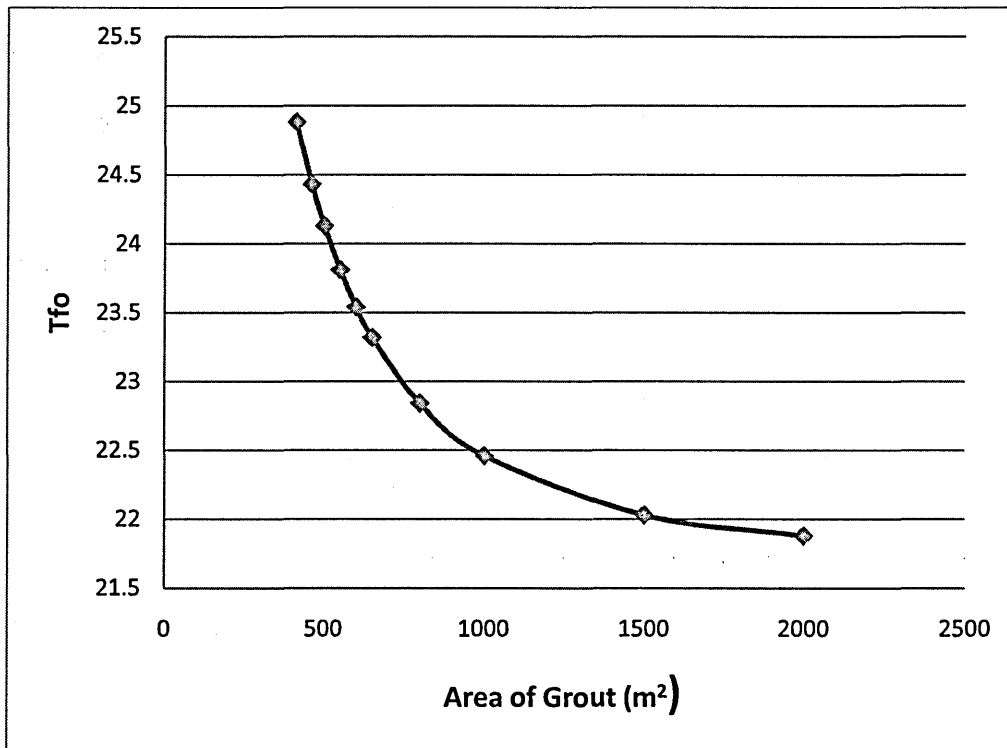


Figure 54 Varying outlet temperature of water from the GHE with area of grout

As the surface area increases the outlet water temperature of the ground heat exchanger will decrease. The cold water absorbs more energy from the condenser and thus improves the performance of the system. Figure 54 shows the temperature (T_{fo}) of water decrease. Steep drop of around 3°C in the range of 400-1000m² is observed. To compare the two results i.e. figure 47 and figure 48, at 100m² area of the grout the slope is reducing quite sharply and flattens at around 2000m². Giving sufficient information the COP does not affect much after the 2000m².

5.1.4.2 Effect of degree of sub cooling and super heating on the performance

The effect of degree of sub cooling at the condenser exit and super heating before the compressor inlet is studied in this section. The effect of super heat is to completely vaporise the refrigerant before entering the compressor with some degree of superheated vapour. Figure 55 show that it is having the positive effect on the performance of the system. The ideal effect of the super heating is represented by the top line in the following figure on average of 10.66. Considering the energy required to super heat vapour, the actual COP is reduced to an average of 5.55. The average difference found to be around 47%; still the degree of super heating has the positive result.

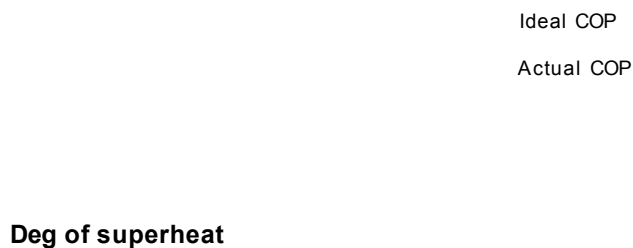


Figure 55 Effect of degree of super heat on COP

The effect is almost linear with the degree of super heat for each 5°C raise in the temperature above the saturated vapour region, gain of around 0.2% of COP is observed. The additional energy required to heat the vapour to the super heated region is gained from the water re-circulated from the condenser or any other heat

exchanger. Similarly the effect of degree of sub cooling is also considered in this work. This affect shows the COP increase is higher for the same range of degree of sub cool temperature when compared to degree of super heat. Figure 56 show the much steeper gradient of the COP compared to previous method. The average gain in the ideal COP curve is about 11.12 and with the actual curve the gain reduces to 6.54. The net effect is quite positive with 41.18% deviation with ideal and actual COP.

The net gain when compared to super heating for the same temperature range is 5.82 %. Considering the other unaccounted 20-30% losses, the net gain will be around 4.6%-4.1%, which is quite practical.

Actual COP

Deg of Sub cooling

Figure 56 Effect of degree of sub cooling on COP

By improving the mechanism of heat transfer in the condenser and using better thermal properties for the material, this objective can be achieved. An

arrangement for cooling mechanisms might be implemented to get the degree of sub cool.

5.1.4.3 P-h-diagram for super heat and sub cooling cycle

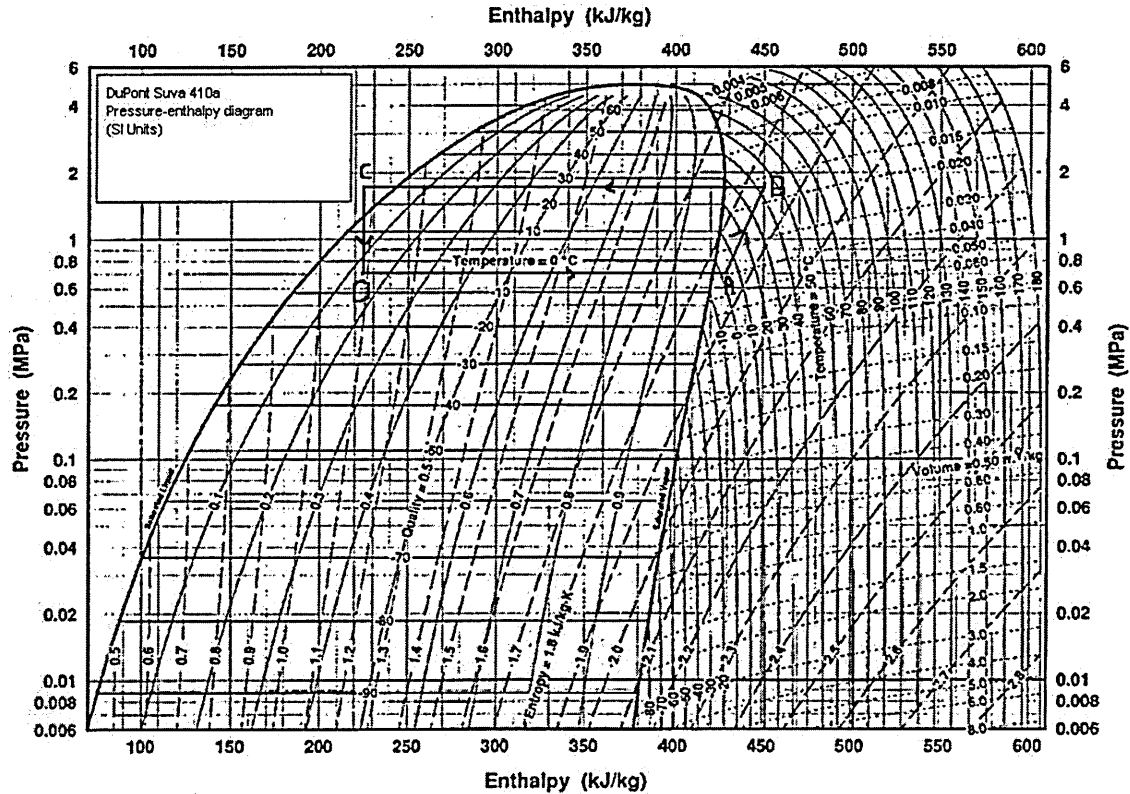


Figure 57 P-h diagram with sub cooling and super heating for a typical cycle

The cycle begins from inlet to the compressor. Point A is in the superheated region above the saturated vapour line. The refrigerant is compressed isentropically from A to B in the super heated region. From point B, the refrigerant at high energy level releases the heat in the condenser and reaches the saturated liquid line. It then sub cooled to the point C with constant pressure. At point C refrigerant is completely in liquid state and enters the throttle valve. The throttling process is represented by process C to D at this point it is liquid-gas mixture. At point D the

refrigerant absorbs the heat in the evaporator and vaporises to reach point on the saturated vapour curve at constant temperature. It is super heated to reach point A to enter the compressor and the cycle repeats. The above section describes the actual cycle for the calculated values of the temperature and enthalpy of the refrigerant. This cycle repeats and changes the position of the points each and every time for different cycles.

5.1.4.4 Effect of U-value on the performance of the system

Improving the material properties to increase the performance is also one possible option, which is analysed in the exercise. The effect of overall heat transfer coefficient for the ground heat exchanger analysed and is shown in figure 54. The effect is not significant raise in COP with additional U value. It gives the limiting value of heat transfer coefficient around $20 \text{ W/m}^2 \text{ }^\circ\text{K}$. Further increase in the U value has only noticeable effect on the performance. The overall gain is observed to be around 0.5% for about $10 \text{ W/m}^2 \text{ }^\circ\text{K}$ and it reduces to about 0.2% above the threshold of $20 \text{ W/m}^2 \text{ }^\circ\text{K}$.

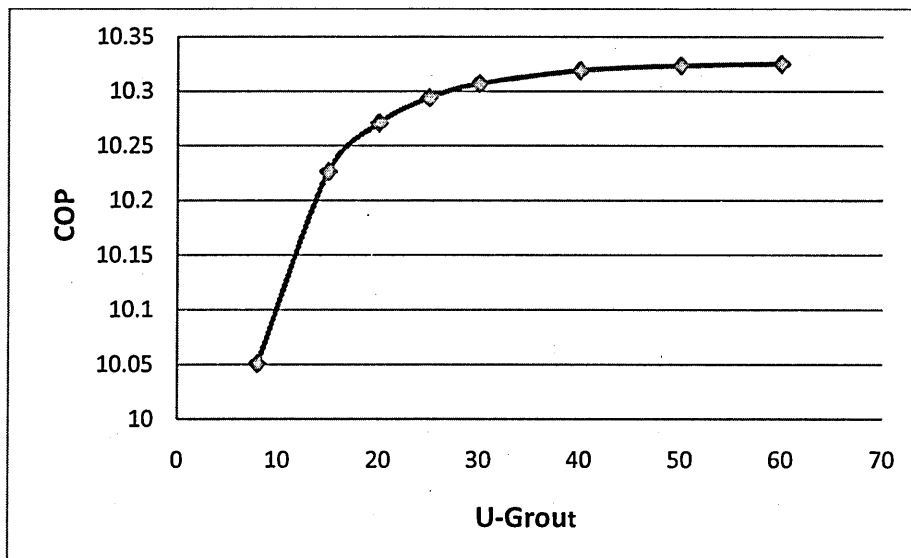


Figure 58 Variation of COP with U value of grout

Improving the U value beyond certain range has the practical difficulty. The heat transfer coefficient is combination of convection and conduction in the pipe and grout. The major share of the heat transfer mechanism lies with convection of water in the pipe. It is worth looking at the fluid part in the pipe.

A CFD model is used for the ground heat exchanger to calculate the convective heat transfer coefficient. Different configuration of the pipe in the ground suggests the variation of the heat transfer coefficient. The common U tube configuration is modelled from the velocity and temperature boundary condition; the convective heat transfer coefficient is calculated.

5.1.5 CFD model

Figure 59 Contours of temperature distribution in the pipe

The experimental value of outlet temperature of circulating water, which is 24°C, is used for the inlet for the CFD model. Temperature at the outer surface of the grout is maintained at 16.5°C, which is the average value calculated from the published experimental work for 200m depth bore hole. The CFD results show the outlet temperature is 22°C, which is very much comparable from the experimental outlet water temperature at 21.5°C. The deviation of around 2.3% can be observed in figure 60 is very negligible.

Figure 60 Contours of velocity profile in the pipe

The value of velocity is obtained from the published data and is also used to calculate the overall heat transfer coefficient in the analytical model. The inlet velocity 0.5m/s with inlet temperature is used for the above solution. Figure 61 also shows the velocity profile at the bend U section below the ground at 200m depths along with the grout.

Figure 61 Contours of velocity in U tube

It is shown that the method used to compare the performance is valid. The effect of increase of grout surface area and the thermal properties of the GHX is also increases the performance. CFD results show the close match to the analytical solution. The convective heat transfer coefficient of the water in the pipe is shown in figure 62. The values are high at the inlet and reaches constant value at the exit to the grout temperature. The CFD value of the heat transfer coefficient is 1611.6 $W/m^2 \text{ } ^\circ K$ maximum and is 1612 $W/m^2 \text{ } ^\circ K$ minimum. If all the values are added up in the fringe plot, the final value is 9.17 $W/m^2 \text{ } ^\circ K$ and the calculated value is 7.88 $W/m^2 \text{ } ^\circ K$ from Appendix A. This deviation of 16% can be minimised by refining the mesh or using the different solving techniques to converge the solution.

Figure 62 Surface heat transfer coefficient on the inner surface of the pipe

Conclusion

Actual and experimental COP's for different power input are in reasonable agreement. The inlet and outlet temperatures of GHE are also predicted to the acceptable range. The effect of increase of area of grout and temperature difference between the air and ground seems to have slight impact on the performance. High values of COP can be expected without considering the effect of power consumption for circulating pumps.

Chapter 6

Introduction

The influence of some parameters was not that significant as it was initially thought of, ground properties might have been the parameter to limit the performance. Complete system performance is reasonably accurate with the assumptions made; the methodology adopted has worked well for some parameters. Modelling the grout with the ground for transient conditions should show the actual impact on the system performance. As discussed earlier in the literature the possibilities are numerous. Outcome of this work is a step towards the better understanding of the complete system behaviour.

6.1 Conclusion and future scope of work

For the optimum design of the GSHP system, it is necessary to estimate its performance and economic feasibility before the installation. In this work an analytical model is proposed and developed for the steady state condition. Complete model is analysed in the MathCAD analytical model, and clear choice has been made to improve the GHE having compared all subsystems overall heat transfer coefficient. The model considered the effect of area of ground heat exchanger on the performance it has the positive impact.

Thermal properties of the materials of the pipe and grout have considerable impact on the performance of the system. The interesting aspect of degree of sub-cooling and super-heating of the refrigerant on the performance of the system clearly

demonstrate the impact on the overall COP of the GSHP. The important test of the performance of the model was with the ideal Carnot cycle performance, gives the clear indication of its practicality of application. The accuracy of the model is verified by the experimental work published by comparing with the circulating water temperature at inlet and exit of the heat pump and power consumption for the compressor.

As a result of this study, many conclusions have come to the attention of the author and many reflections exist as a result of such scientific investigation.

What remains of interest is the temperature difference which drives the heat flow i.e. T^r and T_g has resulted in steady increase of COP for the initial 20°C. The graph gradually reduces the slope with further increase in the difference of temperature. This furthers the premise behind the issue of performance. The performance is significantly affected by the ground temperature T_g . Results clearly shows that as the ground temperature T_g is varied, the raise in COP for 15 °C raise in temperature difference is 10% and with T_g held constant, for the same 15°C raise the COP is increased by 1.5% the net 8.5% raise in COP is observed.

Still further, it is the affect of grout area on the performance that is quite steep, at 2% raise is observed for first 500m² area. The raise is almost steady around 0.5% at every 500m² area. Similar effect can be observed for the drop of temperature of the circulating water, it reduces steeply by 2.5°C for the same area and stabilises for the rest increase in the area.

Furthermore, circulating water temperatures compared with experimental results are very nearly achieved with 2% deviation, which summarises the accuracy of the model. The results again supported by CFD model with 2.3% deviation. This directly suggests the effect of degree of sub-cooling and super-heating of the refrigerant is encouraging. This can be achieved by developing a system to re-circulate the condenser exit auxiliary water to heat the evaporator exit. Similarly the system can be converted to sub-cool the condenser exit. This can lead to further innovation and improvements.

The main improvement in thermal properties of materials has shown increase in the performance for about 2.5% up to $20\text{W/m}^2\text{ }^\circ\text{K}$, and the effect is reduced for further increases in the overall heat transfer coefficient. It is evident that for an increase of U value considering the thermal conductivity of the pipe and grout to be constant, the velocity needs to be increased and this requires more power from the compressor. The model gives the safe range of overall heat transfer coefficient values.

Considering the difficulties to model such a complex and dynamic system, the appropriate assumptions are made to develop this model. The results chosen to compare are from the working range of temperatures. This model is developed to understand the operating parameters, which affect the performance of the system. To the extended of understanding the working methodology, this model gives fairly good results with very good consistency. Further research is needed to understand complex behaviour of the system working in the dynamic condition.

Hybrid model gives more diversified access to improve the methodologies and procedures for these systems. This CFD approach to combine the analytical model is a good example to follow and develop still more sophisticated way to represent challenging and dynamic systems. The possible solutions to offer by hybrid model would be to analyse by considering long time variations such as for monthly or yearly of the weather which CFD will take time to reproduce. But the analytical solution can be obtained in quick time and CFD can help calculate the flow variables due to change in geometric configurations, ground condition etc at ease. Analysing the results in CFD is easier by plotting different variables on any part of the system.

6.2 Future scope of work

The future of work in this field can be focused upon the transient condition, by considering the daily variation of the out side air temperature for a typical day in a month. This can be extended for the month and a whole year. Furthermore, the ground surrounding the grout can be modelled and solved for time varying temperature conditions on the outer surface of the grout. The temperature on the far end of the ground can be fixed assuming infinite source or sink.

The modelling can also be extended to consider the affect of heat interface between the two adjacent legs of the standard U-tube compared with the other configurations such as coil type with different pitch to diameter ratio. Considering the nonlinearity of the system and all the dynamic aspects of the model, it is still challenging task to completely predict the model performance. Influence of

different configuration of the GHE such as coil shape and other simple shapes which are easy to install is worth a try.

Modelling refrigerants with complex working environments is a challenging task. With proper assumptions refrigerant modelling can explore the understanding and can help to develop new and nature friendly refrigerants. Combining complete system cycle with refrigerant modelling for time varying parameters is a complex work. This explores new ways to understand the GSHP system.

Conclusion

In closing, this study serves to promote the continued research into ground heat as a sustainable and alternative energy saving option for the future. Introduction of such a hybrid concept will have a positive impact on the energy sector. With never stopping algorithm developments and computing power of the computer, results can be achieved in a short time. Ideas and methodologies should work together to achieve this common goal of improving the quality of life with cleaner and greener energy.

References

- [1] VICTOR W. GOLDSCHMIDT (1984) *Heat pumps: Basics, Types and Performance Characteristics*. Ann. Rev. Energy. 9:447-72
- [2] S. B RIFFAT, M.C.GILLOT (2002) *Performance of a novel mechanical ventilation heat recovery heat pump system*. Applied Thermal Engineering. 22: 839-845
- [3] GUOHUI GAN, SAFFA B.RIFFAT, C.S.A.CHONG (2007) *A novel rainwater-Ground source heat pump-Measurement and simulation*. Applied Thermal Engineering 27: 430-441
- [4] LUND, J. W. et al. *Geothermal (Ground Source) Heat Pumps- A world overview*, edited and updated version of the article from Renewable Energy World (July-Aug, 2003, Vol 6, No. 4) Geo-Heat Centre (GHC) Quarterly Bulletin, Vol. 25, N0 3, ISSN 0276-1084, 10pp, September 2004.
- [5] Clean energy project analysis (2005): Retscreen engineering and cases. *Ground Source Heat Pump Chapter*. ISBN: 0-662-39150-0 Catalogue no: M39-110/2005E-PDF.
- [6] ROBIN CURTIS (2007). *Geothermal heat pumps-their role in global cooling*. Proceedings of European Geothermal Congress. Unterhaching,
- [7] YUSUF ALI KARA (2007). *Experimental performance evaluation of a closed-loop vertical ground source heat pump in the heating mode using energy analysis method*. Int. J. Energy Res. 3: 1504-1516.
- [8] GEORGIOS FLORIDES, SOTERIS KALOGIROU (2007), *Ground Heat exchangers- A review of systems, models and applications*. Renewable energy 32 : 2461-2478
- [9] Technical report by Aire-Com of KY,LLC. Please follow the link below
<http://www.kycooling.com/webapp/GetPage?pid=187>
- [10] Ground Source Heat Pumps (Earth Energy Systems) (2009). *Heating and Cooling with a Heat Pump*. Natural Resources Canada, Office of Energy Efficiency.
- [11] Energy Efficiency Best Practice in Housing (March 2004) Energy Saving Trust part of Government. Technical documentation
- [12] H. SINGH, A. MUETZE, P.C. EAMES (2009) Factors influencing the uptake of heat pump technology by the UK domestic sector. Renewable Energy 35: 873-878

- [13] *Modern Building Service online-journal*. Please visit the following link http://www.modbs.co.uk/news/fullstory.php/aid/448/Renewable_heat_96_the_era_of_ground-source_heat_pumps.html
- [14] DANIEL E.FISHER, SIMON J. REES (2005). *Modelling ground source heat pump systems in a building energy simulation program (ENERGY PLUS)* "Ninth International IBPSA Conference" Montreal Canada: Aug 15-18
- [15] S.P. KAVANAUGH (1984), *Simulation experimental verification of vertical ground-coupled heat pump systems*, Ph.D. Dissertation, Oklahoma State University
- [16] J.D. DEERMAN AND S.P. KAVANAUGH (1990) *Simulation of vertical U-tube ground-coupled heat pump systems using the cylindrical heat source solution*, ASHRAE Transactions 97: 287-295.
- [17] P.ESKILSON (1987) *Thermal analysis of heat extraction boreholes*, Doctoral Thesis, University of Lund, Department of Mathematical Physics, Lund, Sweden
- [18] L. INGERSOLL, O.ZOBEL, A. INGERSOLL (1954) *Heat conduction with Engineering Geological and Other Applications*, second edition McGraw-Hill
- [19] G HELLSTROM (1991) *Ground Heat Storage, Thermal analysis of Duct storage system*, Ph D thesis, University of Lund Department of Mathematical Physics, Sweden
- [20] KATSUNORI NAGANO, TAKAO KATSURA, SAYAKA TAKEDA (2006) *Development of a design and performance prediction tool for the ground source heat pump system*. Applied Thermal Engineering 26:1578-1592
- [21] SUNDEN, BENGT (2007). *Computational fluid dynamics in research and design of heat exchangers*. (Department of Energy Sciences, Division of Heat Transfer, Lund University) Heat transfer engineering: 28, n 11: 898-910
- [22] FRANK P.INCROPERA, DAVID P.DEWITT (1996). *Introduction to Heat Transfer*, Third edition,
- [23] ETSU, *Heat pumps and heat pump-related R&D in UK Universities* (March 2000), Energy Efficiency Best Practice Programme, General Information Report No. 70
- [24] S.B. RIFFAT, N. ABODAHAB, *Innovative ground source heat pump systems for applications in building* : A Combined Conference of the Second International Conference on Renewable Energy & Environment Protection Technologies and the Fifth Conference on Solar Electricity: Photovoltaic's, Wind and Solar Thermal Technologies, Cairo, Egypt, March 2000.

- [25] P.S. DOHERTY , S. AL-HUTHAILI, S.B. RIFFAT, N. ABODAHAB (2004) *Ground source heat pump-description and preliminary results of the Eco House system*, Applied thermal engineering 24: 2627-2641
- [26] ABDEEN MUSTAFA OMER (2006) *Ground source heat pumps systems & applications*. Renewable and sustainable energy reviews, 12: 344-371
- [27] J. LUND, B. SANNER, L. RYBACH, R. CURTIS, G. HELLSTRO" M (2004) *Geothermal (ground-source) heat pumps. A world overview*, Geo-Heat Centre, Oregon Institute of Technology, Klamath Falls. <http://www.geoheat.oit.edu>
- [28] J. LUND, T. BOYD, A. SIFFORD, G. BLOOMQUIST, (2000) *Geothermal Energy Utilization in the United States*, Geo-Heat Centre, Oregon Institute of Technology, Klamath Falls. <http://www.geoheat.oit.edu>.
- [29] S. KAVANAUGH (2000), *Field tests for ground thermal properties-methods and impact on ground-source heat pump design*, ASHRAE Transactions 106 (1): 851-855.
- [30] D. PAHUD, B. MATTHEY (2001) *Comparison of the thermal performance of double U-pipe borehole heat exchangers measured in situ*, Energy and Buildings 33: 503-507
- [31] ASHRAE Handbook (2003)-HVAC Applications, *American Society of Heating, Refrigerating and Air-Conditioning Engineers*, Chapter 32
- [32] NIKOLAS KYRIAKIS, APOSTOLOS MICHPOULOS, KONSTANTIN PATTAS (2006), *on the maximum thermal load of ground heat exchangers*. Energy and Buildings 38: 25-29
- [33] ZHONGJIAN LI , MAOYU ZHENG (2009) *Development of a numerical model for the simulation of vertical U-tube ground heat exchangers* Applied thermal Engineering 29 : 920-924
- [34] YUJIN HWANG et al (2009) *Cooling performance of a vertical ground-coupled heat pump system installed in a school building*, Renewable Energy 34: 578-582
- [35] C.O POPIEL, J.WOJTKOWIAK, B. BIERNACKA (2001), *Measurement of temperature distribution in ground*, Experimental Thermal and Fluid Sciences 25:301-309
- [36] S.A.BAGGS (1983) *Remote prediction of ground temperature in Australian soil and mapping its distribution*, Solar Energy 30: 351-366
- [37] S.A.BAGGS (1991), *Australian Earth-Covered Buildings*, New South Wales University Press, New South Wales: 154-173 (Appendices)

- [38] LOUIS LAMARCHE, BENOIT BEAUCHAMP (2007) A new contribution to the finite line source model for geothermal boreholes. *Energy and Buildings* 39, 188-198
- [39] Alfalaval technical documentation
- [40] L. INGERSOLL, O.ZOBEL, A. INGERSOLL (1954) *Heat conduction with Engineering Geological and Other Applications*, second edition, McGraw-Hill,
- [41] ARIF HEPBASLI (2005) *Thermodynamic analysis of a ground source heat pump system for district heating*. *International Journal of Energy Research* 29: 671-687
- [42] SZARGUT J, MORRIS DR, STEWART FR. (1988). *Exergy Analysis of Thermal, Chemical, and Metallurgical Processes*. Hemisphere Publishing Co.: New York
- [43] KAVANAUGH, RAFFERTY (1997). *Ground Source Heat Pumps*, Amer society of heating, Publication date 1-6-1997.
- [44] ONDER OZGENER, ARIF HEPBSALI (2005) Performance analysis of a solar assisted ground source heat pump system for green house heating: An experimental study. *Building and Environment* 40: 1040-1050
- [45] G. HELLSTRÖM, B. SANNER, M. KLUGESCHIED T. GONKA, S. MÅRTENSSON, *Experiences with the borehole heat exchanger software EED* : Proceedings of IEAs Seventh Energy Conservation Thermal Energy Storage Conference Megastock'1997, Sapporo, 1997, : 247-252.
- [46] S.P. KAVANAUGH (1992), *Field test of a vertical ground-coupled heat pump in Alabama*, ASHRAE Transactions: Symposia BA-92-9-1: 607-615.
- [47] H. FUJII, R. ITOI, J. FUJII, Y. UCHIDA (2005) *Optimizing the design of large-scale ground coupled heat pump systems using groundwater and heat transport modeling*, *Geothermics* 34 : 347-364.
- [48] WEI BO YANG A, MING HENG SHI A,, HUA DONG (2006) *Numerical simulation of the performance of a solar-earth source heat pump system* - *Applied Thermal Engineering* 26: 2367-2376
- [49] J.M. CRYE, A.E. RUGGLES, W.D. POINTER, D.K. FELDE, P.A. JALLOUK, M.T. MCFEE, M.W. WENDEL JR., G.L. YODER (2002), *Measurement of the heat transfer coefficient for mercury flowing in a narrow channel*, *Transactions of ASME* 124 1034-1038.
- [50] JACO DIRKER, JOSUA P. MEYER (2002), *Heat transfer coefficients in concentric annuli*, *Journal of Heat Transfer* 124: 1200-1203

- [51] K. VAFAI, C.P. DESAI, S.V. IYER, M.P. DYKO (1997), *Buoyancy induced convection in a narrow open-ended annulus*, Journal of Heat Transfer, Transactions ASME 119 (3) 483–494.
- [52] S. KENJERES, K. HANJALIC (1995), *Prediction of turbulent thermal convection in concentric and eccentric horizontal annuli*, International Journal of Heat and Fluid Flow 16 (5) 429–439.
- [53] C.K. LEE, H.N. LAM (2008) *Computer simulation of borehole ground heat exchangers for geothermal heat pump systems* Renewable Energy 33:1286–1296
- [54] NIKOLAS KYRIAKIS, APOSTOLOS MICHPOULOS, KONSTANTIN PATTAS (2006), *On the maximum thermal load of ground heat exchangers*. Energy and Buildings 38:25–29
- [55] D. MARCOTTE, P. PASQUIER (2008) *On the estimation of thermal resistance in borehole thermal conductivity test*. Renewable Energy 33: 2407–2415
- [56] H.J.G. DIERSCH (2002), *FEFLOW Reference Manual*, Institute for Water Resources Planning and Systems Research Ltd. 278
- [57] H. FUJII, ET AL (2005). *Optimizing the design of large-scale ground-coupled heat pump systems using groundwater and heat transport modelling*, Geothermics 34: 347–364.
- [58] YUJIN NAM, RYOZO OOKA, SUCKHO HWANG (2008) *Development of a numerical model to predict heat exchange rates for a ground-source heat pump system*- Energy and Buildings 40: 2133–2140
- [59] W.A. AUSTIN, ET AL (2000). *Development of an in-situ system for measuring ground thermal properties*, ASHRAE Transaction 106 (1) 365–379.
- [60] H.D. RAWLINGS, J.R. SYKULSKI (1999), *Ground source heat pumps: a technology review*, CIBSE A. Building Services & Engineering Research Technology 20 (3) 119–129.
- [61] IEA, *Ground source heat pump systems case studies*, IEA Heat Pump Centre, Report number HPC-AR10, 2002.
- [62] BURKHARD SANNER, CONSTANTINE KARYTSAS (2003), *Current status of ground source heat pumps and underground thermal energy storage in Europe*, Geothermics 32:579–588.
- [63] CANETA Research Inc., *Commercial/institutional ground source heat pump engineering manual*, American Society of Heating, Refrigerating and Air-Conditioning Engineers (ASHRAE), Atlanta, 1995.

- [64] N.D. PAUL (1996.), *The effect of grout conductivity on vertical heat exchanger design and performance*, Master Thesis, South Dakota State University,
- [65] P. ESKILSON (1987) *Thermal analysis of heat extraction boreholes*, Doctoral Thesis, Department of Mathematical Physics, University of Lund, Lund, Sweden,
- [66] A. CAROTENUTO, C. CASAROSA (1997), *An aquifer-well thermal and fluid dynamic model for down-hole heat exchangers with a natural convection promoter*, Int. J. Heat Transfer 40 (18) 4461-4472.
- [67] JUNGI NISHIOKA (1993), *Heat transfer characteristics of an earth-probe model for a ground source heat pump*, Heat Trans. Japanese Res. 22 (7) 661—671.
- [68] A.C. CHIASSON, S.J. REES, J.D. SPITLER (2000), *A preliminary assessment of the effects of ground-water flow on closed-loop ground-source heat pump systems*, ASHRAE Trans. 106 (1) 380-393.
- [69] XINGUO LI, JUN ZHAO, QIAN ZHOU (2005), *Inner heat source model with heat and moisture transfer in soil around the underground heat exchanger*, Applied Thermal Eng. 25 :1565-1577.
- [70] HEYI ZENG, RAIREN DIAO, ZHAOHONG FANG (2003), *Heat transfer analysis of boreholes in vertical ground heat exchangers*, International Journal of Heat Mass Transfer. 46: 4467-4481.
- [71] ESKILSON P 1987. *Thermal analysis of heat extraction boreholes*. PhD thesis. Sweden: University of Lund.
- [72] YAVUZTURK C, SPITLER JD, REE SJ. *A transient two-dimensional finite volume model for the simulation of vertical U-tube ground heat exchangers*. ASHRAE Trans 1999 105: 465-74.
- [73] YAVUZTURK C, SPITLER JD, REES SJ. *A short time step response factor model for vertical ground loop heat exchangers*. ASHRAE Trans 1999 105: 475-85.
- [74] LI Z, ZHENG M. Development of a numerical model for the simulation of vertical U-tube ground heat exchangers. Applied Thermal Eng, in press.
- [75] KAVANAUGH SP (1986). *Simulation and experimental verification of vertical ground coupled heat pump systems*. PhD thesis. Stillwater, Oklahoma: Oklahoma State University
- [76] INGERSOLL LR, PLASS HJ. *Theory of the ground pipe heat source for the heat pump*. ASHRAE Trans 1948 47: 339-48.
- [77] H.S. CARSLAW AND J.C. JAEGER, *Conduction of Heat in Solid*, Oxford University Press, Oxford 1959.

[78] IGSHPA (1991) *Design and installation standards*. Stillwater. Oklahoma: International Ground Source Heat Pump Association

[79] A C CLELAND (1994), *Polynomial curve fits of for refrigerant thermodynamic properties: extension to include R134a*, International Journal of Refrigeration 17: 245-249

[80] F. DE MONTE (2002) *Calculation of thermodynamic properties of R407C and R410A by the Martin–Hou equation of state — part I: theoretical development*, International Journal of Refrigeration 25: 306–313

[81] JOHN D ANDERSON Jr, *Computational Fluid Dynamics the basics with applications*, McGraw-Hill International Editions, 1995

[82] DONALD D HEARN, M PAULINE BAKER (2003) *Computer Graphics with open GL*. Third edition, Prentice hall publication

[83] FLUENT Technical documentation

[84] KIM, BHAVANI V SANKAR (2008), *Introduction to finite element analysis and design*, Wiley Pap/Pas edition

Appendix A - Numerical values for the variables

$$\rho = 1000 \frac{\text{kg}}{\text{m}^3}$$

$$v = 0.5 \text{ m/sec}$$

$$d = 0.032 \text{ m}$$

$$\mu = 8.9 \times 10^{-4} \text{ kg/m sec}$$

$$C_p = 4189 \text{ J/kgK}$$

$$k = 0.59 \text{ W/mK}$$

$$r_1 = 0.016 \text{ m}$$

$$r_2 = 0.02 \text{ m}$$

$$r_3 = 0.075 \text{ m}$$

$$r_4 = 2.5 \text{ m}$$

$$K_{\text{pipe}} = 0.51 \text{ W/mK}$$

$$K_{\text{grout}} = 2.96 \text{ W/mK}$$

$$K_{\text{ground}} = 0.5 \text{ W/mK}$$

$$l = 175 \text{ m}$$

$$n = 24$$

$$Re = \frac{\rho v d}{\mu} = 17977 > 2100$$

It is turbulent flow

$$C_f = \frac{0.079}{Re^{0.25}}$$

$$Pr = \frac{C_p \mu}{k}$$

$$Nu = \frac{\left(\frac{Cf}{2}\right) (Re - 1000) Pr}{1 + 12.7\sqrt{Cf/2} (Pr^{2/3} - 1)}$$

$$Nu = 121.83$$

$$hf = \frac{Nu K}{d}$$

$$hf = \frac{121.83 * 0.59}{0.032} = 2246.2 W/m^2K$$

$$U_g = \frac{1}{\frac{1}{hf} + \frac{r_1}{K_{pipe}} \ln\left(\frac{r_1}{r_2}\right) + \frac{r_1}{K_{grout}} \ln\left(\frac{r_3}{r_2}\right) + \frac{r_1}{K_{ground}} \ln\left(\frac{r_4}{r_3}\right)}$$

$$U_g = 7.88 W/m^2K$$

$$A = \pi d l n$$

$$A = \pi * 0.15 * 175 * 24$$

$$A = 1979 m^2$$

Appendix B: Calculation of Overall Heat transfer Coefficient for heat exchangers

1. Ground Heat Exchanger (GHE)

$$UA_{GHX}=7.88 * 1979 W / ^\circ K$$

$$UA_{GHX}=15594 W / ^\circ K$$

2. Condenser and Evaporator.

Plate heat exchanger have high overall heat transfer coefficient (U) ranging from 1000-2500 W/m^2K , (SWEP Heat Exchanger manufacturer's catalogue)

Assuming the lower value for the safer design at 1000 W/m^2K . Model DBD400 is selected as a condenser for this case. From the dimension of the heat exchanger, with 282 plates

2.1 $(UA)_{con}$ for 282 plates

$$Area \ 0.604 * 0.216 * 282 = 36.5m^2$$

$$(UA)_{con}=1000*36.79 = 36790 W / ^\circ K$$

Similarly P400T model is selected for Evaporator with following dimensions

2.2 $(UA)_{eva}$ for 280 plates

$$\text{Area } 0.601 * 0.25 * 280 = 36.5m^2$$

$$(UA)_{eva}=1000*42 =42000W/^{\circ}K$$

3 Radiators

For cast iron working between air and water the overall heat transfer coefficient is around $7.6 W/m^2K$ with an assumed area $24m^2$

$$(UA)=7.9*24 =1896 W/^{\circ}K$$

With the total mass flow rate of $15.54 Kg/Sec$ for each tube the flow rate is $15.54/24=0.647 Kg/Sec$ for convenient in calculation $0.5 Kg/Sec$ is considered.

Appendix C: MathCAD Calculations- Uses values given in Appendix A

$$C_p := 4189 \frac{\text{J}}{(\text{kg} \cdot \text{K})}$$

$$K_w := 0.69 \frac{\text{W}}{(\text{m} \cdot \text{K})}$$

$$U_2 := 300.2886193 \frac{\text{W}}{(\text{m}^2 \cdot \text{K})}$$

$$U_1 := 1000 \frac{\text{W}}{(\text{m}^2 \cdot \text{K})}$$

$$U_r := 870.1426415 \frac{\text{W}}{(\text{m}^2 \cdot \text{K})}$$

$$A_2 := 20\text{m}^2$$

$$U_{ai} := 10 \frac{\text{W}}{\text{m}^2 \cdot \text{K}}$$

$$A_1 := 36.8013931 \text{ m}^2$$

$$L_w := 0.30 \text{ m}$$

$$A_w := 214.4247086 \text{ m}^2$$

$$T_{\text{air}} := 63^\circ\text{C}$$

$$W_{\text{in}} := 6200 \text{ W}$$

$$C_{\text{pref}} := 600 \frac{\text{J}}{\text{kg} \cdot \text{K}}$$

$$U_{\text{ao}} := 15 \frac{\text{W}}{\text{m}^2 \cdot \text{K}}$$

$$U_g := 7.88 \frac{\text{W}}{(\text{m}^2 \cdot \text{K})}$$

$$T_g := 18^\circ\text{C}$$

$$A_g := 1979 \text{ m}^2$$

$$M_w := 4.814769294 \frac{\text{kg}}{\text{s}}$$

$$M_{w1} := 2.561937614 \frac{\text{kg}}{\text{s}}$$

$$M_{\text{ref}} := 0.35 \frac{\text{kg}}{\text{s}}$$

$$A_r := 24 \text{ m}^2$$

$$F1(T_g, T_{fi}, T_{fo}, U_g, A_g, Q_s) := Q_s - U_g \cdot A_g \cdot \frac{(T_{fo} - T_{fi})}{\ln \left[\frac{(T_{fo} - T_g)}{(T_{fi} - T_g)} \right]}$$

$$F2(M_w, C_p, T_{fo}, T_{fi}, Q_s) := Q_s - M_w \cdot C_p \cdot (T_{fo} - T_{fi})$$

$$F3(T1_{ref}, T_{fi}, T_{fo}, U_1, A_1, Q_s) := Q_s - U_1 \cdot A_1 \cdot \frac{(T_{fo} - T_{fi})}{\ln \left[\frac{(T1_{ref} - T_{fi})}{(T1_{ref} - T_{fo})} \right]}$$

$$F4(Q_s, h1_{ref}, h4_{ref}, M_{ref}) := Q_s - M_{ref} \cdot (h1_{ref} - h4_{ref})$$

$$F5(Q_{sr}, h1_{ref}, h4_{ref}, M_{ref}, W_{in}) := Q_{sr} - M_{ref} \cdot (h1_{ref} - h4_{ref}) + W_{in}$$

$$F6(M_{ref}, h2_{ref}, h4_{ref}, Q_{sr}) := Q_{sr} - M_{ref} \cdot (h2_{ref} - h4_{ref})$$

$$F7(U_2, A_2, T2_{ref}, T2_{in}, T2_{out}, Q_{sr}) := Q_{sr} - U_2 \cdot A_2 \cdot \frac{(T2_{out} - T2_{in})}{\ln \left[\frac{(T2_{out} - T2_{ref})}{(T2_{in} - T2_{ref})} \right]}$$

$$F8(M_{w1}, C_p, T2_{in}, T2_{out}, Q_{sr}) := Q_{sr} - M_{w1} \cdot C_p \cdot (T2_{out} - T2_{in})$$

$$F9(U_r, A_r, T2_{in}, T_r, T2_{out}, Q_{sr}) := Q_{sr} - U_r \cdot A_r \cdot \frac{(T2_{out} - T2_{in})}{\ln \left[\frac{(T_r - T2_{in})}{(T_r - T2_{out})} \right]}$$

$$F10(K_w, A_w, U_{ao}, U_{ai}, L_w, T_r, T_{air}, Q_{sr}) := Q_{sr} - \left[\left(U_{ao} + \frac{K_w}{L_w} + U_{ai} \right) \cdot A_w \cdot (T_{air} - T_r) \right]$$

Constants for function F11 and F12

$$t_c := 72.13^\circ\text{C}$$

$$a1 := 221.174$$

$$b1 := -514.966$$

$$c1 := -631.625$$

$$d1 := -262.274$$

$$e1 := 105$$

$$F11(T1_{ref}, h4_{ref}) := \left[h4_{ref} - 1000 \left[a1 + b1 \cdot \left[\left(1 - \frac{T1_{ref}}{t_c} \right)^{\frac{1}{3}} - x_0 \right] + c1 \cdot \left[\left(1 - \frac{T1_{ref}}{t_c} \right)^{\frac{1}{3}} - x_0 \right]^2 + d1 \cdot \left[\left(1 - \frac{T1_{ref}}{t_c} \right)^{\frac{1}{3}} - x_0 \right]^3 + e1 \cdot \left[\left(1 - \frac{T1_{ref}}{t_c} \right)^{\frac{1}{3}} - x_0 \right]^4 + f1 \cdot \left[\left(1 - \frac{T1_{ref}}{t_c} \right)^{\frac{1}{3}} - x_0 \right]^5 \right] \cdot 1 \frac{J}{kg} \right]$$

$$F12(T2_{ref}, h2_{ref}) := h2_{ref} - \left[-2 \cdot 10^{-11} \cdot \left(\frac{T2_{ref}}{K} - 273.15 \right)^6 \right] - \left[4 \cdot 10^{-9} \cdot \left(\frac{T2_{ref}}{K} - 273.15 \right)^5 \right] - \left[2 \cdot 10^{-7} \cdot \left(\frac{T2_{ref}}{K} - 273.15 \right)^4 \right] - \left[1 \cdot 10^{-5} \cdot \left(\frac{T2_{ref}}{K} - 273.15 \right)^3 \right] - \left[0.003 \cdot \left(\frac{T2_{ref}}{K} - 273.15 \right)^2 \right] + \left[0.28 \cdot \left(\frac{T2_{ref}}{K} - 273.15 \right) \right] + 422.49 \cdot 1000 \cdot 1 \frac{J}{kg}$$

$$T_r := 22^\circ\text{C}$$

$$T_{2\text{ref}} := 7^\circ\text{C}$$

$$T_{2\text{out}} := 21^\circ\text{C}$$

$$T_{2\text{in}} := 15^\circ\text{C}$$

$$T_{1\text{ref}} := 25.173^\circ\text{C}$$

$$T_{\text{fi}} := 21^\circ\text{C}$$

$$T_{\text{fo}} := 24.5^\circ\text{C}$$

$$h_{2\text{ref}} := 424299.0 \frac{\text{J}}{\text{kg}}$$

$$h_{1\text{ref}} := 442112.6857 \frac{\text{J}}{\text{kg}}$$

$$h_{4\text{ref}} := 240716.65758 \frac{\text{J}}{\text{kg}}$$

$$Q_{\text{sr}} := 64391.74\text{W}$$

$$Q_s := 70591.74\text{W}$$

Given

$$F1(T_g, T_{\text{fi}}, T_{\text{fo}}, U_g, A_g, Q_s) = 0$$

$$F2(M_w, C_p, T_{\text{fo}}, T_{\text{fi}}, Q_s) = 0$$

$$F3(T_{1\text{ref}}, T_{\text{fi}}, T_{\text{fo}}, U_1, A_1, Q_s) = 0$$

$$F4(Q_s, h_{1\text{ref}}, h_{4\text{ref}}, M_{\text{ref}}) = 0$$

$$F5(Q_{\text{sr}}, h_{1\text{ref}}, h_{4\text{ref}}, M_{\text{ref}}, W_{\text{in}}) = 0$$

$$F6(M_{\text{ref}}, h2_{\text{ref}}, h4_{\text{ref}}, Q_{\text{sr}}) = 0$$

$$F7(U_2, A_2, T2_{\text{ref}}, T2_{\text{in}}, T2_{\text{out}}, Q_{\text{sr}}) = 0$$

$$F8(M_{w1}, C_p, T2_{\text{in}}, T2_{\text{out}}, Q_{\text{sr}}) = 0$$

$$F9(U_r, A_r, T2_{\text{in}}, T_r, T2_{\text{out}}, Q_{\text{sr}}) = 0$$

$$F10(K_w, A_w, U_{\text{ao}}, U_{\text{ai}}, L_w, T_r, T_{\text{air}}, Q_{\text{sr}}) = 0$$

$$F11(T1_{\text{ref}}, h4_{\text{ref}}) = 0$$

$$F12(T2_{\text{ref}}, h2_{\text{ref}}) = 0$$

$$\begin{pmatrix} T_1 \\ T_2 \\ T_3 \\ T_4 \\ T_5 \\ T_6 \\ T_7 \\ Q_1 \\ Q_2 \\ h_1 \\ h_2 \\ h_3 \end{pmatrix} := \text{Minerr}(T_r, T2_{\text{in}}, T2_{\text{out}}, T2_{\text{ref}}, T1_{\text{ref}}, T_{\text{fi}}, T_{\text{fo}}, Q_{\text{sr}}, Q_s, h1_{\text{ref}}, h4_{\text{ref}}, h2_{\text{ref}})$$

Residue calculation for an initial guess

$$Q_s - U_g \cdot A_g \cdot \frac{(T_{fo} - T_{fi})}{\ln \left[\frac{(T_{fo} - T_g)}{(T_{fi} - T_g)} \right]} = -3.20142135 \times 10^{-10} \text{ W}$$

$$Q_s - M_w \cdot C_p \cdot (T_{fo} - T_{fi}) = -1.16415322 \times 10^{-10} \text{ W}$$

$$Q_s - U_1 \cdot A_1 \cdot \frac{(T_{fo} - T_{fi})}{\ln \left[\frac{(T_{1ref} - T_{fi})}{(T_{1ref} - T_{fo})} \right]} = 8.73114914 \times 10^{-10} \text{ W}$$

$$Q_s - M_{ref} \cdot (h_{1ref} - h_{4ref}) = -1.45519152 \times 10^{-11} \text{ W}$$

$$Q_{sr} - Q_s + W_{in} = 0 \text{ W}$$

$$Q_{sr} - M_{ref} \cdot (h_{2ref} - h_{4ref}) = 0 \text{ W}$$

$$Q_{sr} - U_2 \cdot A_2 \cdot \frac{(T_{2out} - T_{2in})}{\ln \left[\frac{(T_{2out} - T_{2ref})}{(T_{2in} - T_{2ref})} \right]} = 1.45519152 \times 10^{-10} \text{ W}$$

$$Q_{sr} - M_{w1} \cdot C_p \cdot (T2_{out} - T2_{in}) = 2.98314262 \times 10^{-10} \text{ W}$$

$$Q_{sr} - U_r \cdot A_r \cdot \frac{(T2_{out} - T2_{in})}{\ln \left[\frac{(T_r - T2_{in})}{(T_r - T2_{out})} \right]} = -1.14232535 \times 10^{-9} \text{ W}$$

$$Q_{sr} - \left(U_{ao} + \frac{K_w}{L_w} + U_{ai} \right) \cdot A_w \cdot (T_{air} - T_r) = 1.30967237 \times 10^{-10} \text{ W}$$

$$\left[h4_{ref} - 1000 \left[a1 + b1 \cdot \left[\left(1 - \frac{T1_{ref}}{t_c} \right)^{\frac{1}{3}} - x_0 \right] + c1 \cdot \left[\left(1 - \frac{T1_{ref}}{t_c} \right)^{\frac{1}{3}} - x_0 \right]^2 + d1 \cdot \left[\left(1 - \frac{T1_{ref}}{t_c} \right)^{\frac{1}{3}} - x_0 \right]^3 + e1 \cdot \left[\left(1 - \frac{T1_{ref}}{t_c} \right)^{\frac{1}{3}} - x_0 \right]^4 + f1 \cdot \left[\left(1 - \frac{T1_{ref}}{t_c} \right)^{\frac{1}{3}} - x_0 \right]^5 \right] \cdot 1 \frac{\text{J}}{\text{kg}} \right] = 0 \frac{\text{J}}{\text{kg}}$$

$$h2_{ref} - \left[-2 \cdot 10^{-11} \cdot \left(\frac{T2_{ref}}{K} - 273.15 \right)^6 \right] - \left[4 \cdot 10^{-9} \cdot \left(\frac{T2_{ref}}{K} - 273.15 \right)^5 \right] - \left[2 \cdot 10^{-7} \cdot \left(\frac{T2_{ref}}{K} - 273.15 \right)^4 \right] - \left[1 \cdot 10^{-5} \cdot \left(\frac{T2_{ref}}{K} - 273.15 \right)^3 \right] - \left[0.003 \cdot \left(\frac{T2_{ref}}{K} - 273.15 \right)^2 \right] + \left[0.28 \cdot \left(\frac{T2_{ref}}{K} - 273.15 \right) \right] + 422.49 \cdot 1000 \cdot 1 \frac{\text{J}}{\text{kg}} = 0 \frac{\text{J}}{\text{kg}}$$

Sample data for the calculation of COP with varying power input to the compressor

W_{in} (Watts)	Q_{sr} (Watts)	Q_s (Watts)	T_r (°C)	T_{2in} (°C)	T_{2out} (°C)	T_{2ref} (°C)	T_{1ref} (°C)	T_{fi} (°C)	T_{fo} (°C)	h_1 (J/Kg)	h_2 (J/Kg)	h_4 (J/Kg)	COP (Actual)	COP (Exp)
1250	14573	15823	21.28	15.038	19.076	3.981	25.55	21.18	24.88	439181	423556	241389	11.65	10.2
1450	15225	16675	21.01	14.91	19.79	3.879	25.57	21.19	24.91	439808	423558	241427	10.5	9.8
2500	21750	24250	20.12	14.89	19.85	3.561	25.62	21.21	24.94	441061	423561	241504	8.7	7.8
4000	32000	36000	18.63	14.78	20.091	3.12	25.67	21.22	24.98	442314	423564	241580	8	7.1
5000	34350	39350	17.49	14.39	20.36	2.96	25.71	21.24	25.02	443567	423567	241657	6.87	6.5